

DEPOSITIONAL HISTORY OF THE DESMOINESIAN SUCCESSION
(MIDDLE PENNSYLVANIAN) IN THE PERMIAN BASIN

Wayne Wright

Bureau of Economic Geology
Jackson School of Geosciences
The University of Texas at Austin
Austin, Texas

ABSTRACT

Distribution of the Desmoinesian reflects two large phases of deposition. Earliest Strawn Group deposition is reflected by widespread, generally uniformly thick carbonate deposition (that is, Odom Formation and equivalents). Carbonate deposition was followed by “downwarping” and subsidence of the Midland Basin, which resulted in a more geographically stable carbonate platform/shelf developing. This shelf edge strikes north-south and is generally coincident with the Fort Chadbourne Fault System (Fort Chadbourne High). Deposition of carbonates and siliciclastics is cyclic, although the shelf margin is largely stationary and reflects aggradation. The overall depositional environment detailed on the Eastern Shelf (for example, Odom and Goen, etc.) appears to be reflected in other parts of the Permian Basin. The ‘Lower’ Strawn is generally a relatively uniform thickness at approximately 225 to 275 ft, with a characteristic wireline-log signature. In localized areas of increased accommodation, the Strawn carbonate succession thickens dramatically (750 to 900 ft). Many of the historically termed Strawn siliciclastics have subsequently been reinterpreted using high-resolution 3D seismic and other means to actually be Permian (dominantly Wolfcampian) in age.

Desmoinesian-age units in the Permian Basin record a weak 2nd-order transgression. In general, calculations for rate of global sea-level rise are less steep in the Desmoinesian than in the underlying Atokan. The 2nd-order transgression is punctuated by high-amplitude 3rd-order regressive and transgressive events occurring at a very high frequency.

Desmoinesian carbonates were deposited over a much larger area in the Permian Basin than previously documented. Algally dominated bioherms and higher energy facies (oid grainstones) affected by burial diagenesis and subsequently fractured compose the best carbonate reservoirs. Because producing carbonate reservoirs within the Midland Basin are products of both meteoric and deep-burial diagenesis, many zones can be linked to facies type and sequence stratigraphic surfaces.

Two new paleogeographic reconstructions of the Desmoinesian of the Permian Basin are presented (figs. 1, 2). Figure 1 is reconstructed at an early Desmoinesian time (Strawn Caddo to Lower Odom equivalent), whereas figure 2 is a late Desmoinesian reconstruction at approximately the Anson Bank depositional period.

In brief, early Desmoinesian-age alluvial, deltaic, and marine siliciclastics are distributed over the Llano Uplift, margins of the Eastern Shelf, parts of western Val Verde Basin (Kerr Basin), and the northern Delaware Basin. Siliciclastic shale deposition is volumetrically and physiographically isolated, with occurrences in the southern Delaware Basin and portions of the Midland Basin (southern Reagan County and parts of Martin, Howard, and Mitchell Counties). Widespread ramp to platform-carbonate deposition of a relatively uniform thickness dominates throughout the Permian Basin. Deeper basinal carbonates and shales are largely restricted to the Delaware Basin. The

small number of Precambrian inliers that were exposed during the Atokan are transgressed in early Desmoinesian time. The Pedernal Uplift provided limited sediment input for the northwest shelf, and the Bravo Dome area appears to have been exposed, although providing little in the way of material.

During the late Desmoinesian, structural downwarping of the Midland Basin appears to have initiated. This downwarping and subsidence led to an increased area of deeper water within the Midland Basin, and carbonates around the margins responded to the increased accommodation by aggrading substantially. This aggradation led to development of the first well-defined Pennsylvanian shelf margin of the Permian Basin. Initial development of the Val Verde Basin in Terrell County also occurred during the late Desmoinesian. The northern Eastern Shelf and north of the Llano Uplift comprise a series of cyclic carbonate and siliciclastic units. In figure 2 marginal marine and alluvial siliciclastics are feeding the Bowie and Perrin Deltas in the west (Jack, Young, and Clay Counties). To the west of the deltas, the Anson carbonate bank and shelf complex developed, which is part of the Eastern Shelf margin and shelf interior facies. To the west of the Anson Bank, across a shallow basin, are thick aggradational carbonates on the Red River Uplift (King County). A shallow trough possibly runs from the Knox and Baylor County area (Knox-Baylor Trough) and connects to the Midlands in Mitchell and Fisher Counties. A deepening of the basin also occurred in the Hockley-Lubbock County area. Subsidence in this area potentially led to development of a carbonate shelf margin in Hockley and Lubbock Counties, which would roughly correspond to the northern margin of the Horseshoe Atoll. The paleogeographic summary at the end of this chapter should be referred to for a more detailed discussion of Desmoinesian paleogeography.

INTRODUCTION

This chapter discusses styles of deposition and facies development of Desmoinesian-age sediments, concluding with a discussion of revised paleogeography for the Desmoinesian Permian Basin (figs. 1, 2; Summary). The chapter is divided into discussions of siliciclastic and carbonate Desmoinesian deposition. In each section a regional model for facies patterns and deposition is proposed. Data from areas adjacent to the Permian Basin are used as analogs for facies that are predicted to be present within the study area. More localized studies are used to illustrate certain key aspects (for example, facies type, reservoir quality). However, an initial introduction to the area, placing it in a global perspective, is first presented.

GLOBAL TECTONIC SETTING

Desmoinesian-age sediments in the Permian Basin are characterized by being deposited at a near (8 to 12° south) equatorial position during the middle stages of icehouse, high-amplitude, high-frequency eustatic sea-level fluctuations. It was an area undergoing increased tectonic activity of both uplift and subsidence related to Ouachita-Marathon orogeny and birth of the greater ancestral Rocky Mountains. Figure 3 illustrates the position of Texas (in orange) relative to major tectonic plates and the equator at the beginning of the Pennsylvanian (circa Atokan–Desmoinesian age). During Desmoinesian times, Texas continued its northward migration toward an equatorial position (fig. 3).

REGIONAL TECTONIC SETTING AND FACIES DISTRIBUTION

The outline of the Permian Basin and the major geologic features commonly associated with the basin are illustrated in figure 4. All features did not develop simultaneously but were in the early to middle stages of development during the Desmoinesian. Figures 5 through 7 illustrate previous interpretations of facies distribution, uplift, and subsidence patterns for Desmoinesian-age sediments in the Permian Basin and surrounding areas. Revised Desmoinesian Permian Basin paleogeography is presented and discussed in the summary. Interpretations suggest that most of the Permian Basin was an area of net subsidence during the Desmoinesian. The basin is inferred to be rimmed by carbonate-platform to shelfal environments, with substantial uplifted areas in the Diablo Platform and Central Basin Platform (CBP) (Ye and others (1996) (fig. 5).

The areas of uplift, subsidence, and facies distribution in figures 5 through 7 do not all match, although figures 5 and 7 are broadly similar. On the basis of Kluth (1986), most of the Permian Basin area is illustrated as an area of net subsidence, with rate ranges from $\leq 50\text{m/Ma}$ to $\sim 200\text{--}300\text{m/Ma}$ (fig. 6). One of the most important differences apparent between figures 5, 6, and 7 is the extent of uplift on the CBP. Uplifted parts range from the almost entire platform in interpretations of Ye and others (1996) and Blakey (2005) to the south region only in Kluth (1986) (figs. 4 through 7). Correcting inconsistencies in the regional paleogeography of the Permian Basin and outlining more detailed depositional patterns are the major goals of this chapter (figs. 1, 2).

GENERAL STRATIGRAPHY AND NOMENCLATURE

Desmoinesian-age sediments within the Permian Basin include those termed Strawn Formation (predominantly carbonates)—those of the Strawn Group and the underlying Caddo Limestone. Within the Permian Basin, most Desmoinesian-age sediments are referred to as Strawn Formation, and they are overwhelmingly carbonates. However, on the Eastern Shelf, the stratigraphy is more complicated, with multiple carbonate and siliciclastic units having been cyclically deposited during the Desmoinesian.

Nomenclature

As is true of the underlying Morrowan and Atokan intervals, stratigraphic nomenclature of the Desmoinesian interval on the Eastern Shelf is complicated (for example, Gunn, 1979; Cleaves, 1993). The reader is referred to figure 8 for detailed correlation of named units of Desmoinesian age on the Eastern Shelf. The Desmoinesian interval as defined in this study contains all formations, groups, and members that lie within the Strawn Group. Historically in the Midland Basin, CBP, and Delaware Basin regions, Desmoinesian-age rocks were referred to only as Strawn, regardless of lithology.

SILICICLASTIC DESMOINESIAN DEPOSITION

General Depositional Setting

Deltaic, fan delta, and incised-valley systems occur throughout the Desmoinesian. Incised-valley systems are largely restricted to north-central Texas, west of the Fort Worth Basin. Multiple deltaic depocenters were active during the Desmoinesian, funneling sediment onto the northeast and east margin of the Eastern Shelf. Delta-front

sediments are present in Coke, Runnels, and Coleman Counties along the Eastern Shelf. The Pedernal Uplift appears to have remained in a stage of quiescence that was established in the Atokan. Aerially restricted minor amounts of marginal marine to open marine deltaic to shelfal siliciclastic sedimentation may be present in the extreme northwest corner of the Permian Basin. The Bravo Dome in Roosevelt and Cochran Counties is thought to have been exposed during the Desmoinesian; however, no siliciclastic plays have been identified in this region yet. Overall, 2nd-order marine transgression during the Desmoinesian resulted largely in deposition of carbonates at the expense of siliciclastic lithologies.

Reservoir Potential

Updip fluvial, amalgamated, stacked channels and thick fan-delta units have the best reservoir potential and quality. However, it appears that most of the proximal facies occur to the east of the Permian Basin. Delta-front and channel-mouth bars along the Eastern Shelf have good reservoir quality (up to 15.2 percent porosity, mean 5.3 percent, and up to 387 md permeability). Trapping mechanisms range from structural to stratigraphic. In delta-front systems, bidirectional facies pinch-out of sand lenses to prodelta and delta-plain mudstones is a common trap style.

Diagenesis

Desmoinesian-age deltaic sediments reflect a long diagenetic history, with extensive cementation by quartz and calcite. Postcementation secondary dissolution and leaching of calcite cement and framework grains (for example, feldspar, rock fragments) produced/recovered current porosity in the facies.

Climate

The Desmoinesian was a time of expansive ice-sheet development typified by a highly fluctuating sea level. Amplitude and frequency of sea-level change are higher in the Desmoinesian than in underlying Atokan- and Morrowan-age units. Highly fluctuating sea levels generally result in thinner, higher frequency cycles and numerous periods of exposure.

PERMIAN BASIN

Eastern Shelf

Detailed studies were performed by Cleaves (1975, 1993, 2000) and Cleaves and Erxleben (1982, 1985) on the siliciclastic depositional patterns of the Desmoinesian northern Eastern Shelf. Figure 8 illustrates a schematic representation of Desmoinesian sedimentation patterns along the northern Eastern Shelf and farther eastward into the greater Fort Worth Basin area. During the Desmoinesian, siliciclastic sediments encroached fully only on the Eastern Shelf (that is, within the boundaries of the current Permian Basin, as defined in figure 4) (equivalent to Odom Bank Limestone) (fig. 8). In the northern Eastern Shelf, these two influx episodes are associated with Buck Creek and Dobbs Valley sandstones (fig. 8). In the Desmoinesian, because no highstand deltaics prograded across the entire shelf (Eastern Shelf), ramp and shelf-margin sediments are either carbonate or condensed marine shales. Highstand Desmoinesian deltaic lobes contain conglomeratic channel fill at the top of progradational parasequences, whereas lowstand deposits lack these deposits (Cleaves, 1993). Lowstand delta lobes appear to aggrade vertically at the delta front and delta plain, and coarser material is deposited

more proximally in the upper delta and coastal plain. An alternative explanation for the coarse fill at the top of the highstand systems tract is that the channel is actually part of overlying lowstand systems tracts in an incised-valley system. Figure 9 illustrates possible superimposition of highstand and lowstand deltaic systems tracts.

Within King County, delta facies interfinger with the carbonate ramp and platform in Bateman and Anne Tandy fields (Boring, 1993). Two large regressive and transgressive cycles are present in this area of the Knox-Baylor Trough. Tandy 5400 and Anne Tandy sandstones are in a basal cycle, and the Twin Peaks sandstone is in an upper cycle. Desmoinesian-age limestones interfinger with and transgress deltaic sediments; however, correlation is not sufficient to identify the carbonate sequences (for example, Odom, Goen, or Anson). The Tandy 5400 sandstone may be equivalent to the Hog Mountain sandstone to the east (fig. 8). The Tandy 5400 is interpreted as a distributary bar finger comprising crossbedded sandstones, whereas the Anne Tandy is a lobate delta. The Twin Peaks sandstone is thought to represent an offshore bar system (Boring, 1993). Most of this succession was previously interpreted as being deposited in deep-water conditions (Gunn, 1979). Given the regional geology gathered in this study, it appears that this succession is predominantly shallow water deltaic in origin.

Farther to the south of the area detailed in figure 8, within Taylor County, the “Gray Sandstone or Gray Interval” is time-equivalent to the Buck Creek Sandstone. The Gray Sandstone in West Tuscola field is the basal siliciclastic interval in a series that includes Gardner and Jennings intervals and is stratigraphically between the basal Caddo limestone and the upper Goen limestone (figs. 8, 10)

The facies present in the delta system at Tuscola field (Taylor County) comprise prodelta black shales; delta-front, bar-slope, burrowed, and intercalated carbonaceous sandstones with silty claystones; delta-front, bar-crest, laminated sandstones; delta-front, crossbedded coarse sandstones; delta-plain, carbonaceous shales; and shallow marine sandstones (fig. 11). Bar-crest, laminated sandstones are the main producing interval. Secondary production also comes from delta-front channels. The overall upward-shallowing succession from prodelta shales to highstand channels mimics the succession studied by Cleaves (1993) for the northern Eastern Shelf. Figure 12 illustrates core photographs of cross-laminated and rippled sandstones from the Desmoinesian deltaic facies.

Reservoir Quality

Reservoir quality in the Tuscola sandstones and siltstones ranges from 0 to 15.2 percent, with a mean of 5.3 percent. Permeability for the same units ranges from 0 to 387 md (Dutton, 1977). In deltaic sediments of the Tandy 5400 sandstone of King County, porosity averages 25 percent, and permeability ranges from 77 to 250 md. Within Tuscola field, precement porosity was approximately 22 percent; however, extensive cementation (up to 47 percent total volume of rock) substantially reduced reservoir quality. Cementation took place in several phases, starting with chlorite (minimal effect), followed by overgrowth quartz formation (major effect—50-percent porosity reduction), then calcite (major effect—40- to 50-percent further porosity reduction). After calcite cementation, the rocks were generally completely occluded. Secondary development of porosity was provided by dissolution of the calcite cement, thereby reestablishing a porosity of about 11 percent. Further dissolution of framework

grains (replaced by calcite and pristine), such as feldspar and clay clasts, appears to have augmented overall porosity by approximately 4 percent. Postdissolution cementation was limited to minor kaolinite (up to 5 percent), barite (1 percent), and, lastly, ferroan dolomite. Overall, precement porosity was similar in all coarser grained facies. Current porosity indicates that delta-front channel sandstones have the highest porosity, followed by delta-front, bar-crest facies. In general, highest porosities are found in high-energy, winnowed sandstones at the base of distributary channels and on mouth-bar crests. These facies have the largest mean grain size and the least amount of matrix and shale. Judging from isotopic and petrographic data, diagenesis of Tuscola deltaic sediments took place over a period of 300 Ma (Land and Dutton, 1978). Hydrocarbon maturation may have produced acidic fluids as a by-product of CO₂ degassing and H₂S generation, which have leached and dissolved calcite, feldspar, and rock fragments in the last 75 Ma.

MIDLAND AND DELAWARE BASINS

Siliciclastic deposition in Midland and Delaware Basins appears largely restricted to basin-center shales. No data are available about the sedimentology of these facies. In general, it appears that basin subsidence in both Midland and Delaware Basins was minimal during the early Desmoinesian (fig. 1) and increased dramatically in the late Desmoinesian (fig. 2). Therefore, regional distribution of the shales is greater in the late Desmoinesian relative to the early Desmoinesian.

DISTRIBUTION OF DESMOINESIAN SILICICLASTIC SEDIMENTS

Interpretation of Desmoinesian sedimentation patterns historically relied heavily on structural interpretation of the CBP. According to seismic and wireline-log correlations it appears that the entire CBP was transgressed and covered by carbonate sediments by the early Desmoinesian. Regional reconstructions by Tai and Dorobek (1999, 2000) show no influence by the CBP on Desmoinesian sedimentation patterns in the Midland, Delaware, or Val Verde Basin (figs. 13, 14). Desmoinesian-age sediments are relatively uniform in thickness and have a consistent aerial distribution across Delaware and Midland Basins (Van der Loop, 1990; Yang and Dorobek, 1995). Yang and Dorobek (1995) illustrated numerous cross sections of the Delaware and Midland Basins, illustrating only differential erosion of Desmoinesian sediments (lower and upper Strawn) (figs. 13, 14). Most sedimentation patterns appeared largely unaffected by uplift. A pre-Desmoinesian unconformity does exist, which results in the cutting out of variable amounts of the stratigraphic section in parts of the Val Verde Basin. Post-Desmoinesian differential uplift of blocks within the CBP resulted in erosion from Upper Pennsylvanian units down to the Precambrian basement. Desmoinesian sediments (dominantly carbonate lithologies) were pervasive across much of what would become the CBP during the Missourian to Virgilian. Major uplift of the CBP occurred during Missourian to Virgilian time.

SUMMARY OF DESMOINESIAN SILICICLASTIC SEDIMENTS

Desmoinesian siliciclastic deposition in and around the Permian Basin is even more aerielly restricted than in the Atokan. Desmoinesian siliciclastic deposition is

reciprocal with carbonate sedimentation and is largely restricted to the northern Eastern Shelf. A 2nd-order transgression appears to have dominated throughout the rest of the Desmoinesian; however 3rd- and 4th-order, high-amplitude, sea-level fluctuations occurred at a high frequency. The result was an almost interlayered carbonate and siliciclastic stacking pattern on a 3rd-order scale.

Deltaic sediments continued their westward progradation from the Fort Worth Basin farther onto the Eastern Shelf. This progradation initiated in the Atokan and was governed largely by convergence of the Ouachita thrust foldbelt to the east of the Fort Worth Basin. During the early Desmoinesian, because subsidence in the Midland Basin, Fort Worth Basin, and Eastern Shelf was minimal, siliciclastic progradation advanced to its westwardmost point (that is, Buck Creek and Dobbs Valley sandstone sequences). During the mid- to late Desmoinesian, uplift and compression of the Ouachita diminished, and subsidence of the Midland Basin accelerated. These two factors, coupled with a 2nd-order rising sea level, resulted in eastward backstepping of the clastic to carbonate transition zone and a geographical fixing of the carbonate shelf. In the Permian Basin, distal parts of the deltaic systems are the most common. Coarser grained alluvial delta feeder systems are generally farther east.

DESMOINESIAN CARBONATE DEPOSITION

Approach

Carbonate rocks of Desmoinesian age in the Permian Basin have been studied extensively in the Midland and Delaware Basins and the Northwest and Eastern Shelves. The carbonate formations of the Eastern Shelf, including the Caddo (Desmoinesian

interval), Branson Bridge, Odom, Goen, Anson, Capps, and Village Bend, span the same time interval as the carbonate Strawn Formation in Midland, Delaware, and Val Verde Basins.

General Depositional Setting

The carbonate depositional environment during the Desmoinesian was varied in style (for example, ramps, patch reefs, shelf-margins, rimmed shelves) and geographic distribution. Early Desmoinesian-age carbonates were deposited almost ubiquitously across the Permian Basin in dominantly ramp settings. In the middle to late Desmoinesian, regional subsidence patterns changed, and the Midland, Delaware, and parts of the Val Verde Basins began to subside rapidly. Along the margin of these basins, carbonates aggraded almost vertically in response to increased accommodation. The carbonate margins became more steep sided in geometry, as opposed to ramplike, and in general a true shelf margin developed and became fixed geographically. Thick accumulations of shallow-water facies, including phylloid algal mounds and grainstones, developed through time (for example, south margin of the Horseshoe Atoll). Most of the thicker Desmoinesian sections underpin later Missourian and Virgilian carbonate growth. High-amplitude and high-frequency sea-level falls exposed the Desmoinesian carbonates on numerous occasions.

Reservoir Potential and Diagenesis

Shallow-water phylloid algal bioherms, *Chaetetes* reefs, and bioclastic packstone/grainstones are the most favorable reservoir facies. Overall, phylloid algae are common and tend to dominate the bioherm community during the Desmoinesian, which is a change from the Atokan and Morrowan, when *Komia*, *Donezella*, and *Cuneiphycus*

dominated the algal assemblage. Commonly, in the Desmoinesian, primary porosity was occluded largely during early diagenesis, and present reservoir quality is related to the extent of alteration during subaerial exposure. Within the Val Verde Basin, reservoir quality is also linked to late-stage fracturing and fluid flow. Reservoir intervals are not confined to a particular facies or exposure surface but commonly exist at the top of 10- to 30-ft-thick upward-shallowing cycles. Geometry of a potential reservoir interval varies radically between different carbonate depositional settings (for example, small and ovoid for patch reefs, narrow in width but long in strike length for shelf-margin buildup). The duration of exposure events during the Desmoinesian was less than in the Missourian or Virgilian. The resulting extent of diagenetic alteration during meteoric diagenesis is often only poorly developed. One exposure event appears to be correlative across a large area and may have regional sequence stratigraphic significance. The wireline-log expression of this event is confirmable only using spectral gamma-ray logs.

MIDLAND BASIN

In the Midland Basin, data relating to the depositional style of Desmoinesian carbonates (Strawn Formation) can be taken from regional cross sections and seismic data, originally gathered and interpreted for the younger Canyon and Cisco Formations in the Horseshoe Atoll. Figure 15 illustrates the general distribution of the Strawn Formation. The infrequently termed 'lower Strawn' appears to be a regionally consistent thickness of 225 to 275 ft. This part of the Strawn interval is represented in figure 15 as the thinnest interval underlying the gray Canyon deep-water shales. Thickness estimates for the Strawn increase on the Eastern Shelf and on the Horseshoe Atoll to a maximum of

around 750 ft. Increased thickness of the upper Strawn is a response to increased accommodation caused by accelerated rates of subsidence in the Midland Basin. Regional seismic data across the Horseshoe Atoll indicate a uniform Strawn, with possible small moundlike features (fig. 16) (Waite, 1993; Saller and others, 2004). Across the Horseshoe Atoll area (including fields of Diamond M, Kelly-Snyder, Cogdell, and Salt Creek), Waite (1993) defined the Strawn as a one- to three-reflector package comprising a single 3rd-order seismic sequence. However, in the areas of increased Strawn thickness, more seismic sequences may be present, although difficult to define (Waite, 1993). More recent vintage seismic and new processing techniques indicate that there is much more internal structure within the Strawn interval in the Midland Basin (figs. 17, 18). Major differences exist on the seismic pick for the top of the Strawn (for example, Waite, 1993; Saller and others, 2004). These differences result in very different interpretations of development of the Desmoinesian carbonate succession, as well as their relationship to the overlying Missourian (Canyon) and Virgilian (Cisco) and underlying Atokan and Mississippian. Figures 19 and 20 illustrate a regional correlation based on seismic indicating that the Strawn Formation was forming topographic highs (reefs/mounds?) in response to increased accommodation. These highs are the nucleation point for later Canyon and Cisco mounds. The Strawn section, according to biostratigraphic data, is approximately 500 ft thick, composing a major part of the entire Pennsylvanian reef complex, even in the off-mound position (figs. 19, 20). The alternative interpretation indicates that Desmoinesian carbonates had little effect on overlying depositional geometries of the Canyon and Cisco (fig. 18). Given the biostratigraphic control provided from the Waite (1993) study, it appears that a substantial part of the Missourian (Canyon)

section in figure 18 is actually Desmoinesian (Strawn). Previous interpretations rarely indicate the presence of an Atokan or Morrowan interval above the Mississippian in the Horseshoe Atoll area. This Mississippian section ranges from 100 to 290 ft in thickness and is largely unconstrained biostratigraphically. According to interpretations of previous chapters, Morrowan- and Atokan-age sediments are likely to be present under the Desmoinesian-age section.

In the Kelly-Snyder region, the Strawn comprises five cycles (parasequences) that are defined using wireline logs and biostratigraphy (fig. 20). Waite (1993) considered the contact between the underlying Mississippian and the Desmoinesian (Strawn Formation) a Type 1 sequence boundary evidenced by seismic onlap of the lowermost Strawn onto a top Mississippian erosional surface (Waite, 1993). However, as evidenced in figure 19, a conformable sequence of Atokan and Desmoinesian units is inferred for part of the Horseshoe Atoll near Vealmore and Oceanic fields. The exact nature of the contact between the Desmoinesian and their underlying units is still debatable. Most wells used for correlation across the Midland Basin do not penetrate to this level, and biostratigraphic dating of this interval is lacking. The uppermost contact between the Strawn and overlying Canyon/Cisco or Wolfcampian shales is equivocal. In the Mobil #1-380 McDonnell well, facies and associated seismic signature are interpreted to indicate depositional continuity, with subtidal facies overlying grainstones and packstones (Waite, 1993) (fig. 20). An alternative interpretation for the Mobil #1-380 McDonnell well is that the Canyon A interval is a transgressive flooding interval and the top of the Strawn is a sequence boundary, although not exposed in the Kelly-Snyder area. The Strawn-Canyon contact is considered a Type 1 sequence boundary marked by

subaerial exposure outside the Permian Basin (for example, Stafford, 1959; Boardman and Barrick, 1989; Reid and Reid, 1991). On the proto-CBP, it appears that the top of the Strawn is marked by a significant exposure event (for example, Saller and others, 1999a). The regional differences in exposure of the top of the Strawn may be related to accommodation and growth rates. In a high-angle (0.25°) ramp-type system, a large sea-level fall of 20 m would displace the lowstand and shoreface 4.6 km seaward, whereas in a more platform system with steeper sides (5 to 10°), the shoreline is displaced only 228 to 112 m basinward relative to the initial point. Differences in amount of carbonate exposed during a lowstand event and subject to exposure-related diagenesis are profound (5 km vs. 200 m).

The Desmoinesian (Strawn Formation) interval in the Mobil #1-380 McDonnell well is interpreted to comprise five 4th- to 5th-order cycles in an overall 3rd-order sequence (Waite, 1993). Judging solely from the Dunham character of the rocks, the entire Strawn sequence appears to shallow upward (for example, wackestones/packstones at the base, overlain by algal packstones, and overlain by grainstones) (fig. 20). This large-scale packaging with phylloid-rich algal packstones and wackestones above mudstones/wackestones and below grainstones is the same as that identified for the Strawn in the South Andrews area, University Block 9 field (Andrews County) and St. Lawrence field (Glasscock County). However, caution must be exercised in overinterpreting the significance of facies similarities. This type of cyclicity also occurs at 4th- and 5th-order scales, and biostratigraphic and wireline-log data are required to confirm whether equivalent sections of comparable duration are truly being compared. The Strawn succession in Seminole field (Gaines County) has a similar facies-stacking

pattern; however, the entire interval studied at Seminole equates only to the lower $\frac{1}{3}$ to $\frac{1}{2}$ of the Andrews or Block 9 intervals (Mazzullo, 1983).

Studies of the South Andrews area and Block 9 field provide detailed data on facies distribution and reservoir quality of the Strawn Formation. Figure 21 illustrates a three-well correlation of Pennsylvanian facies types within Andrews County. The Strawn is subdivided into four gross packages: (1) a lower package (wackestone and spiculitic mudstone dominated), (2) a *Komia*-rich package (calcareous algae) (wackestone and bioclastic grainstone dominated), (3) a phylloid-algae-rich package (phylloid wackestone and boundstone dominated), and (4) an upper package (basal spiculitic mudstone overlain by ooid-peloidal grainstones). The contact of the Strawn and lower Canyon is considered a sequence boundary. As interpreted for figure 20, the lower Canyon basal sequence indicates a transgression (deep-water spiculitic limestones overlying grainstones) over the sequence boundary. In detail, the lower part of the Strawn (8 to 15 m thick) contains fossiliferous wackestones and spiculitic mudstones, but cycles are hard to define, and no distinct upward shallowing or deepening trends or subaerial exposure surfaces are noted (Saller and others, 1999b). Deposition of the lower Strawn package (fig. 21) is interpreted to have occurred in deep water (30 to 100 m), with grainy intervals forming as products of debris flows. The *Komia*-rich second package is divided into three upward-shallowing cycles, capped by erosion surfaces (interpreted by Saller and others, 1999b, as subaerial exposure). The *Komia* package, approximately 20 m thick in the South Andrews field area, is characteristic of shallow shelf deposition. The phylloid-algal middle Strawn package, the thickest interval at about 50 m, comprises phylloid-rich wackestones, packstones, and boundstones with corals, as well as shaly and cherty intervals. The unit

was divided into nine cycles (seven bound by subaerial exposure; Saller and others, 1999a, b). The depositional environment is thought to be shallow shelf dotted by phylloid algal mounds and intermound areas. Both upward-deepening and -shallowing cycles are present in this interval, indicating an overall grouping of facies from separate systems tracts. Saller and others (1999a, b) interpreted the cycle trends (deepening or shallowing) as reflecting dramatic sea-level rises and falls. However, diagenesis associated with exposure still appears minimal, and many of the abrupt trends could be due to autocyclic switching between mound and intermound areas. The upper Strawn package (10 to 15 m thick) consists of two cycles each, with crossbedded ooid grainstones overlying cherty (spiculitic) mudstones. Both cycles, capped by exposure surfaces, have diagenetic alteration extending 1 to 2 m below the surface. Saller and others (1999b) suggested that at least a 20-m sea-level drop had occurred from the beginning to the end of each cycle.

Identification of sequence boundaries (both higher and lower orders) and exposure events is vital to understanding and predicting the reservoir quality and diagenesis of the Strawn Formation in Midland, Delaware, and Val Verde Basins. A hierarchy of exposure events is based on data from the Strawn Formation in the Southwest Andrews area (Saller and others, 1999a, b). Four stages of diagenetic alteration linked to subaerial exposure are postulated. Stage 1 is very brief to no exposure. Stage 2 is brief to moderate exposure. Stage 3 is moderate exposure, and Stage 4 is prolonged exposure. Each stage is characterized by its distinct (1) style of alteration below the exposure surface, (2) cycle thickness, (3) position on a Fisher plot, and (4) stable isotope composition. No Stage 3 or 4 exposure was identified by Saller and others (1999a) in the Southwest Andrews field study.

The lower and middle Strawn is characterized by Stage 1 diagenesis—that is, cycles with little petrologic evidence of subaerial exposure or meteoric diagenesis. Cycles are generally thick and about 4 m (although some are thin owing to low carbonate production in deep water), and $\delta^{18}\text{O}$ and $\delta^{13}\text{C}$ compositions are heavy (marine signature) (Saller and others, 1999a, b). Figure 22 illustrates the facies character, isotope profile, and wireline-log signature of a Strawn Stage 1 event. Figure 23 is the core photographs of this same interval, on which proposed Stage 1 exposure events are marked. From the core data, it is difficult if not impossible to infer evidence of exposure at proposed boundaries. Surfaces at the proposed exposure boundaries could alternatively be interpreted as transgressive surfaces. Note that the upper, high, total gamma-ray peak (with associated high thorium) is not in a shale, but in a fusulinid wackestone. Total gamma-ray signatures and their correlations can be misleading when compared with those of the actual rock. The lower proposed exposure surface in figure 23 is even more enigmatic and difficult to identify than that of the upper surface. Overall, exposure is taking place during deposition of the Strawn Formation; however, past studies appear to have overinterpreted the extent, value, and number of these surfaces. Saller and others (1999b) proposed a total of 16 cycles for the Strawn, most of which were interpreted to be capped by a subaerial exposure surface. In general, probably four to five cycles can and should be correlated in the field and possibly regionally.

The upper Strawn Formation is characterized by Stage 2 diagenesis, with minor to moderate alteration during subaerial exposure affecting most of the cycles. Caliche crusts, soil-related mottling, and rhizoliths occur in the upper 1 m of many of the cycles (Saller and others, 1999a, b). A few small vugs and fissures are present below the exposure surfaces. Cycles are

generally thick, 3 to 8 m. Light $\delta^{18}\text{O}$ occurs at the top of the cycles and extends deeply into them, suggesting alteration by meteoric water. Light $\delta^{13}\text{C}$ is confined to the uppermost meter of Stage 2 cycles, suggesting that exposure was not intense or prolonged. Figure 24 illustrates the Stage 2 diagenetic profile at the top of the Strawn in the Parker X-1 well. Five cycle tops (each with possible exposure) were interpreted by Saller and others (1999). The exposure event at 9,452 ft, 6 inches, has no visible manifestation on the spectral gamma-ray log. The interval above the top of the Strawn is characterized by a high thorium peak, indicating exposure. The total gamma spike at 9,480 ft appears to represent a small flooding or deepening event. In the absence of spectral gamma, the exposure surface at 9,440 ft (top of the Strawn) would probably be interpreted solely as a flooding event.

Figures 25 through 27 are core photographs of the entire interval described in figure 24 for well X-1. In figure 25, the upper dark crinoidal unit corresponds to the beginning of the Canyon Formation. Note that the high thorium values on the spectral gamma ray (fig. 24) correspond only to the basal 2 ft of this unit. Note that an intervening tight packstone facies is between the upper cycle boundary and the lower cycle boundary on top of the grainstone reservoir facies (figs. 24, 25). Even with core in good condition, these exposure events are difficult to identify and in some instances may indicate only a cycle top and not an exposure event. The lowermost unit in the figure marks the beginning of the upper Strawn reservoir interval (fig. 25).

Figure 26 illustrates finer scale cycles within the reservoir zone of the X-1 well. Several small cycles within the reservoir interval are proposed and are marked by blue sawtooth lines (fig. 26). On the original core description and wireline-log diagram, these facies are not highlighted; however, porosity type and overall reservoir quality are affected

by these facies changes. The surface at about 9,470 ft denotes the top of a laminated facies (peritidal muds?), which was identified in a neighboring well within the field at the same stratigraphic position and possesses similar wireline-log characteristics. This facies may indicate that the grainstone facies of figures 24 and 26 for well X-1 may be split into two cycles, which are separated by peritidal facies. This type of observation, only possible with core data, has a bearing on the lateral and vertical homogeneity of the reservoir interval. In a well about 2 mi away from X-1, the same interval has essentially no reservoir quality largely because the facies are different. The effects of exposure and diagenesis are therefore different. Figure 27 illustrates the lower facies and cycles from figure 24, from 9,475 to 9,495 ft. Yellow boxes outlining the facies from 9,480 to 9,482 ft correspond to the 2nd-highest total gamma-ray spike in the entire Strawn interval within well X-1. Note that the gamma-ray peak is composed almost entirely of uranium and the peak does not correspond to the darkest or most “organic-rich” facies. The use of this peak as a possible maximum flooding surface (MSF) is equivocal when viewed in association with the core and further highlights that spectral gamma ray should be used for correlation, not total gamma ray.

Reservoir Quality

Reservoir quality in the Desmoinesian carbonates of the Midland Basin is controlled by facies and grain type, as well as extent of diagenetic alteration occurring during subaerial exposure. Stage 1 diagenetic intervals, as defined by Saller and others (1999a, b) are dominated by wackestones and packstones with low present porosity. Average porosity in limestones is 1.6 percent (7.5 percent of the total limestone is reservoir grade [>4 percent]). Limestone affected by Stage 2 exposure has an average

porosity of 4.3 percent (35 percent of total limestone is reservoir grade). Grainstones at the top of the cycles tend to have calcite cement filling most intergranular pores; however, dissolution of aragonitic grains has resulted in moldic secondary porosity.

Figures 24 and 26 illustrate subtler changes in porosity and permeability related to facies type. Given the core porosity and permeability and wireline-log data, the entire reservoir interval is good quality, with a maximum of 20 percent porosity and permeabilities slightly above 10 md. Within the reservoir interval's upper facies, pore types are generally moldic and microintercrystalline. Fracture and interparticle porosity appear to increase in the underlying facies with a concomitant permeability increase. The lowest facies in the reservoir interval has dominantly moldic and fracture porosity (figs. 24, 26). Figure 28 illustrates the regional architecture of the reservoir interval on the basis of core porosity of the South Andrews field area. A similar pattern also exists for the University Block 9 area. The most porous zones are present directly below the sequence boundary and exposure surface marking the Strawn to lower Canyon transition. However, the same zone is clearly only weakly developed in well V#7. This situation is linked to the fact that facies present in well V7, at that depth, are dominantly wackestones and packstones, as opposed to grainstone shoals in the other two wells. The photomicrograph illustrates the high porosity (21.5 percent) but low permeability (0.99 md) commonly found in these moldic ooid grainstone reservoirs. Also on the diagram is a violet dashed line placed above the porous zone at approximately 2,940 ft in well X#1. This proposed surface corresponds to a second regional exposure surface that appears to be present across much of the Midland Basin. Below this surface lies a reservoir interval in areas such as Seminole field (Gaines County). The facies of this

lower Strawn interval in Seminole field are similar to those described for the Southwest Andrews field area. The uppermost unit (3.7 to 6 m thick) underlying this lower (second) exposure surface is composed of grainstones bearing fragments of *Chaetetes* and *Komia* and in situ bioherms of *Chaetetes* and *Komia*. Seminole field is interpreted as an isolated patch reef similar to the Goen patch reefs of the Eastern Shelf. Reservoir quality in the grainstone section averages 13 percent porosity and 29 md permeability (maximum permeability 94 md). Average reservoir thickness is 8.5 ft. Porosity and permeability in Seminole field are linked directly to diagenesis occurring as a consequence of exposure and influx of meteoric water. Fracturing does play a role in enhancing reservoir quality of the Strawn at Seminole field (Mazzullo, 1983). Fractures are dominantly vertical, open at the hairline, and larger scale. This fracturing is related to post-Strawn deformation in the area. Products of late-burial diagenesis are also present in the Strawn Formation, mainly in the form of coarsely crystalline to saddle dolomite. Dolomitization occurs as replacements and as cement. Reservoir quality reduction due to late diagenesis appears to be minimal.

In general, depositional facies determine limestone porosity and permeability in the subsurface. Phylloid boundstones are rare, but where present, they have moderate to high porosity (4 to 17 percent) and variable but commonly high permeability (1 to 300 md). Grainstones at the top of the cycles, below subaerial exposure surfaces, are good reservoirs, but grainstones in the transgressive part of the systems tract are usually not porous. Phylloid-rich wackestones to packstones in the Strawn can have good porosity and permeability. Matrix porosity is the main type that develops during subaerial exposure. Porosity is rare and widely scattered in the lower Strawn because of limited

exposure, whereas the more grainstone dominated upper Strawn has experienced brief but significant exposure. Porosity zones in the upper parts of the cycles may be less than a few hundred meters to several kilometers across.

Within the Midland Basin, the Strawn Formation, especially the lower interval, is not as predictable as the Canyon and Cisco (Missourian and Virgilian) units in terms of lateral connectivity of porous and permeable zones (Saller and others 1999a, b). The duration of exposure events may be linked directly to establishment of better reservoir intervals. The Strawn is thought to have experienced exposure events with durations several orders of magnitude less than expected for limestones in general and the overlying Desmoinesian and Virgilian (Yang, 2001). However, this assertion does not factor in differences in facies type (susceptibility to diagenetic alteration) or accommodation issues (that is, ramp vs. platform- to shelf-type margins).

NORTHWEST SHELF

Data regarding distribution and sedimentology of Desmoinesian (Strawn Formation) carbonates on the Northwest Shelf are restricted primarily to Parkway-Empire South fields (Eddy County, New Mexico). Strawn Formation carbonates are distributed in a broad arc trending southwest-northeast across Eddy and Lea Counties, New Mexico (figs. 1, 2, 29). Figure 29 illustrates the interpretation of James (1985) for distribution of Desmoinesian carbonates. In this interpretation, Strawn Formation limestones and reservoirs are thought to comprise elongate phylloid algal mounds trending northeast-southwest. In this study, with the addition of more regional data, the width and orientation of the “mound trend” in figure 29 are expanded eastward into the area James

(1985) considered uplifted (CBP Highlands). A large carbonate platform to ramp setting dominated across the CBP and Northwest Shelf during both the early and late Desmoinesian. The true shelf edge or slope transition into more basinal facies occurred much farther to the south, in what is currently Culberson and Reeves Counties. The mound trend noted by James (1985) probably relates to single or multiple phases of eustatic change during the Desmoinesian, where water depths on the ramp reached optimal conditions for phylloid algal growth. The eustatic influence on carbonates in these ramp settings can result in superimposition of both lowstand and highstand carbonates (including bioherms) or alternatively result in a mix of facies (and reservoirs) that geographically define a wide trend but were deposited at very different times and in very different conditions. The mound trend illustrated in figure 29 is probably a result of the latter.

Figure 30 is the wireline-log signature of the Strawn Formation interval from Parkway field (Eddy County, New Mexico), which is similar in its gamma-ray profile, porosity trends, and thickness to other Strawn successions (for example, Andrews, Gaines, Yoakum, Ector, and Scurry Counties) (for example, fig. 20). The gamma-ray spike (red box) with its underlying more-porous zone (orange box) is most likely related to exposure and may be correlative across much of the Permian Basin. In the Parkway Empire field area, Strawn thickness (“clean carbonate”) isopachs define mounded to oblong structures that have a maximum 100-ft vertical dimension (James, 1985). Effective porosity (4 to 10 percent) is often greatest over the apex of the mounds in a vertical zone of 10 to 40 ft, probably indicating more alteration during exposure. However, a direct correspondence of mound shape to porosity is not present, and areas

exist where no mound is defined and a porous interval is present, and vice versa. Because a “clean carbonate” well log cutoff was used in the derivation of the maps (not core data), facies variations were probably missed, resulting in a lack of correspondence between architecture and porosity. In Humble City and Knowles fields (Lea County near Lovington, S.E., field), porous Strawn intervals are found in both crinoidal and foraminiferal debris mounds, as well as phylloid algal-*Chaetetes* bioherms (Mazzullo, 1989). These bioherms and debris mounds are small (<1.0 ×1.0 mi), generally equidimensional, with up to 75 ft of relief. Parkway Empire field, Strawn Formation, reservoirs most likely exhibit the same facies variations as those in Lea County.

Data on the Desmoinesian for the middle and southern Delaware Basin are extremely sparse. The Strawn succession in Block 16 field (Ward County) appears similar to successions in Upton and Andrews Counties.

EASTERN SHELF

The Eastern Shelf Desmoinesian succession comprises multiple carbonate units from differing depositional and geometric settings (fig. 8) (Cleaves, 2000). The following table illustrates depositional architecture, relative age, formation, and location of Desmoinesian carbonates on the Eastern Shelf.

Table 1. Relative age, formation, and location of different carbonate depositional architectures in the Eastern Shelf Desmoinesian succession.

Architecture	Relative Age	Group (Fm/Mbr)	Location
Ramp Shelf- interior banks Patch reefs	Early Desmoinesian	Lower Strawn (Caddo equivalent)	Western margin of 'Concho platform' facing the Midland Basin to the Eastern Shelf
	Middle Desmoinesian	Lower to middle Strawn (Odom) upper Strawn (Capps)	
	Middle Desmoinesian	Lower to middle Strawn (Goen) (for example, Fuzzy Creek and Pony Creek fields—Runnels and Concho Counties)	
	Late Desmoinesian	Upper Strawn (Capps)	
Shelf-margin /rimmed shelf	Late Desmoinesian	Upper Strawn (Anson Bank) (for example, Nena Lucia, Nolan County)	Eastern Shelf
Periplatform pinnacle reef (rare)	Middle-late Desmoinesian	Strawn	Parallel to Eastern Shelf and Ozona Arch area

Desmoinesian carbonate deposition on the Eastern Shelf evolved through several stages of development. Deposition started on a poorly defined carbonate ramp that graded westward from the Eastern Shelf into deeper water carbonates and areas of isolated shale deposition (Caddo and Odom Formations) (fig. 8). After deposition of Buck Creek and Dobbs Valley siliciclastic successions, the lower to middle Strawn Goen patch reefs established themselves in areas of low fluvial-deltaic input. Note that in figure 8 the extent of the Ada Sandstone is much smaller than either previous or subsequent siliciclastic depositional episodes. Rimmed-shelf and shelf-margin carbonate-bank growth started with development of the Anson Ramp (late Desmoinesian), which transformed into the true shelf-margin system of the Anson Bank. The Anson Bank

system was largely aggradational, with minor backstepping up section. The Capps limestone of the uppermost Desmoinesian appears to be a reestablishment of the Anson Bank aggradational shelf margin after a minor hiatus in carbonate deposition.

On the Eastern Shelf in Fisher, Nolan, and Coke Counties there is a series of Desmoinesian-age carbonate reservoirs (for example, Millican, Jameson, and Nena Lucia fields). The Strawn succession in Coke County (Jameson field) was divided into three units: (1) a lower unit comprising cherty limestones and thought to cover the entire Midland Basin except for topographic highs, (2) a middle massive carbonate to dark limestone with shale breaks (not present in the Midland Basin; Hopkins and Ahr, 1985), and (3) an upper buildup succession composed of shelf, reef, and back-reef facies (Hopkins and Ahr, 1985). The upper buildup succession is the producing interval at Jameson Reef field.

The tripartite system used for Strawn division on the Eastern Shelf clearly does not equate to the system used in the southwest Andrews field area (Midland Basin) (Saller and others, 1999a) or the Horseshoe Atoll (Waite, 1993). To further confuse matters, to the east of Jameson Reef field, in Concho and Runnels Counties, the proximity to siliciclastic input results in cyclic deposition of carbonates and siliciclastics throughout the Desmoinesian (fig. 8) (Marquis and Laury, 1989). In general, the Strawn interval in Jameson Reef field appears to be relatively low energy (dominated by wackestones and packstones). Grainstone cycle caps are present but very limited in distribution. Hopkins and Ahr (1985) interpreted the Jameson Reef to have formed on preexisting mud-mound accumulations, which were then colonized by *Chaetetes* and

Komia. These more-framework-type mounds coalesced into large, thicker (up to 300 m) ‘reef’ intervals.

The Strawn interval in St. Lawrence field (Glasscock County) has similarities to both the southwest Andrews field area and Seminole field of the Midland Basin (fig. 31). Two main producing zones are present in the St. Lawrence interval (one below the uppermost exposure surface, and one below the lower exposure surface, fig. 31). The lower surface is in a similar position relative to the wireline-log signature of both Seminole and Kelly-Snyder field examples. The sequence stratigraphic framework of the Glasscock “X” Fee #4 Strawn interval is interpreted to reflect a transgressive systems tract above the Atokan contact, with a possible maximum flooding surface at 9,910 ft. The highstand systems tract culminated in a 10-ft-thick crossbedded grainstone (which is the thickest producing interval in the well). A sequence boundary is inferred at the top of the grainstone, above which more open-marine, deeper water facies are noted and the overall gamma-ray signature increases. A thin lowstand systems tract may exist; however, data are equivocal. In the uppermost transgressive systems tract, sedimentation appears to have taken place largely in the open marine environment (dominated by sponge spicules, brachiopods, bryozoans, corals and echinoderms. From 9,845 to 9855 ft, dolomitization is common, as well as silicification (dissolution of sponge spicules). The dolomitized interval does not appear to have better reservoir quality than the limestones. Given the spatial proximity of the dolomitized interval to Canyon sediments, the dolomite may be associated with an undocumented sequence boundary/surface separating the underlying Strawn Formation from overlying Canyon sediments. The three major cycles below the proposed mid-upper Strawn sequence boundary are capped by higher energy facies.

These grain-rich (ooids, peloids, bioclasts) are the primary reservoir facies of the Strawn. Extensive development of exposure surfaces was indicated by Sivils (2002). However, some of these surfaces, when compared with other studies of the Strawn (for example, Saller and others, 1999a, b), are enigmatic and difficult to identify in core. The Glasscock “X” Fee #4 well in this study is interpreted to have four major cycles within the Strawn. Overall, many of the small-scale cycles noted by Sivils (2002) may not indicate upward shallowing but autocyclic switching from phylloid mound to intermound. These extremely fine scale cycles are usually only definable in a localized area. Defining the proper scale for a Strawn Formation sequence stratigraphic framework will result in better prediction of reservoir facies in other areas.

Farther eastward on the Eastern Shelf, in Runnels and Concho Counties, sedimentology and reservoir characteristics of the Desmoinesian Goen Limestone were discussed by Marquis and Laury (1989). Underlying the Goen limestone are four other Desmoinesian carbonate intervals, the Jennings, Gardner, Odom, and Caddo. Biostratigraphically the entire Eastern Shelf Desmoinesian succession (including younger Capps limestones) equates to the succession present in the Horseshoe Atoll, as well as in Andrews and Gaines Counties. The Eastern Shelf Desmoinesian succession is approximately 800 ft thick in Concho County. The Goen interval within it is approximately 70 ft thick.

The Goen limestone is considered a patch reef situated on the interior of a carbonate ramp (Marquis and Laury, 1989; Cleaves, 2000). Figure 32 is a schematic illustration of a Goen patch reef (Marquis and Laury, 1989), which comprises five facies: (1) a lower-ramp, outer subtidal zone dominated by clayey, spiculitic wackestone and

shales (>50 m water depth) and (2) a middle ramp (which also contains the foreound area) with mound-associated facies dominated by foraminiferal wackestones and packstones. Within the (3) mound community there are phylloid algal wackestones, packstones, and boundstones, with associated localized *Chaetetes* colonies. The (4) shallow-water upper-ramp facies is dominated by bryozoan-coral-green algae wackestones. (5) This facies is a very fine grained sandstone present in the middle ramp. The generalized model proposed for the Goen limestone is three upward-shallowing cycles all capped by transgressive marine mudstones and shales (Marquis and Laury, 1989). Nena Lucia field (Nolan County) represents an Eastern Shelf example of a middle to late Desmoinesian carbonate-rimmed shelf (fig. 33). The close proximity of the carbonate shelf to Desmoinesian siliciclastics (prodelta succession) results in interleaving of carbonate and siliciclastic facies. In the rimmed-shelf environment there is decided depositional relief between the shelf-margin interior and the outer shelf (fig. 33). Total carbonate thickness (Caddo+Odom+Anson Bank) ranges from about 600 ft at the shelf margin (reef) and interior (back reef) to about 300 ft on the outer shelf. The siliciclastic sequence capping the Anson Bank Formation is probably equivalent to the Brazos River Sandstone succession (fig. 8). Nena Lucia field parallels the shelf-margin crest for approximately 10 mi along depositional strike.

Reservoir Quality

Strawn reservoir quality in Jameson Reef field is different from that of Andrews, Block 9, or Seminole fields. In general, the process for causing secondary porosity is subaerial exposure, as in the other areas. However, the depositional mounded topography

resulted in uniform diagenesis across multiple facies. The coarser grained, higher energy facies (grainstones and packstones) appear to have been cemented early. The mound core facies, which are dominantly bioclastic wackestones, were subjected to more numerous and intense leaching episodes during exposure and meteoric water influx. Therefore, in more isolated reef mounds, like at Jameson, the reservoir is the structurally high, low-energy facies. These low-energy facies average 10 percent porosity but have small layers with up to 25 percent porosity.

As with the Midland Basin examples, two of the producing intervals in St. Lawrence field (Glasscock County) are associated with grain-rich facies below multiple exposure surfaces. The secondary dissolution of grains during exposure resulted in moldic and vuggy porosity. Maximum core porosity in the Strawn is 10 percent (fig. 31).

Atypically in Concho County (fig. 32), middle-ramp, shallow subtidal, foraminiferal wackestones (facies 2) and bryozoan, coral, algal wackestones (facies 4) are the reservoir intervals, whereas in other Goen patch reefs phylloid algal and *Chaetetes* boundstones and wackestones of the mound facies (facies 3) are the dominant reservoir (fig. 32). In the Concho County Goen patch reef, facies 2 reservoir quality ranges from 0.4 to 13 percent porosity (mean 2.9 percent) and 0.02 to 25 md permeability. Facies 4 reservoir quality averages 4.2 percent porosity (0.3 to 12.7 percent) and has a permeability range of 0.03 to 325 md. Facies 2 and 4 average 7.0 percent porosity in as many as six different zones (4.0 ft average thickness). Primary porosity is largely occluded by cementation. Secondary dissolution pores after phylloid algae and calcispheres are the dominant macropores. Vug and channel porosity is also important in

the reservoir and is generally the result of solution enlargement after algae dissolution. This porosity is common in the back reef (facies 4), not in the main algal mounds. Figure 34 illustrates the porosity-permeability relationship defined by Marquis and Laury (1989) for the Goen limestone, and four regions are defined on the poro/perm plot. Type IV is characterized by algal, moldic, vug channel, and fracture pores that have been significantly occluded by cementation; however, the micropores remain open. Type III is characterized by open fracture and/or stylolitic pores. Types I and II contain solution-enlarged algal moldic, vug, and channel pores. Type II differs from Type I only by having a slight occlusion of the pores, whereas in Type I, pore space is entirely open. As is obvious from figure 34, samples with Type I characteristics have the best reservoir quality.

Porosity in shelf-margin-style carbonate successions (for example, Nena Lucia field, Nolan County) is linked to dissolution of phylloid algae during subaerial exposure (fig. 33). Shelf-margin plays are better overall targets than many other Desmoinesian carbonate plays (for example, patch reefs or shelf-interior banks). The shelf-margin carbonate successions (especially on the Eastern Shelf) are generally thicker, have large lateral continuity along strike, and are easier to locate on seismic data. Also, Desmoinesian and subsequent Missourian shelf margins became largely fixed geographically by the middle Desmoinesian, resulting in a series of stacked reservoir intervals ranging from the Anson Ramp through the Missourian Palo Pinto Bank (fig. 8).

VAL VERDE BASIN

In the Val Verde Basin, identification of a productive Desmoinesian interval occurred in 1993 after drilling of the Tom Brown Inc. 49-1 ACU well. Following completion of that well, major advances in seismic acquisition and numerous 3D and 2D swath surveys resulted in development of the thrustured Strawn play (figs. 35, 36). The bulk of the data relating to the structure, sedimentology, and reservoir quality of the Strawn in the Val Verde Basin come from Terrell County and the area encompassing South Park, Deer Canyon, South Branch, ACU, and Pakenham fields (figs. 35, 36). Figure 35 illustrates a schematic representation of the thrustured Strawn reservoir style in the South Park field area. Along with the northward-thrustured Strawn interval, an underlying, unthrustured Strawn interval has been identified. This interval has not been developed yet, largely because of the drilling depths required (>15,000 ft in the Pakenham field area) and its dry-gas-only potential (Montgomery, 1996).

The area is structurally complex, and multiple interpretations have been put forward for the geometry of the thrusting. According to data from Pakenham field, the thrusting appears to have resulted in northward-verging, piggy-back thrust sheets crosscut and divided by numerous back thrusts (figs. 37, 38) (Montgomery, 1996; Newell and others, 2003). Khan and others (2002) proposed an alternative structural model based on seismic interpretation, proposing that the Strawn Formation (as well as Mississippian and Permian sections) is deformed by a single thrust sheet broken up by back thrusts and overlying possibly more deeply buried wrench-faulted pop-up structures (figs. 39, 40). The structural interpretation of this area is vitally important because the first interpretation results in multiple stacked reservoir intervals within the Strawn Formation,

whereas the later model (for example, Khan and others, 2002) results in a single Strawn target interval. A review of uninterpreted seismic from Pakenham field (fig. 41) and the wireline-log signature of the Riata Mitchell 11-1 well reveal that multiple thrust sheets of the Strawn Formation are present. However, given the size of individual thrusts (2.5 mi/4.0 km), it is likely that in other regions of the frontal thrust belt that only a single thrust package could be present and/or dominate. Structural interpretation data from Pakenham field can be compared directly with the log signature from the Riata Mitchell 11-1 well. The piggy-back nature of Strawn Formation thrust sheets resulted in two producing intervals within the Riata Mitchell 11-1 well (figs. 37, 42). The structural complexity of the thrust sheets appears to increase downward, resulting in multiple closures (fig. 43). The third Strawn interval is interpreted to back thrust in the well path of the Riata Mitchell 11-1 well, which may have resulted in migration of the hydrocarbons out of this interval (figs. 37, 42, 43). Thickness of the Strawn interval appears to increase with depth (figs. 37, 42). This increase is thought to be primarily depositional because the wireline-log character of the bottom sections of all three Strawn intervals is very similar. Juxtaposition of sediments from different facies environments would be expected in this type of structural setting. The depositional thickness changes are probably related to changes from a more outer shelf/outer ramp (for example, thin) to a more reef crest/inner ramp (for example, thick), as illustrated for Nena Lucia field in figure 33.

Sedimentological and reservoir-quality data for the Strawn succession in the Val Verde Basin comes from the South Park-Deer Canyon-South Branch complex of fields (Terrell County) (Newell and others, 2003) (fig. 36). Strawn lithofacies comprise graded

packstone to mudstone facies (lower third of the Creek Ranch #10-1 core), a very fine grained packstone to laminated wackestone facies (upper two-thirds of the Creek Ranch #10-1 core and lowest 10 ft of the Anna McClung #3-1 core), a structureless wackestone facies (lowest 10 ft of the Alex Mitchell #2-1R core), phylloid algal wackestone and packstone facies (most of the Anna McClung #3-1 and Alex Mitchell #2-1R cores), and a phylloid algal boundstone facies (top of the Anna McClung #3-1) (Newell and others, 2003) (fig. 44). These facies are arranged in multiple repetitive, shallowing, and upward-coarsening packages from 10 to 30 ft thick. The predominance of phylloid algae and other bioclasts also increases upward in each package. The boundary between the packages (cycles) is represented by a dark, laminated, poorly fossiliferous wackestone (base of next cycle) abruptly overlying the coarse phylloid algal packstone/wackestones (fig. 44). In general, cycle thickness appears to be decreasing toward the upper contact of the Strawn Formation (figs. 44 through 46).

Along with the standard facies, three breccia types were identified in the South Park-Deer Canyon-South Branch complex cores. The first breccia type is a polymict angular breccia, which is restricted to the Creek Ranch core. The second breccia is interpreted as a diagenetic pseudobreccia (fig. 45). The third breccia type is an autoclastic fitted breccia (fig. 46). Newell and others (2003) concluded that the intensity of brecciation does not have a strong correspondence to cycle boundaries. The breccias may have formed via early faulting, collapse of burrow pores, or karstic collapse (Newell and others, 2003). Atypically, cycle boundary tops show no evidence of subaerial exposure (paleosols, bird's-eye fabrics, root casts, etc.) according to Newell and others (2003). However, isotopic and textural data suggest that exposure did occur at several of the

cycle boundaries. In the Anna McClung #1-3 core, a pronounced 4-per-mil negative isotopic shift in both carbon and oxygen occurs at and below the cycle boundary at 11,062 ft (fig. 45). This isotopic excursion was interpreted by Newell and others (2003) as not indicative of exposure; however, this surface meets the geochemical criterion devised by Saller and others (1999) for at least a Stage 3 exposure surface. The texture of the “pseudobreccia” in figure 45 also appears to be diagenetic at the top of the sample, whereas the lower brecciation appears sedimentary. Overall, it does appear that the Strawn-age carbonate succession in the Val Verde Basin was subjected to subaerial exposure on several occasions. The depositional model for the Strawn Formation in the South Park-Deer Canyon-South Branch complex is a simple ramp setting, with the McClung and Mitchell cores representing shallow-water, ramp-crest, phylloid-algal buildups and debris, whereas the Creek Ranch core represents deeper water, distal-ramp facies, possibly of turbiditic origin (Newell and others, 2003).

Reservoir Quality

The diagenetic history of the Strawn succession in the Val Verde Basin is long lived and complicated (Newell and others, 2003). Intergranular and intragranular porosity (moldic) developed diagenetically early, via leaching of predominantly phylloid algae. Much of this early porosity was occluded by early and late calcite cements. The bulk of the present porosity is related to late burial diagenesis. The primary events important for the current reservoir porosity are (1) continued development of stylolites that crosscut all early diagenetic features; (2) fracturing; (3) dissolution to create moldic, vug, and enlarged fracture porosity; and (4) porosity reduction by late saddle dolomite and calcite cements (Newell and others, 2003). Fracturing and dissolution in the reservoir intervals

are linked. Moldic and vuggy pores correspond to zones of increased open and cemented fractures, and solution enlargement of pores occurred after stylolitization. The best porosity zone (up to 12 percent log values) is present in packstones and wackestones (for example, McClung core). The Creek Ranch core has virtually no porosity, which indicates that facies type played a crucial role in defining the location of the porous zones. This indication is contradictory to the assertion by Newell and others (2003) that porosity development is dominantly a secondary, late event. Porosity is slightly reduced by late calcite spar and saddle dolomite (found in 10 percent of the samples). Oil migration into the system was contemporaneous with the late-stage calcite and dolomite cementation (primary oil-filled (40+ API) fluid inclusions). Because the Strawn Formation in the Val Verde Basin is primarily a gas and condensate reservoir, the oil either migrated out of the succession or was flushed out by gas (Newell and others, 2003). This 'early' migration/flushing indicates that updip of the Strawn system, probably along thrust-fault paths, oil may have accumulated. Fluid-inclusion analysis of the saddle dolomite indicates maximum trapping temperatures of 136°C/277°F, which is approximately 45°C/113°F above the current formation temperature. Isotopic and fluid-inclusion data from dolomite and late calcite cements support a fluid origin of evolved connate, basinal, high-temperature brine. Newell and others, (2003) contended that the migration of high-temperature basinal fluids into a 'cooler' host rock (Strawn Formation) resulted in cooling-induced undersaturation of the fluid, which then leached the limestones. Overall, reservoir quality in the Val Verde Strawn succession is tied to facies-type extent of subaerial exposure and is overprinted by compression-induced fracturing followed by migration of connate, high-temperature, oil-bearing fluids.

DISTRIBUTION OF DESMOINESIAN-AGE CARBONATES

Desmoinesian-age carbonates were widespread in distribution in several different geologic settings (for example, ramps, shelf margins, patch reefs, etc.). Basin subsidence played a particularly important role in defining and changing the architecture of the carbonate depositional system in the Midland Basin. The east margin of the Midland Basin has been historically defined as the zone to the west of the Concho Arch (Galley, 1958). The Concho Arch is interpreted to trend northwest from the Llano Uplift through Concho, Runnels, Nolan, Fisher, Stonewall, and King Counties (fig. 47). In this study, given the regional data, the site for the east margin of flexure in the Midland Basin is the Fort Chadbourne Fault Zone (also referred to as the Fort Chadbourne High), which trends north-south from Schleicher to King Counties (fig. 47). There is a direct correspondence between the location of the mid- to upper Desmoinesian shelf margin and the Fort Chadbourne Fault Zone. It is proposed that downward, to-the-west flexure along this fault zone resulted in establishment of the topographic gradient that became the nucleation point for shelf-margin accretion during the mid- to late Desmoinesian and the Missourian. Continued downwarping along this flexure zone possibly impacted the distribution of facies during the Missourian.

SUMMARY OF DESMOINESIAN CARBONATE SUCCESSION

In summary several key issues come to bear on understanding Desmoinesian-age carbonates. Many of these issues have a direct bearing on exploitation of, and exploration for, new reservoirs in the Permian Basin.

1. Scale: Studies within and external to the Permian Basin need to be put into a regional sequence stratigraphic context. Several surfaces relating to 3rd-order sequences appear to be correlative within the Desmoinesian succession. The Eastern Shelf carbonate succession needs to be fully integrated and correlated into the Midland Basin. Unraveling the juxtaposed carbonate depositional motifs is required to get a true sense of facies distribution and establish relevant play trends. The use of spectral gamma-ray logs should be adopted to better correlate carbonate successions and help identify exposure surfaces.
2. Diagenesis: Reservoir development is linked to extent of subaerial exposure and to facies type. Multiple facies types can have good reservoir quality. However, shallow-water, phylloid algal bioherms generally are the best reservoirs. Structural interpretation in the Val Verde Basin appears crucial for identifying fluid-flow pathways, which controlled secondary reservoir development.
3. Structure: The currently supported structural model indicates that uplift of the Central Basin Platform was very limited during the Desmoinesian. Carbonate deposition was widespread across that area. Down-to-the west flexure along the Fort Chadbourne Fault Zone occurred during the mid- to late Desmoinesian, establishing a north-south-trending shelf margin for the remainder of the Desmoinesian and the Missourian.
4. Nomenclature: A concerted effort must be made to unify the stratigraphic nomenclature applied to Desmoinesian carbonates. The Eastern Shelf succession of Desmoinesian carbonates must be fully integrated and correlated into the Midland Basin.

DISCUSSION AND SUMMARY OF THE DESMOINESIAN IN THE PERMIAN BASIN

Within the Permian Basin, Desmoinesian siliciclastic deposition is confined to the Eastern Shelf. These siliciclastics are generally fine grained and associated with distal parts of deltaic lobes. The siliciclastics illustrated in figures 1 and 2 in Kinney and Uvalde Counties (that is, Kerr Basin) appear to have had an easterly source, but they did not migrate into the Val Verde Basin area because of a buttress provided by the carbonate platform on the paleohigh of the Devils River Uplift.

Carbonate deposition dominated the Desmoinesian and varied from shallow-water, high-energy to basinal, low-energy facies. Myriad carbonate depositional settings were present during the Desmoinesian, and a general transition from ramplike to steep-shelf margin occurred in the second half of the Desmoinesian within the Midland Basin. Defining water depths for the Desmoinesian facies is difficult. Off-platform and lower-ramp spiculitic facies can occur in water depths that range from as little as ten to hundreds of meters. This range makes defining ramp and shelf margins difficult without the use of 3D seismic. The effects of 3rd- and 4th-order sea-level falls are manifested in carbonates as subaerial exposure surfaces. These surfaces/events often control development of reservoir intervals within the Desmoinesian carbonates throughout the Permian Basin.

PALEOGEOGRAPHIC SUMMARY

Proposed distribution of early and late Desmoinesian-age sediments across the Permian Basin and surrounding areas based on interpretations that were mentioned earlier

is illustrated in figures 1 and 2. The following discussion refers to interpretations represented in those figures.

Early Desmoinesian-age siliciclastics dominated deposition only at the very periphery of the Permian Basin (primarily in the east). A thin band of marine open-shelf siliciclastics are thought to have existed in the extreme northwest corner of the Permian Basin. A tongue of marginal marine to deltaic sediments encroached on the eastern Permian Basin in Fisher County (Knox-Baylor Trough). In general, siliciclastics reached their farthest westward extent during the early Desmoinesian. The predominance of carbonate facies across most of the Permian Basin is due to (1) lack of siliciclastic supply and (2) continued overall 2nd-order rising sea level. Deep-water carbonates and carbonate and siliciclastic shales are only minor in distribution. These facies are centered in Howard, Reagan, and Reeves Counties. The early Desmoinesian carbonate succession is uniform in distribution and thickness across most of the Permian Basin. The CBP, not uplifted at this time, also possesses a blanket of carbonate sediments.

Precambrian inliers along the Matador Arch were uplifted during the Desmoinesian (for example, Bravo Dome, Roosevelt County). Carbonates appear to have dominated sedimentation around these uplifts. Siliciclastics in the Kerr Basin (for example, Kinney, Uvalde, and Zavala Counties) were sourced from the east Ouachita foldbelt. Although illustrated as alluvial to marine in figures 1 and 2, these siliciclastics are largely sedimentologically undefined. Areas of shale deposition in the northern Midland and Delaware Basin reflect ensuing subsidence of these two basins, which becomes more prominent in the late Desmoinesian.

The late Desmoinesian reflects a sedimentation pattern similar to that of the early Desmoinesian, with two notable exceptions. Basin subsidence begins in earnest during the middle to late Desmoinesian. Westward downwarping along the Fort Chadbourne Fault Zone defined the first true Permian Basin carbonate shelf margin during the Pennsylvanian. And the proto-Midland Basin was born. Concurrently the Delaware Basin continued to subside and expand, and the Val Verde Basin began to develop. The Eastern Shelf succession is represented by carbonates of the Anson Ramp to Bank succession. Carbonate development was punctuated by major siliciclastic deltaic progradation, which covered largely the same area but in general did not extend past the shelf edge of the previous cycle. Increased accommodation in areas surrounding the Permian Basin promoted aggradation of the Desmoinesian carbonates (Strawn, Anson Bank Formations). The Palo Duro Basin was characterized by shallow- and deep-water carbonate deposition. Juxtaposition of the deeper water carbonate facies of the Palo Duro and Midland Basins starts to define what is referred to as the Horseshoe Atoll. Overall, carbonate deposition dominated throughout the middle to late Desmoinesian. However, deposition was being affected by tectonic forces, which resulted in myriad carbonate environments being preserved across the Permian Basin.

KEY CONCLUSIONS

- Desmoinesian-age units in the Permian Basin reflect a continuation of 2nd-order transgression being established during the Atokan; 3rd- and 4th-order sea-level falls are crucial to development of reservoir-grade porosity in the carbonate succession.

- Desmoinesian-age siliciclastics occur primarily on the Eastern Shelf to the east of the Permian Basin. Shales within this succession can provide the regional correlation surfaces needed to integrate the Eastern Shelf mixed carbonate and siliciclastic succession into the rest of the Permian Basin.
- Siliciclastic deposition on the Eastern Shelf of the Permian Basin is dominated by distal delta-front and channel-mouth-bar facies. Coarser grained siliciclastic facies occur primarily to the east of the Permian Basin.
- Desmoinesian shallow-water carbonates were deposited over most of the Permian Basin. Carbonate deposition in the early Desmoinesian was uniform in distribution and thickness throughout the Permian Basin (including the CBP, Eastern Shelf, Val Verde Basin, and the Ozona Arch). The early Desmoinesian is characterized by ramp-like depositional settings. The middle to late Desmoinesian is characterized by a variety of carbonate depositional environments (for example, ramps, shelf/reef margins, and patch reefs). Regional analysis of Desmoinesian carbonates indicates multiple exposure surfaces and sequence boundaries, some of which appear to be correlative on a regional scale. Phylloid-algal-dominated bioherms affected by subaerial exposure and burial diagenesis compose the best carbonate reservoirs. Desmoinesian *Chaetete* reefs are also good reservoirs, being more common than in the older Atokan or younger Missourian rocks. Fracturing and late diagenesis appear crucial in reservoir development in the Desmoinesian carbonate succession of the Val Verde Basin.

REFERENCES

- Blakey, R. C., 2005, Paleogeography and geologic evolution of ancestral Rocky Mountains, *in* Geological Society of America Annual Meeting, Salt Lake City , v. 37, p. 442
- Boardman, D. R., and Barrick, J. E., 1989, Glacial-eustatic control of faunal distribution in Late Pennsylvanian strata of the Midcontinent—implications for biostratigraphy and chronostratigraphy, *in* Franseen, E. K., and Watney, W. L., eds., *Sedimentary modeling: computer simulation of depositional systems*: Kansas Geological Survey, Subsurface Geology Series, p. 79–81.
- Boring, T. H., 1993, Upper Strawn (Desmoinesian) carbonate and clastic depositional environments, Southeast King County, Texas, *in* Johnson, K. S., and Campbell, J. A., eds., *Petroleum-reservoir geology in the southern Midcontinent*, 1991 symposium: University of Oklahoma, p. 195–198.
- Cleaves, A., 1993, Sequence stratigraphy, systems tracts, and mapping strategies for the subsurface Middle and Upper Pennsylvanian of the eastern shelf, *in* Crick, R. E., ed., *American Association of Petroleum Geologists Southwest Section, Regional Meeting, Transactions*: Fort Worth Geological Society, p. 26-42.
- Cleaves, A.W., 1975, Upper Desmoinesian-lower Missourian depositional systems (Pennsylvanian), North-Central Texas: The University of Texas Austin, Ph.D. dissertation.
- Cleaves, A. W., 2000, Sequence stratigraphy and reciprocal sedimentation in Middle and Late Pennsylvanian carbonate-bank systems, eastern shelf of the Midland Basin, north-central Texas, *in* Johnson, K. S., ed., *Platform carbonates in the southern Midcontinent*, 1996 symposium: University of Oklahoma, v. 101, p. 227–257.
- Cleaves, A.W., and Erxleben, A.W., 1982, Upper Strawn and Canyon (Pennsylvanian) depositional systems, surface and subsurface, North-central Texas, *in* Cromwell, D. W., ed., *Middle and Upper Pennsylvanian System of North-Central and West Texas (outcrop to subsurface): symposia and field conference guidebook*: West Texas Geological Society, v. 82-21, p. 49–85.
- Cleaves, A. W., and Erxleben, A. W., 1985, Upper Strawn and Canyon cratonic depositional systems of Bend Arch, north-central Texas, *in* McNulty, C. I., and McPherson, J. C., eds., *Transactions of the American Association of Petroleum Geologists Southwest Section Regional Meeting*: Fort Worth Geological Society, p. 27–46.
- Dalziel, I. W. D., Lawver, L. A., Gahagan, L. M., Campbel, D. A., and Watson, G., 2002, Texas through time Plate Model, The University of Texas at Austin, Institute for Geophysics, http://www.ig.utexas.edu/research/projects/plates/movies/Texas_Through_Time_020312.ppt.
- Dutton, S. P., 1977, Diagenesis and porosity distribution in deltaic sandstone, Strawn series (Pennsylvanian), North-Central Texas: Gulf Coast Association of Geological Societies Transactions, v. 27, p. 272–277.
- Ewing, T. E., 1990, Tectonic map of Texas: The University of Texas at Austin, Bureau of Economic Geology.

- Galley, J. E., 1958, Oil and geology in the Permian Basin of Texas and New Mexico, *in* Weeks, L. G., ed., *Habitat of oil: American Association of Petroleum Geologists Special Publication*, p. 395–446.
- Gunn, R. D., 1979, Desmoinesian depositional systems in the Knox-Baylor Trough, *in* Hyne, N. J., ed., *Pennsylvanian sandstones of the Mid-continent: Tulsa Geological Society*, p. 221–234.
- Hopkins, K. W., and Ahr, W. M., 1985, Reconstruction of the paleoenvironments of Jameson (Strawn) Reef Field, Coke County, Texas, *in* Transactions of the 35th annual meeting of the Gulf Coast Association of Geological Societies AAPG regional meeting and the 32nd annual meeting of the Gulf Coast Section of the Society of Economic Paleontologists and Mineralogists, v. 35, p. 117–124.
- James, A. D., 1985, Producing characteristics and depositional environments of Lower Pennsylvanian reservoirs, Parkway-Empire South area, Eddy County, New Mexico: *American Association of Petroleum Geologists Bulletin*, v. 69, p. 1043–1063.
- Khan, A., Ferris, C., Burdick, C., and Grant, N., 2002, A look into the Val Verde Basin, Texas: *The Leading Edge*, v. 21, p. 872–874.
- Kluth, C. F., 1986, Plate tectonics of the ancestral Rocky Mountains, *in* Peterson, J. A., ed., *Paleotectonics and sedimentation in the Rocky Mountain region, United States: American Association of Petroleum Geologists*, v. 41, p. 353–369.
- Land, L. S., and Dutton, S. P., 1978, Cementation of a Pennsylvanian deltaic sandstone: isotopic data: *Journal of Sedimentary Research*, v. 48, p. 1167–1176.
- Marquis, S. A., and Laury, R. L., 1989, Glacio-eustasy, depositional environments, diagenesis, and reservoir character of Goen Limestone cyclothem (Desmoinesian), Concho Platform, central Texas: *American Association of Petroleum Geologists Bulletin*, v. 73, p. 166–181.
- Mazzullo, S. J., 1983, Lower Strawn reservoir, Seminole S.E. Field, Midland Basin, Texas, *in* Shaw, R. L., and Pollan, B. J., eds., *Permian Basin Cores—a workshop: Permian Basin Section, SEPM*, v. 2, p. 69–93.
- Mazzullo, S. J., 1989, Subtle traps in Ordovician to Permian carbonate petroleum reservoirs, Permian Basin: an overview, *in* Search for the subtle trap: hydrocarbon exploration in mature basins: *West Texas Geological Society*, v. 89-85, p. 155–180.
- Montgomery, S. L., 1996, Val Verde Basin; thrusting Strawn (Pennsylvanian) carbonate reservoirs, Pakenham Field area: *American Association of Petroleum Geologists Bulletin*, v. 80, p. 987–998.
- Newell, K. D., Goldstein, R. H., and Burdick, C. J., 2003, Diagenesis and late-stage porosity development in the Pennsylvanian Strawn Formation, Val Verde Basin, Texas, U.S.A., *in* Ahr, W. M., Harris, P. M., Morgan, W. A., and Somerville, I. D., eds., *Permo-Carboniferous carbonate platforms and reefs: Society for Sedimentary Geology (SEPM)*, v. 78, p. 333–350.
- Reid, A. M., and Reid, S. T., 1991, A postmortem of the Cogdell Field, Horseshoe Atoll, Midland Basin, Texas, *in* Candelaria, M. P., ed., *Permian Basin plays: tomorrow's technology today: West Texas Geological Society*. p. 39–66.
- Saller, A. H., Dickson, J. A. D., and Matsuda, F., 1999a, Evolution and distribution of porosity associated with subaerial exposure in upper Paleozoic platform

- limestones, West Texas: American Association of Petroleum Geologists Bulletin, v. 83, p. 1835–1854.
- Saller, A. H., Dickson, J. A. D., Rasbury, E. T., and Ebato, T., 1999b, Effects of long-term accommodation change on short-term cycles, upper Paleozoic platform limestones, West Texas, *in* Harris, P. M., Saller, A. H., and Simo, J. A., eds., Advances in carbonate sequence stratigraphy; application to reservoirs, outcrops and models: Society for Sedimentary Geology (SEPM), v. 63, p. 227–246.
- Saller, A. H., Walden, S., Robertson, S., Nims, R., Schwab, J., Hagiwara, H., and Mizohata, S., 2004, Three-dimensional seismic imaging and reservoir modeling of an upper Paleozoic “reefal” buildup, Reinecke Field, West Texas, United States, *in* Eberli, G. P., Masafarro, J. L., and Sarg, J. F. R., eds., Seismic imaging of carbonate reservoirs and systems: American Association of Petroleum Geologists, v. 81, p. 107–122.
- Shannon, J. P., and Dahl, A. R., 1971, Deltaic stratigraphic traps in West Tuscola field, Taylor County, Texas: American Association of Petroleum Geologists Bulletin, v. 55, p. 1194–1205.
- Sivils, D. J., 2002, Reservoir characterization of the Strawn Formation (Desmoinesian) for the St. Lawrence Field, Glasscock county, Texas, *in* American Association of Petroleum Geologists Southwest Section Meeting Transactions: Ruidoso, New Mexico, p. 193–197.
- Stafford, P. T., 1959, Geology of part of the Horseshoe atoll in Scurry and Kent counties, Texas: U.S. Geological Survey Professional Paper P 0315-A.
- Tai, P. -C., and Dorobek, S. L., 1999, Preliminary study on the late Paleozoic tectonic and stratigraphic history at Wilshire Field, central Upton County, southwestern Midland Basin, West Texas, *in* Grace, D. T., and Hinterlong, G. D., eds., The Permian Basin: providing energy for America: West Texas Geological Society, v. 99-106, p. 19–29.
- Tai, P. -C., and Dorobek, S. L., 2000, Tectonic model for late Paleozoic deformation of the Central Basin Platform, Permian Basin region, West Texas, *in* DeMis, W. D., Nelis, M. K., and Trentham, R. C., eds., The Permian Basin: proving ground for tomorrow’s technologies: West Texas Geological Society, v. 00-109, p. 157–176.
- Van der Loop, M., 1990, Amacker-Tippett Wolfcamp Field, Upton County, Texas, *in* Flis, J. E., and Price, R. C., eds., Permian Basin oil and gas fields: innovative ideas in exploration and development: West Texas Geological Society, v. 90-87, p. 133–151.
- Waite, L. E., 1993, Upper Pennsylvanian seismic sequences and facies of the eastern and southern Horseshoe Atoll, Midland Basin, West Texas, *in* Loucks, R. G., and Sarg, J. F., eds., Carbonate sequence stratigraphy; recent developments and applications: American Association of Petroleum Geologists, v. 57, p. 213–240.
- Yang, K. -M., and Dorobek, S. L., 1995, The Permian Basin of West Texas and New Mexico: tectonic history of a “composite” foreland basin and its effects on stratigraphic development, *in* Dorobek, S. L., and Ross, G. M., eds., Stratigraphic evolution of foreland basins: SEPM (Society for Sedimentary Geology), v. 52, p. 149–174.

- Yang, W., 2001, Estimation of duration of subaerial exposure in shallow-marine limestones: an isotopic approach: *Journal of Sedimentary Research*, v. 71, p. 778–789.
- Ye, H., Royden, L., Burchfiel, C., and Schuepbach, M., 1996, Late Paleozoic deformation of interior North America; the greater ancestral Rocky Mountains: *American Association of Petroleum Geologists Bulletin*, v. 80, p. 1397–1432.

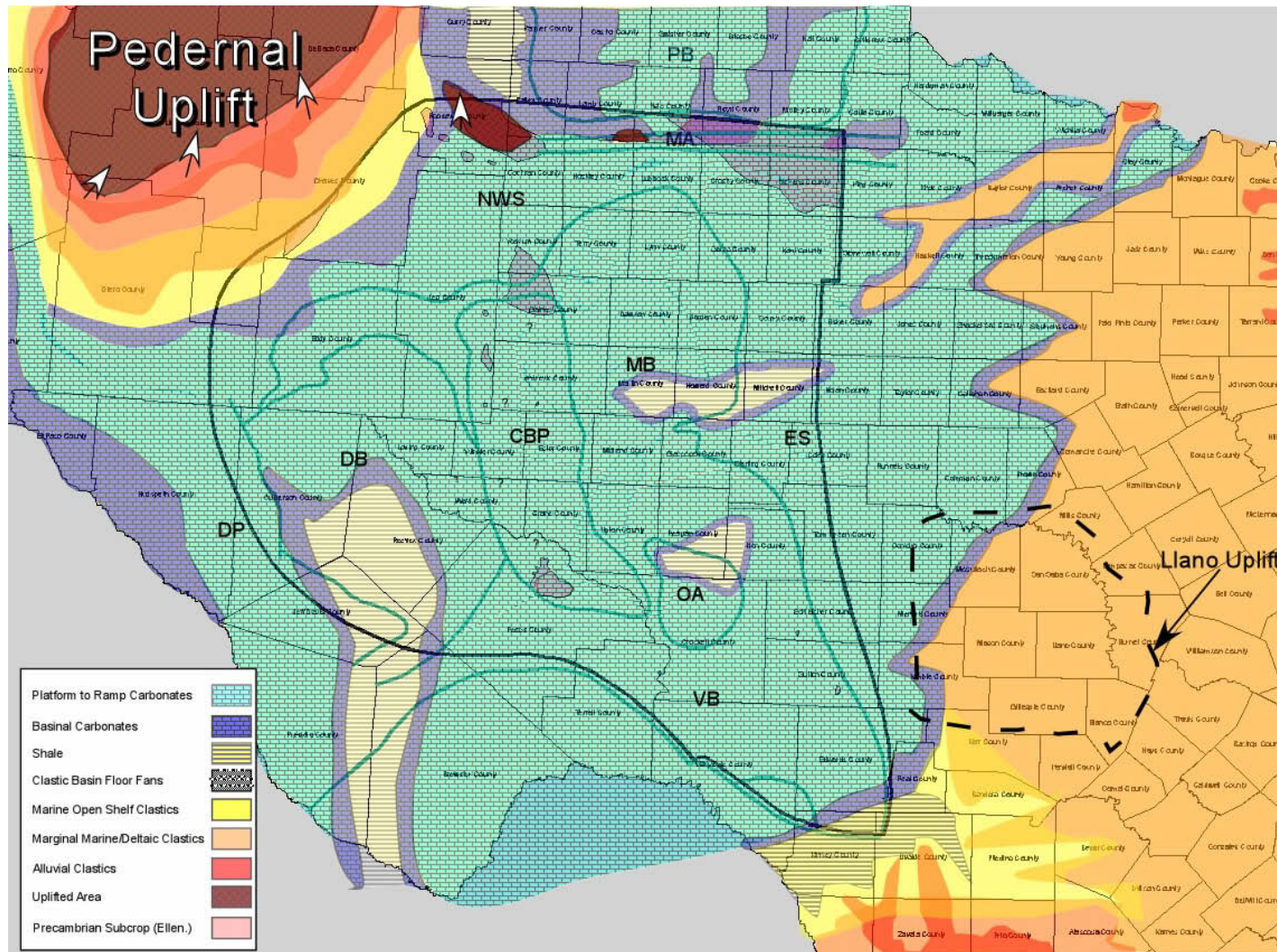


Figure 1. Early Desmoinesian paleogeography and facies distribution map of the greater Permian Basin region. The illustration is based on a time-slice equivalent of the lower Desmoinesian Caddo and early Odom limestone depositional event. Major subregions (outlined in dark green): CBP = Central Basin Platform, DB = Delaware Basin, DP = Diablo Platform, ES = Eastern Shelf, MA = Matador Arch, MB = Midland Basin, NS = Northwest Shelf, OA = Ozona Arch, PB = Palo Duro Basin, VB = Val Verde Basin. The orange siliciclastic zone centered on Knox and Baylor Counties corresponds to the Knox-Baylor Trough. The Fort Worth Basin is centered on Wise County. All geometries are schematic only and may not correspond to actual size or distribution. Llano Uplift area outlined by black dashed line. Sizes of arrows surrounding the Pedernal and other uplifted areas correspond to relative amount of uplift (that is, larger arrow, greater relative uplift).

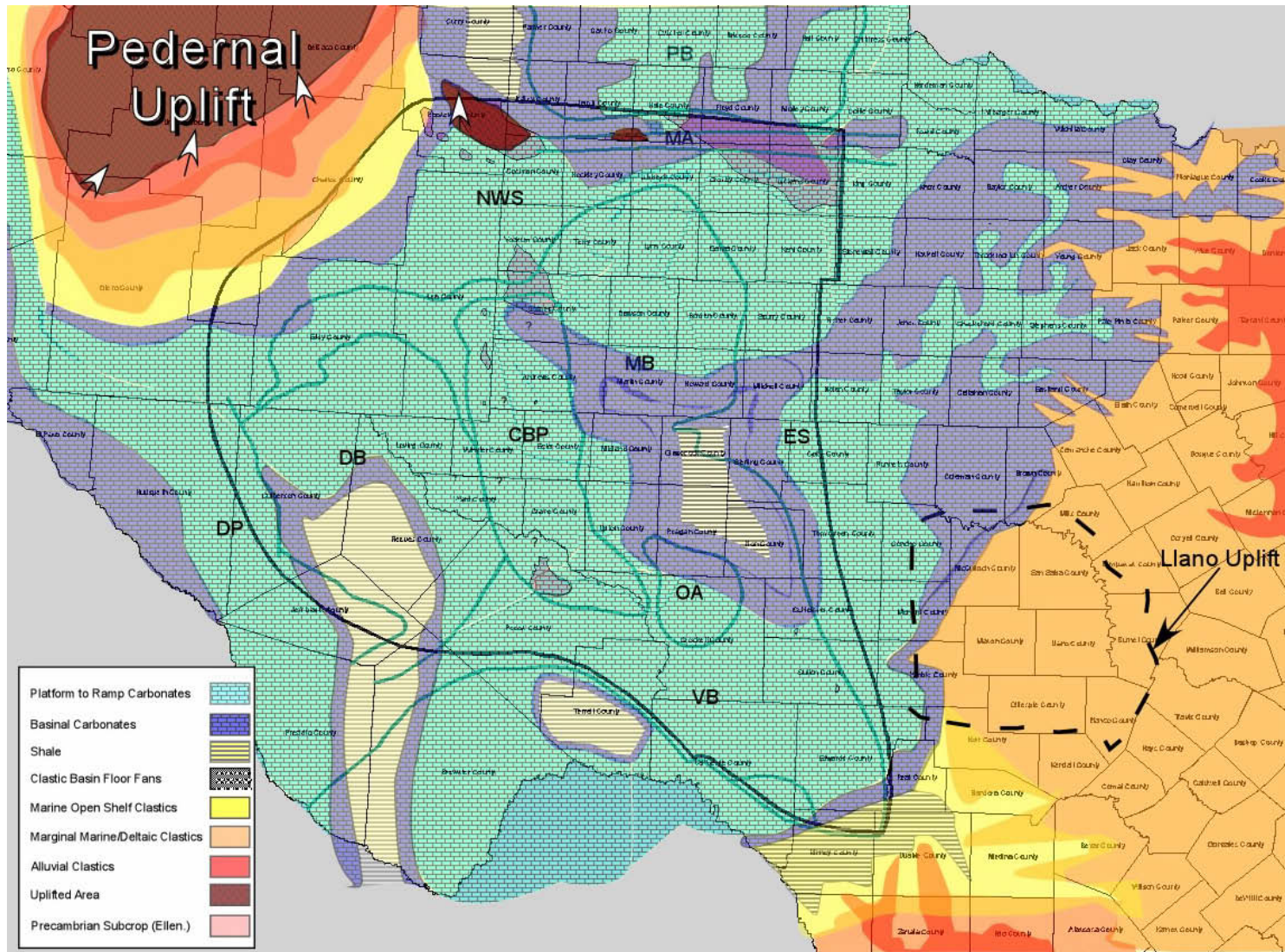


Figure 2. Late Desmoinesian paleogeography and facies distribution map of the greater Permian Basin region. The illustration is based on a time-slice equivalent of the upper Desmoinesian Anson Bank limestone depositional event. Major subregions (outlined in dark green): CBP = Central Basin Platform, DB = Delaware Basin, DP = Diablo Platform, ES = Eastern Shelf, MA = Matador Arch, MB = Midland Basin, NS = Northwest Shelf, OA = Ozona Arch, PB = Palo Duro Basin, VB = Val Verde Basin. The orange siliciclastic zone centered on Knox and Baylor Counties corresponds to the Knox-Baylor Trough. The Fort Worth Basin is centered on Wise County. All geometries are schematic only and may not correspond to actual size or distribution. Llano Uplift area outlined by black dashed line. Sizes of arrows surrounding the Pedernal and other uplifted areas correspond to relative amount of uplift (that is, larger arrow, greater relative uplift).

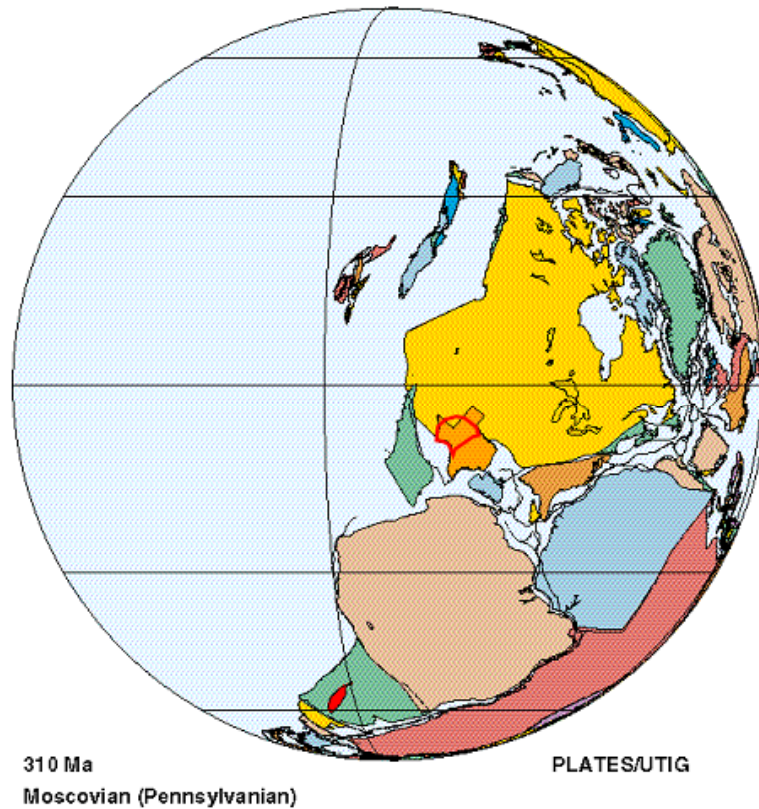


Figure 3. Atokan- to Desmoinesian-age (circa 310 Ma) Texas plate tectonic reconstruction. Note the marine (light-blue) to continental (light-orange) transition, which occurs across Texas (dark-orange) in the area of the Permian Basin. Suturing of the continents has resulted in partly restricted marine subbasin between the plates. Diagram modified from Dalziel and others (2002). The Permian Basin has migrated north (that is, more equatorial) relative to its Morrowan/Atokan position.



Figure 4. Permian Basin outline (dashed red) and major geologic features. Many of the features were developing during the late Desmoinesian. Compare figure 4 with figures.5 through 7 for previous models of facies distribution relative to the basin outline. Figure 1 illustrates facies distribution in the greater Permian Basin area derived from this study. The west margin of the Forth Worth Basin runs north-south through Palo Pinto County.

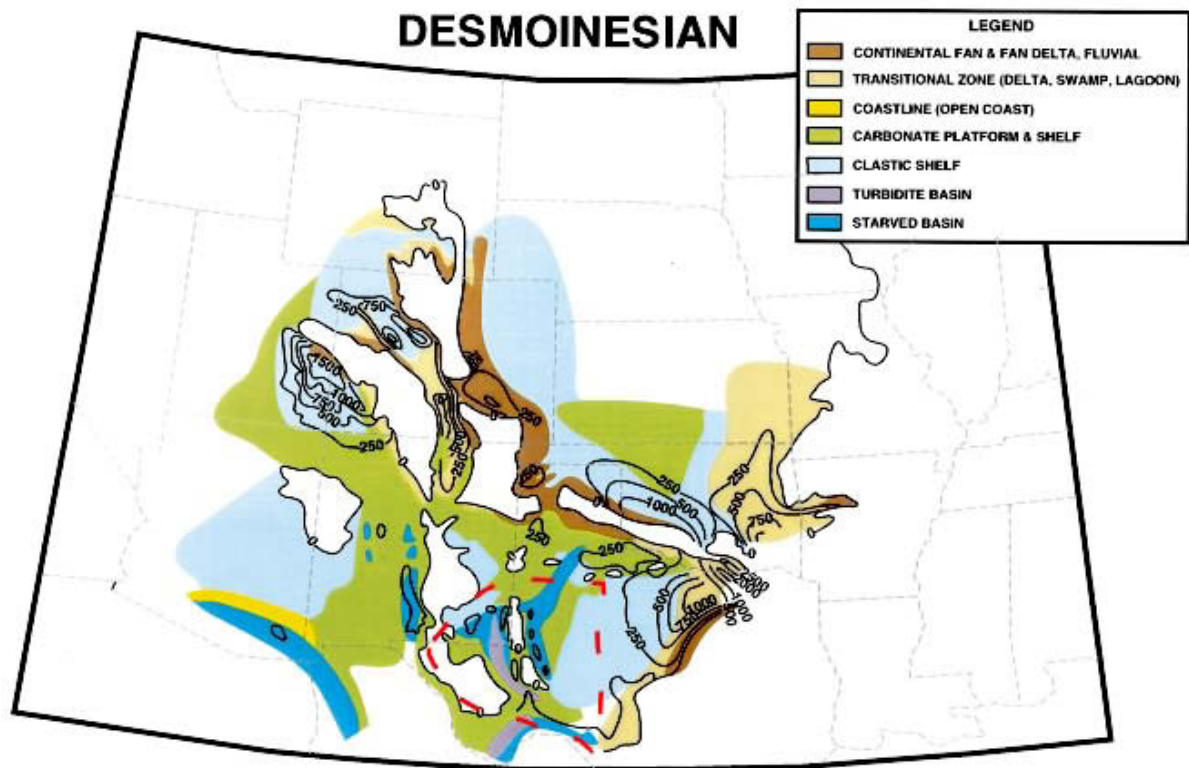


Figure 5. Generalized Rocky Mountain Region and Southern Midcontinent Desmoinesian Paleogeography (from Ye and others, 1996). White areas indicate either nondeposition or erosion (not clarified in original text). The Permian Basin is outlined by the dashed red polygon. Note that the Permian Basin is split into the Delaware and Midland Basins in this representation. The centers of both Midland and Delaware Basins are thought to be starved of sediment or to contain deep-water turbidite facies. Each of the basins is largely rimmed by carbonate-platform to shelfal sediments. A small siliciclastic shelf is represented near the Pedernal Uplift area, and a large siliciclastic shelf dominates most of the Eastern Shelf and Llano Uplift area. One major difference between figures 5 and 6 is the large uplifted areas spanning most of the Diablo Platform and western Delaware Basin. Refer to figure 4 for localities of major geologic features in the greater Permian Basin.

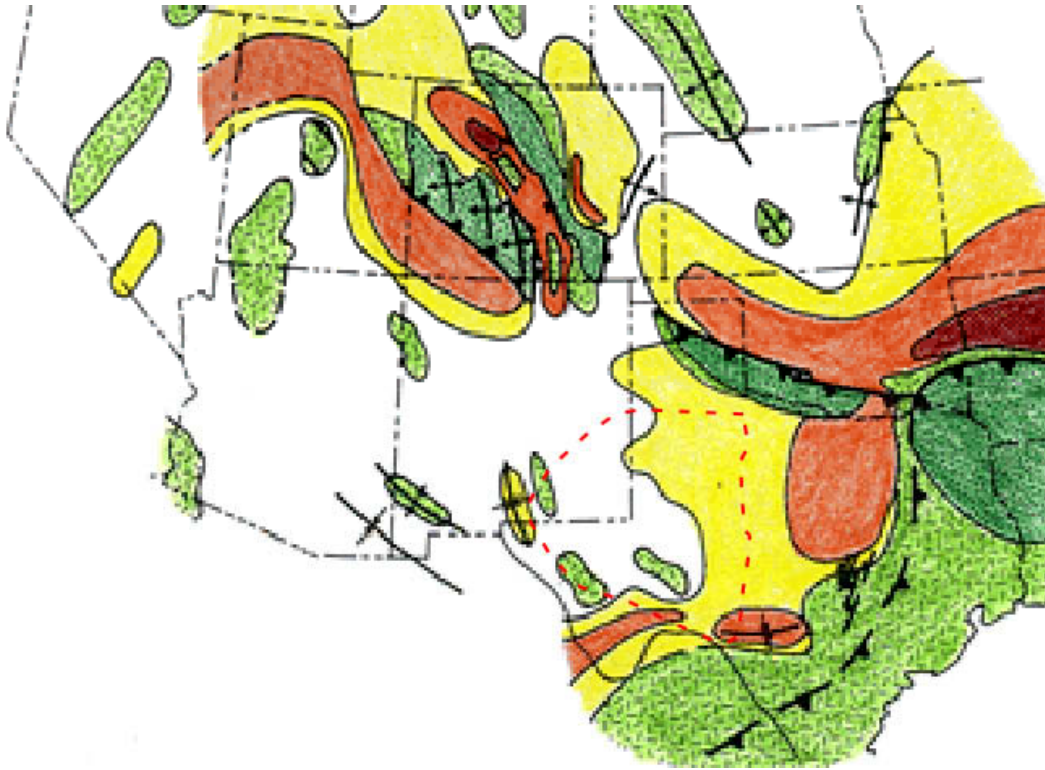


Figure 6. Areas of net subsidence (white $< 50\text{m/Ma}$ to red $> 300\text{m/Ma}$) and net uplift (light-green $< 50\text{m/Ma}$) for the Atokan Series (after Kluth, 1986). Permian Basin outlined by red dashed polygon. Kluth (1986) indicated that the south part of the Central Basin Platform area is uplifting along with the Diablo Platform area. All other areas, along with the Permian Basin, are undergoing net subsidence ranging from less than 50m/Ma in the Delaware Basin to more than 300m/Ma in the Val Verde and Fort Worth Basins.

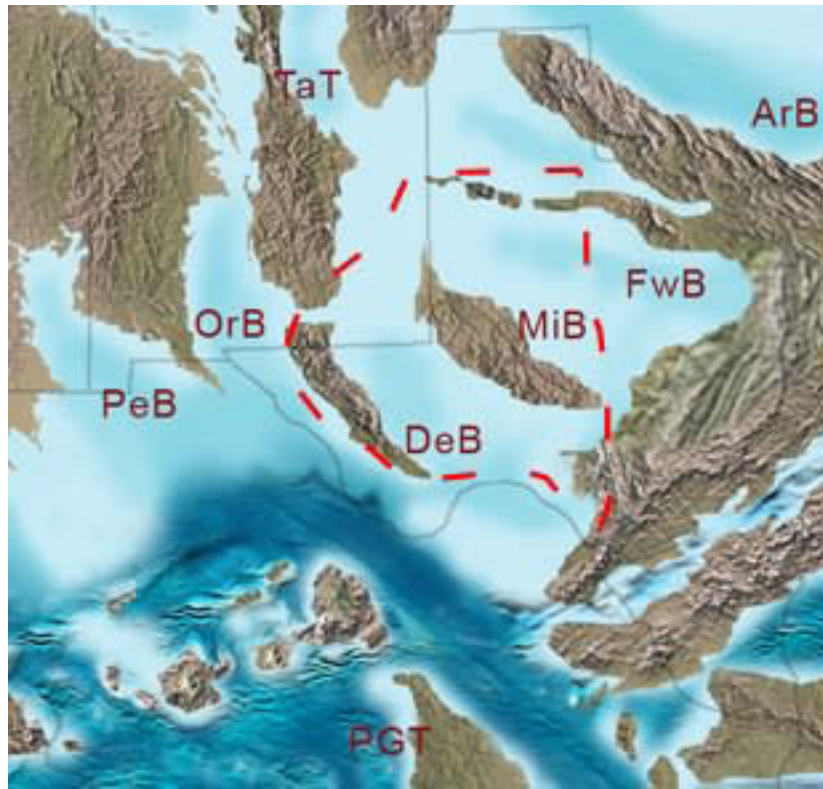


Figure 7. Regional paleogeography of the Desmoinesian (circa 310 Ma). DeB and MiB = Delaware and Midland Basins, respectively. Permian Basin outlined by red dashed polygon. ArB = Anadarko Basin, FwB = Fort Worth Basin, OrB = Orogrande Basin, PeB = Pedregosa Basin, TaT = Taos Trough. Uplifted areas represented by browns, shallow marine by light- to medium-blues, and deep marine by dark-blue (from Blakey, 2005). Prominent differences in uplifting and subsiding areas when compared with those of figure 6, especially with respect to eastern and southeastern New Mexico and location of Pedernal Uplift and Central Basin Platform.

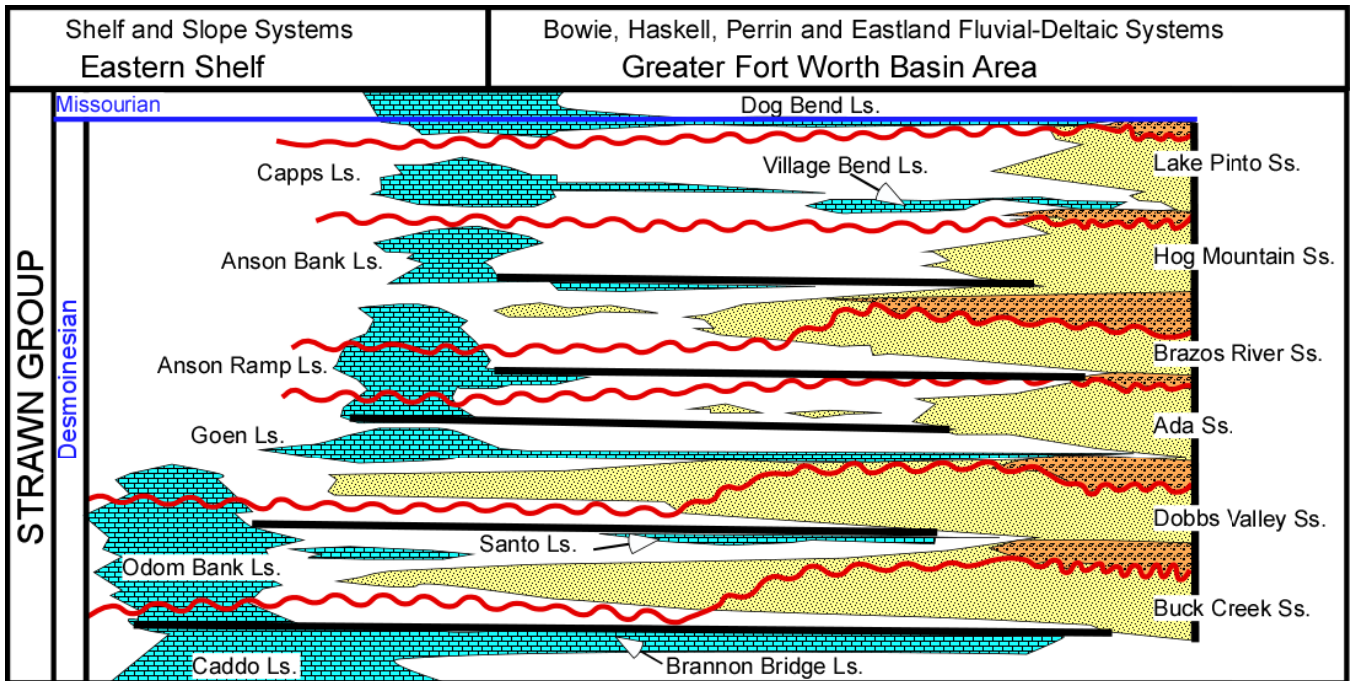


Figure 8. Regional schematic representation of the Desmoinesian-age Strawn group on the Eastern Shelf and the greater Fort Worth Basin area (modified from Cleaves, 1993, 2000). Red irregular lines are major sequence boundaries, and solid straight black lines are regional maximum flooding surfaces. Siliciclastic and carbonate sediments are represented by a series of at least six cyclic packages. The basal two packages, which include the Caddo and Brannon Bridge limestone to Buck Creek sandstone and the Odom Bank limestone and Dobbs Valley sandstone, extend the farthest west into the Permian Basin.

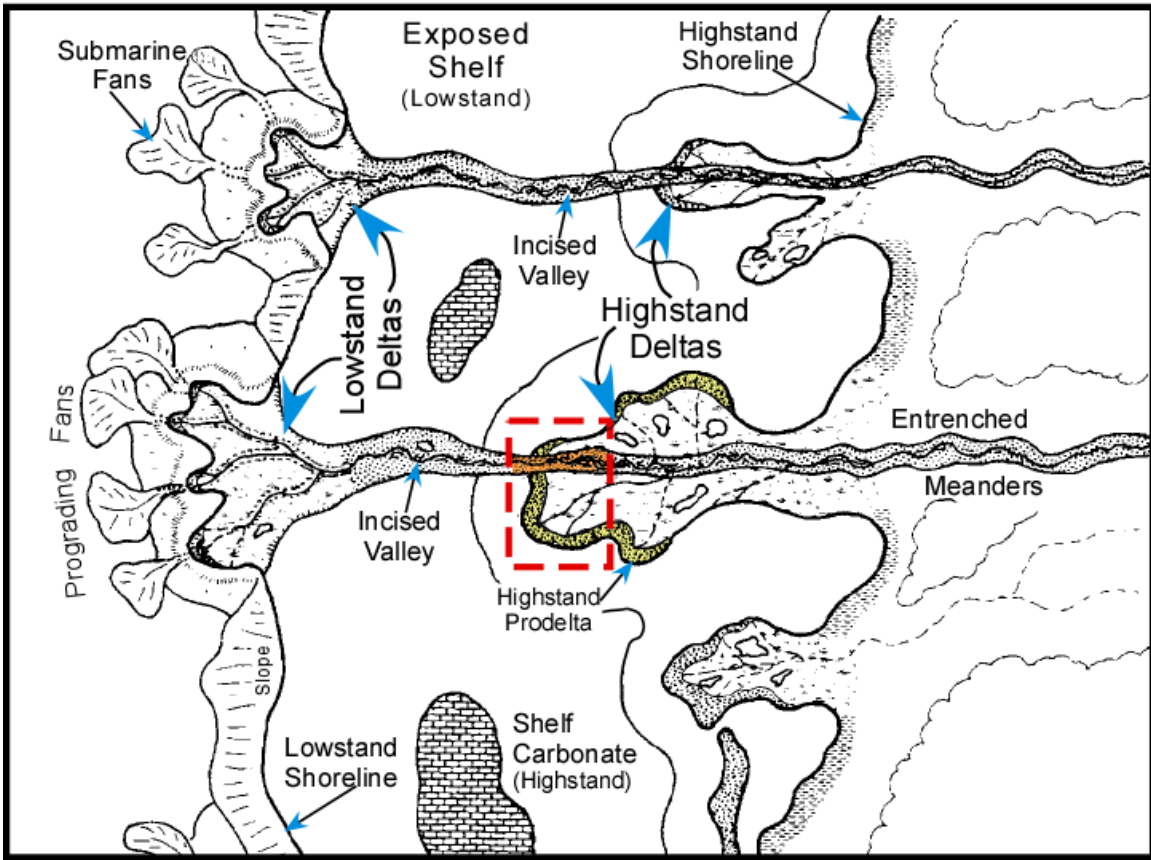


Figure 9. Schematic diagram illustrating possible superimposition of facies when a lowstand deltaic system progrades and downcuts across a highstand delta (after Cleaves, 1993). Red dashed box highlights an area of lowstand channel deposits incising into underlying delta-front bar crest and slope. This area may be analogous to Tuscola field (Taylor County) in figure 10.

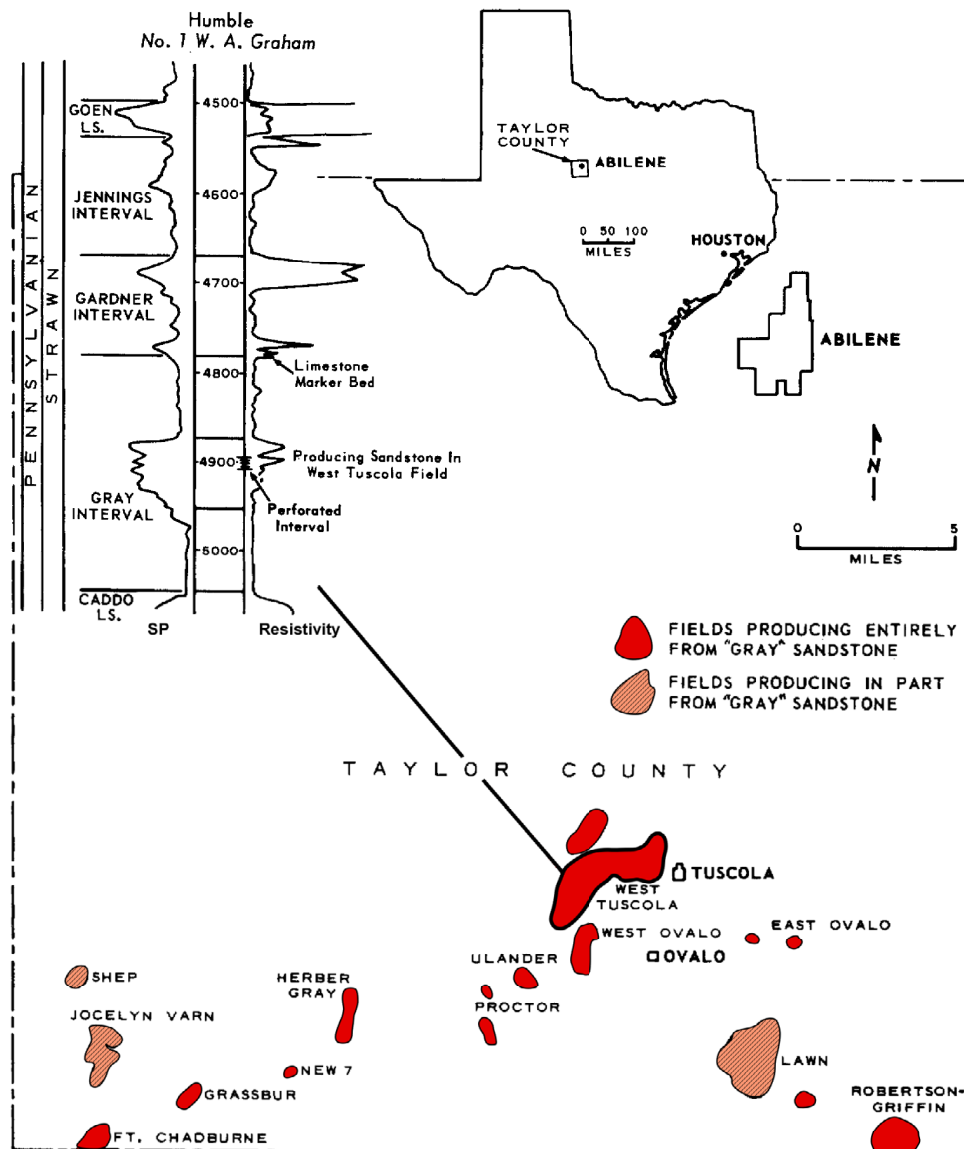


Figure 10. SP- and resistivity-log signature of southern Eastern Shelf siliciclastic interval (after Shannon and Dahl, 1971). 'Gray' producing zone comprises delta-front sediments. West Tuscola field is part of an elongate depositional trend that strikes toward Nolan and Coke Counties in the Permian Basin.

W

E

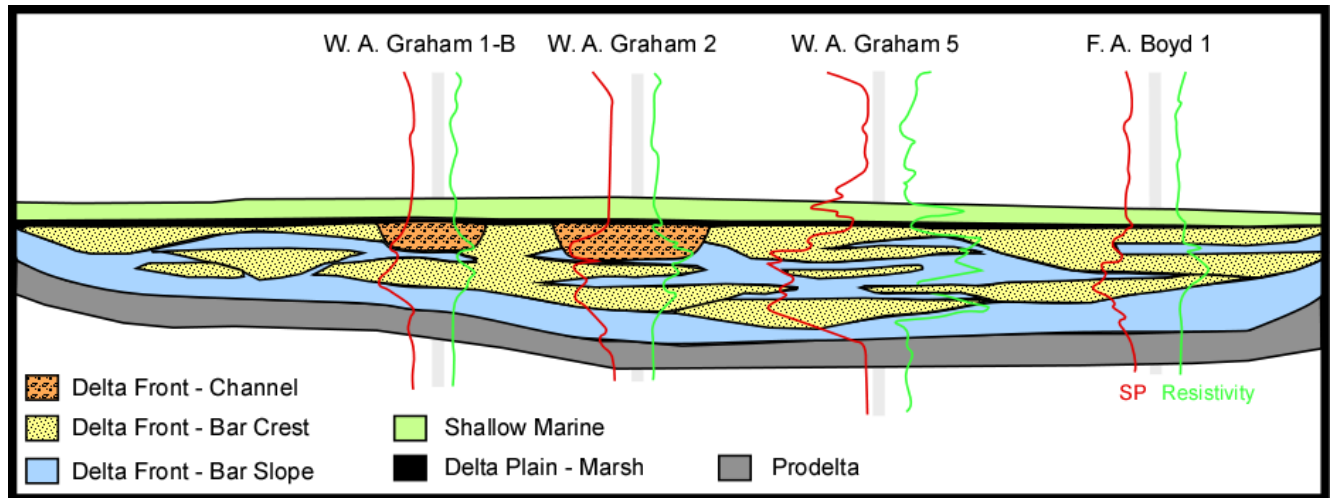


Figure 11. West-east, strike-oriented cross section of the 'Gray Interval,' West Tuscola field, Taylor County (after Shannon and Dahl, 1971). Entire thickness represented by wireline logs approximately 195 ft. The schematic representation of superimposed lowstand channels on a highstand delta in figure 9 may be representative of this field.

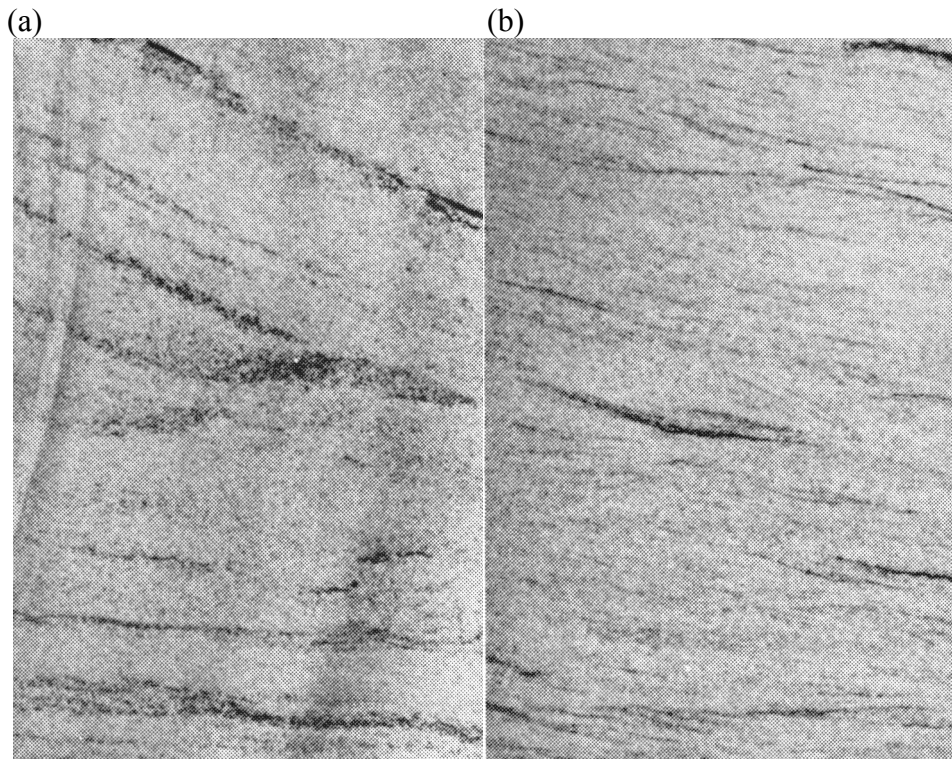


Figure 12. Core photographs of crossbedded and ripple-laminated deltaic facies of the 5,400-ft Anne Tandy Sandstone (Y-22-A, Anne Tandy field, King County). Modified from Gunn (1978). (A) Crossbedded sandstone 5,396 ft. (B) Ripple-laminated sandstone 5,405 ft. Core width is 2.25 inches. Porosity of these facies averages 25 percent, and permeability ranges from 77 to 250 md.

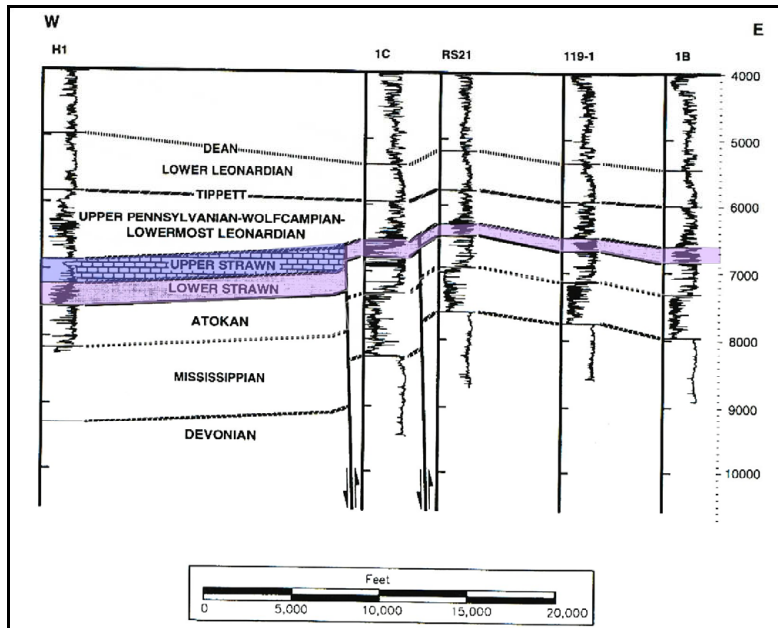


Figure 13. West-east structural cross section of 3D seismic grid over Wilshire field (Upton County). W2 cross section modified from Tai and Dorobek (1999). Note the Desmoinesian Strawn Formation highlighted in purple and blue, which shows thickness changes related to later differential erosion.

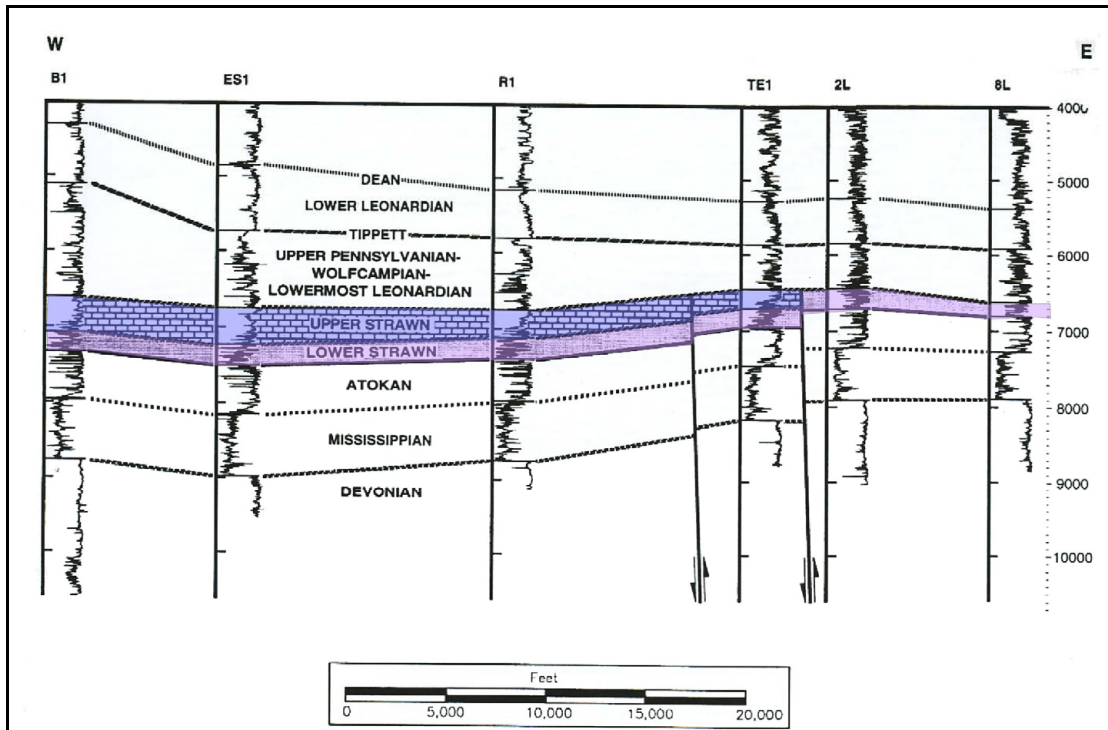


Figure 14. West-east structural cross section of 3D seismic grid over Wilshire field (Upton County). W3 cross section after Tai and Dorobek (1999). Note the Desmoinesian (Strawn Formation) highlighted in purple and blue, which shows differential erosion, not thickness changes, related to deposition.

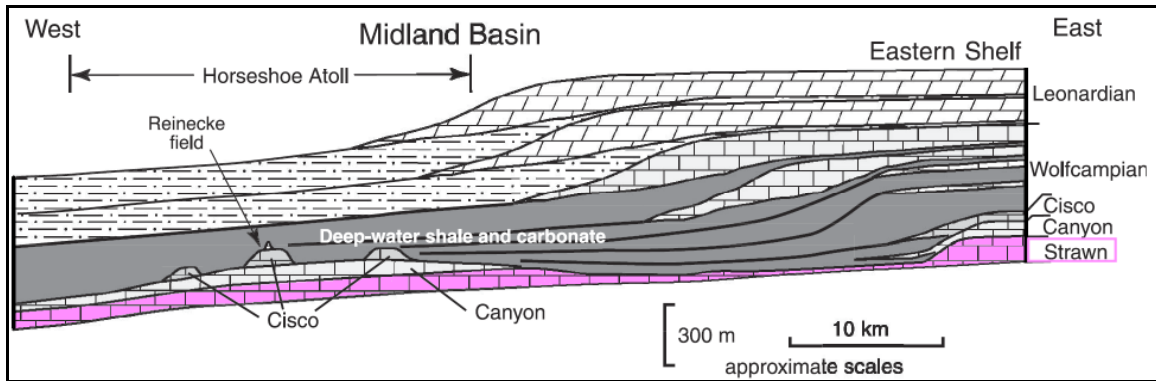


Figure 15. Regional conceptual diagram of Pennsylvanian and Permian facies distribution from the Midland Basin in the west eastward to the Eastern Shelf. After Saller (2004). Strawn interval highlighted in purple. Note that the thinnest part of the Strawn is still approximately 225 ft thick. The thinnest interval of the Strawn is the 'lower' Strawn of Waite (1993).

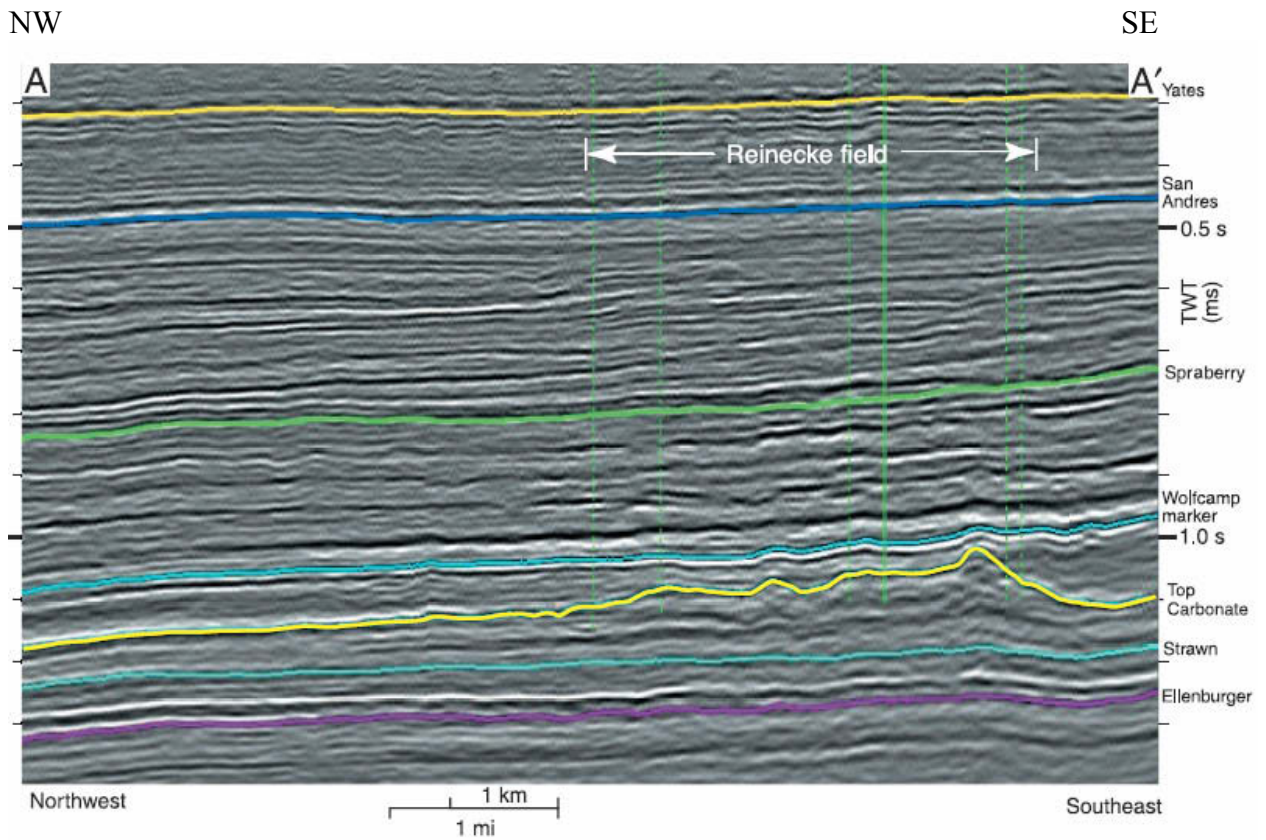


Figure 16. Regional NW-SE seismic cross section of Pennsylvanian and Permian facies distribution from Reinecke field area (Borden County) in the Midland Basin. After Saller (2004). Top of Strawn interval highlighted in cyan. Seismically the Strawn Formation is uniform in thickness. The high-amplitude reflection in the base of the Strawn to Ellenburger interval is either the Atokan Shales or the Mississippian Barnett Formation. The thinnest part of the Strawn is still approximately 225 ft thick. Orientation of line A-A' illustrated in figure 17.

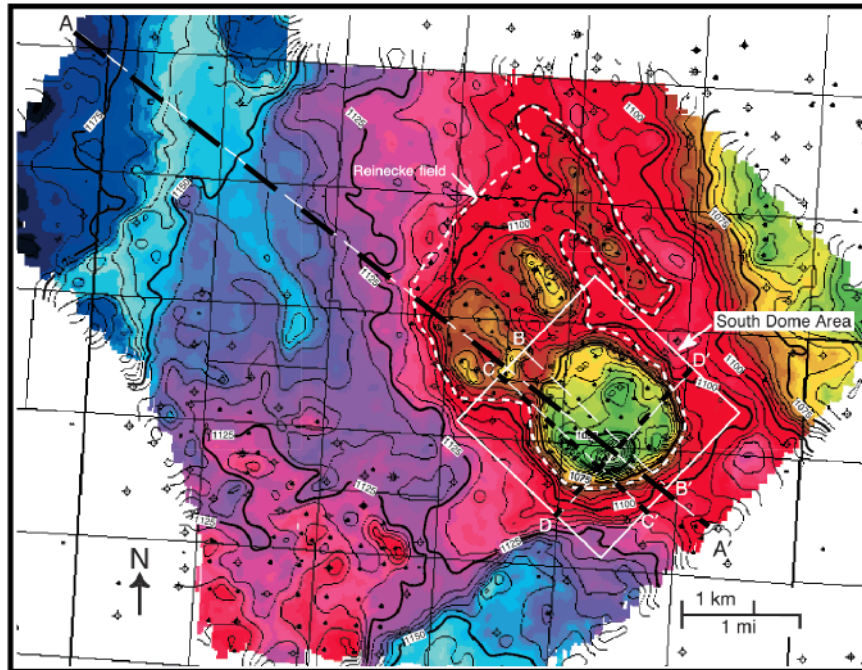


Figure 17. Seismic structure map of the Upper Pennsylvanian-lowest Permian carbonate across Reinecke field at 5-ms contours. Seismic lines A-A' (Figure 16), C-C' and D-D' (figure 18) illustrated by thick dashed black line. All three seismic cross sections go through main mound area and have data down to the Ordovician (Ellenburger).

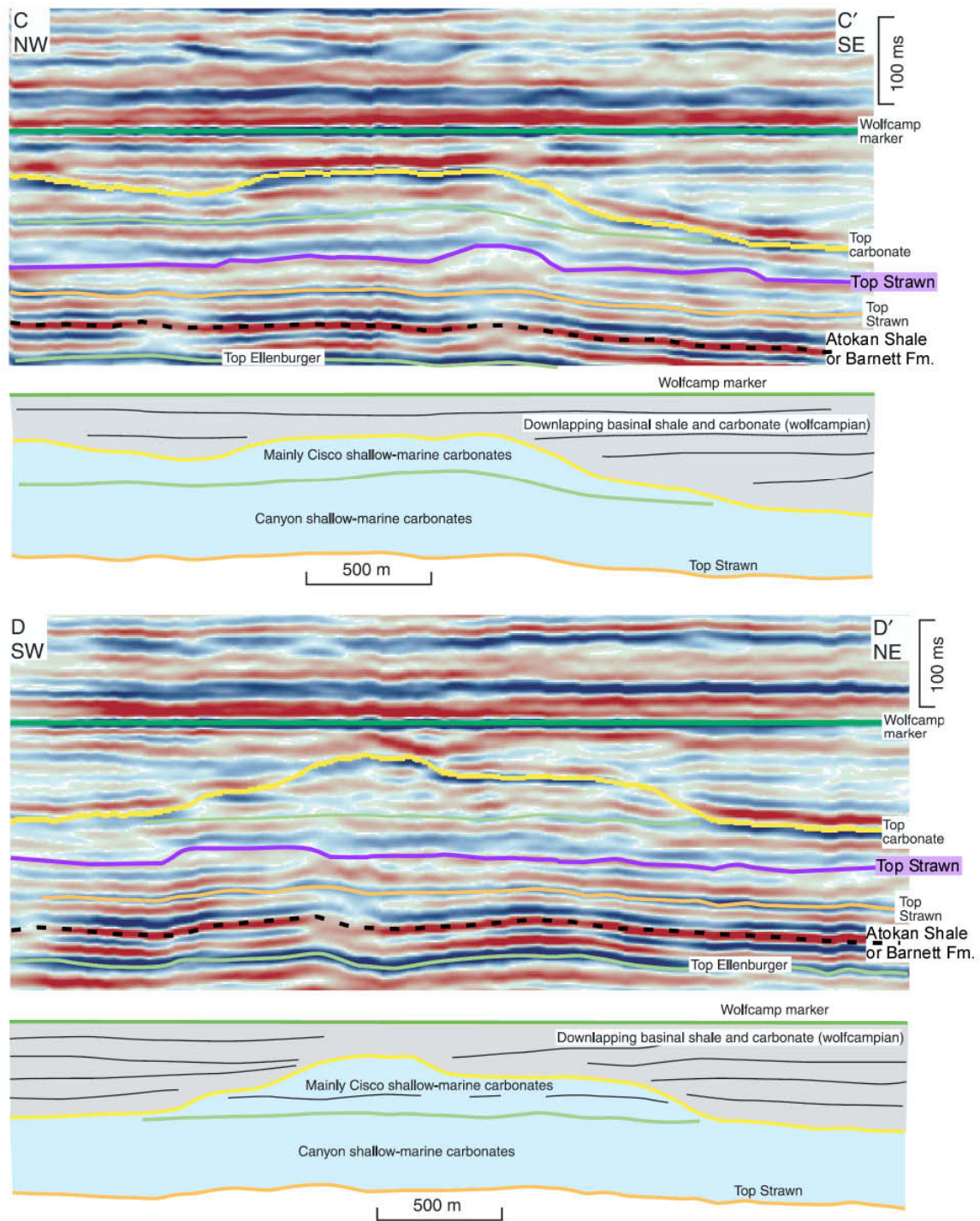


Figure 18. NW-SE (C-C') and SW-NE (D-D') seismic sections of Reinecke field After Saller (2004). For section orientation, see figure 17. On each seismic line, original interpretations of Saller and others (2004) are present, as well as new interpretations from this study. Revised top of Strawn indicated by purple line and proposed Atokan shale or Barnett Formation indicated by dashed black line. Interpreted shale underlying the Strawn Formation equivalent to high-amplitude reflector between Ellenburger and Strawn picks on figure 16.

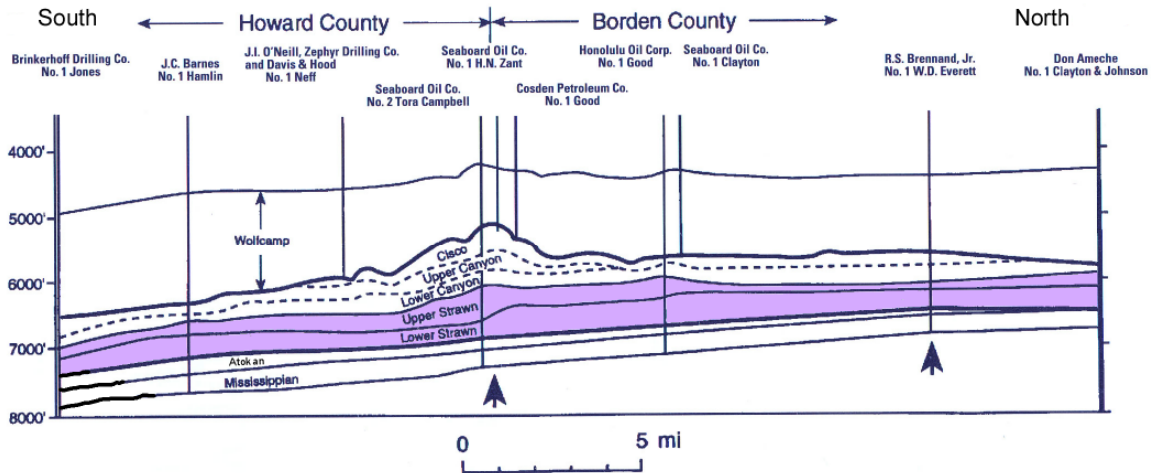


Figure 19. Regional south-north schematic, seismic-based cross section of Vealmoore and Oceanic fields After Waite (1993). Desmoinesian (Strawn Formation) highlighted in purple. Note addition of Atokan (previously referred to as Bend) interval, which was interpreted previously to thin northward. The Strawn Formation as illustrated above has dramatic thickness changes and appears to profoundly control subsequent growth and architectures of Missourian and Virgilian carbonates (Canyon and Cisco).

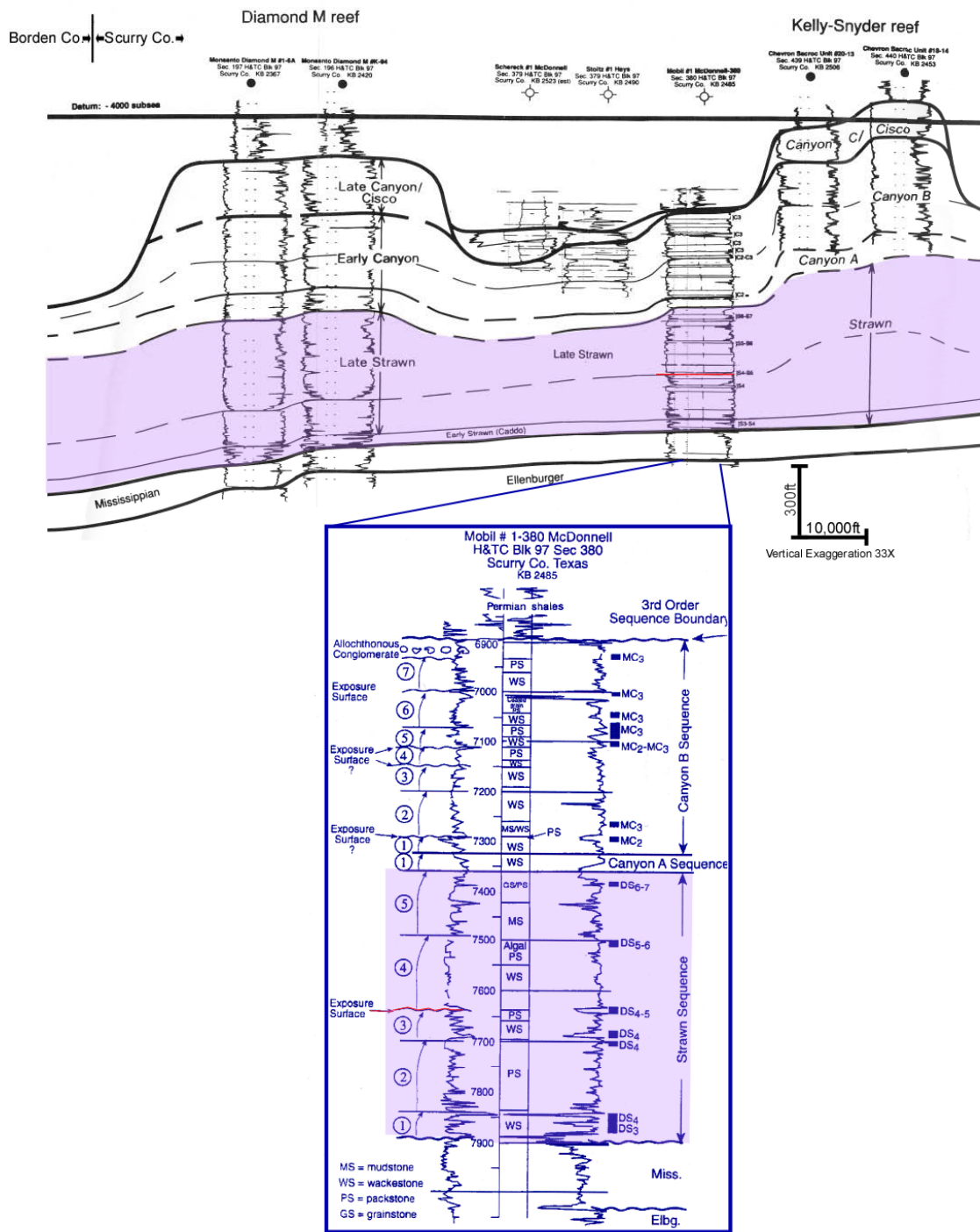


Figure 20. Regional schematic W-E, seismic-based cross section of Diamond M and Kelly Snyder Fields After Waite (1993). Desmoinesian (Strawn Formation) highlighted in purple. Mobil #1-390 well used in correlation illustrated at expanded scale. Circled numbers indicate 4th- to 5th-order cycles proposed by Waite (1993). Fusulinid biostratigraphic zone data provided on right side of log (for example, DS3-DS-7). Note that earliest Desmoinesian zones DS1 and DS2 are not represented in this well. Note exposure surface at top of cycle 3 within the Strawn (Waite, 1993). This surface may hold regional correlation potential. Overall facies stacking pattern indicates upward-shallowing succession. Note cycles stacking with wackestones and packstones underlying phylloid algal packstones, which are overlain by grainstones. This stacking pattern is typical of the Strawn.

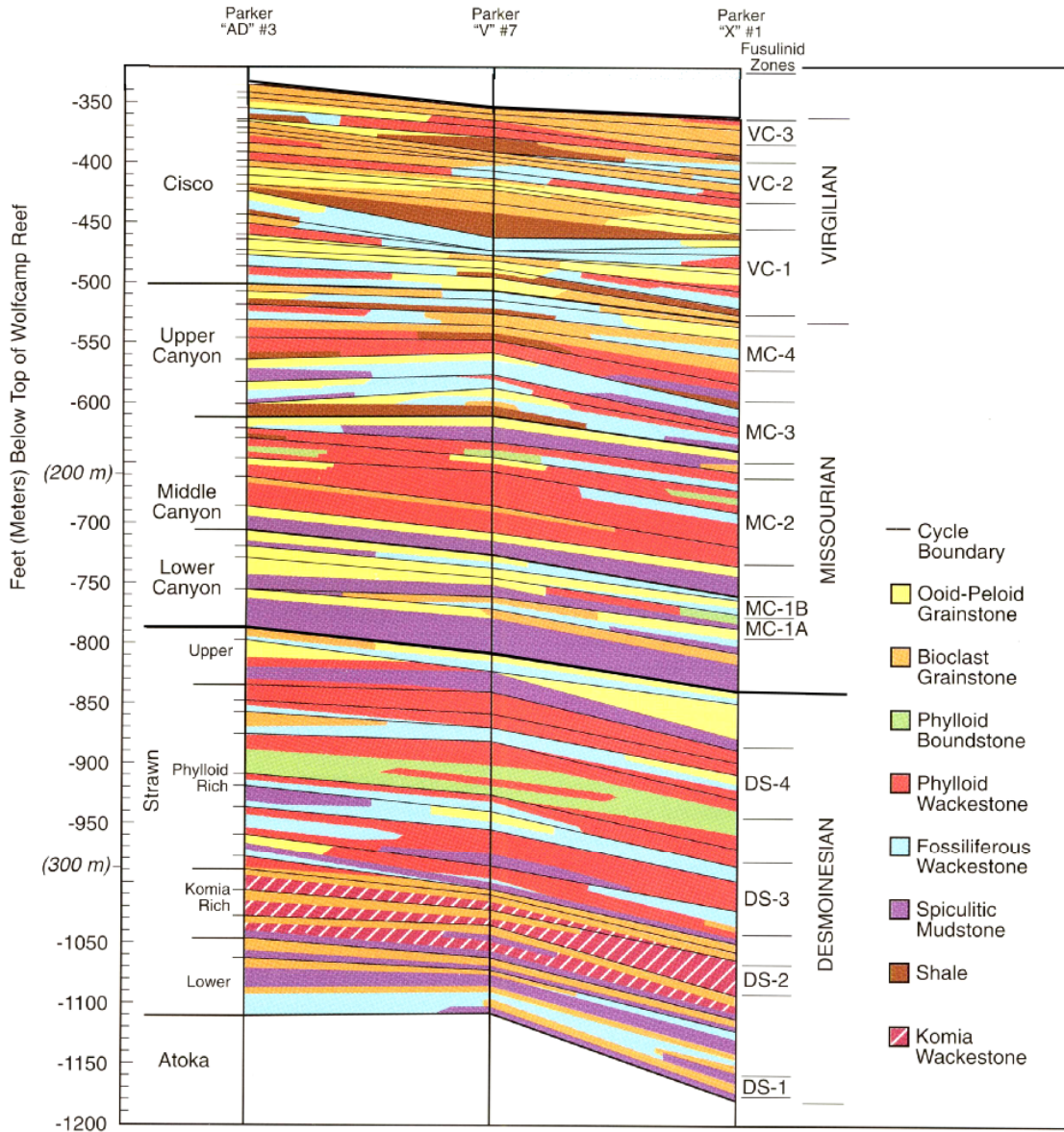


Figure 21. Three well facies and cycle boundary correlation of Pennsylvanian units in Southwest Andrews field Area (Parker, Andrews, and Deep Rock fields) (Andrews County). After Saller and others (1999). The Strawn is subdivided into four gross packages: (1) a lower wackestone and spiculitic mudstone-dominated unit; (2) a *Komia*-rich unit (wackestone and bioclastic grainstone dominates); (3) a phylloid-algal rich unit (phylloid wackestone and boundstone dominate); (4) upper unit (basal spiculitic mudstone overlain by ooid-peloidal grainstones). Contact of Strawn and lower Canyon considered a sequence boundary. As discussed in figure 20, the lower Canyon basal sequence indicates a transgression (deepwater spiculitic limestones overlying grainstones).

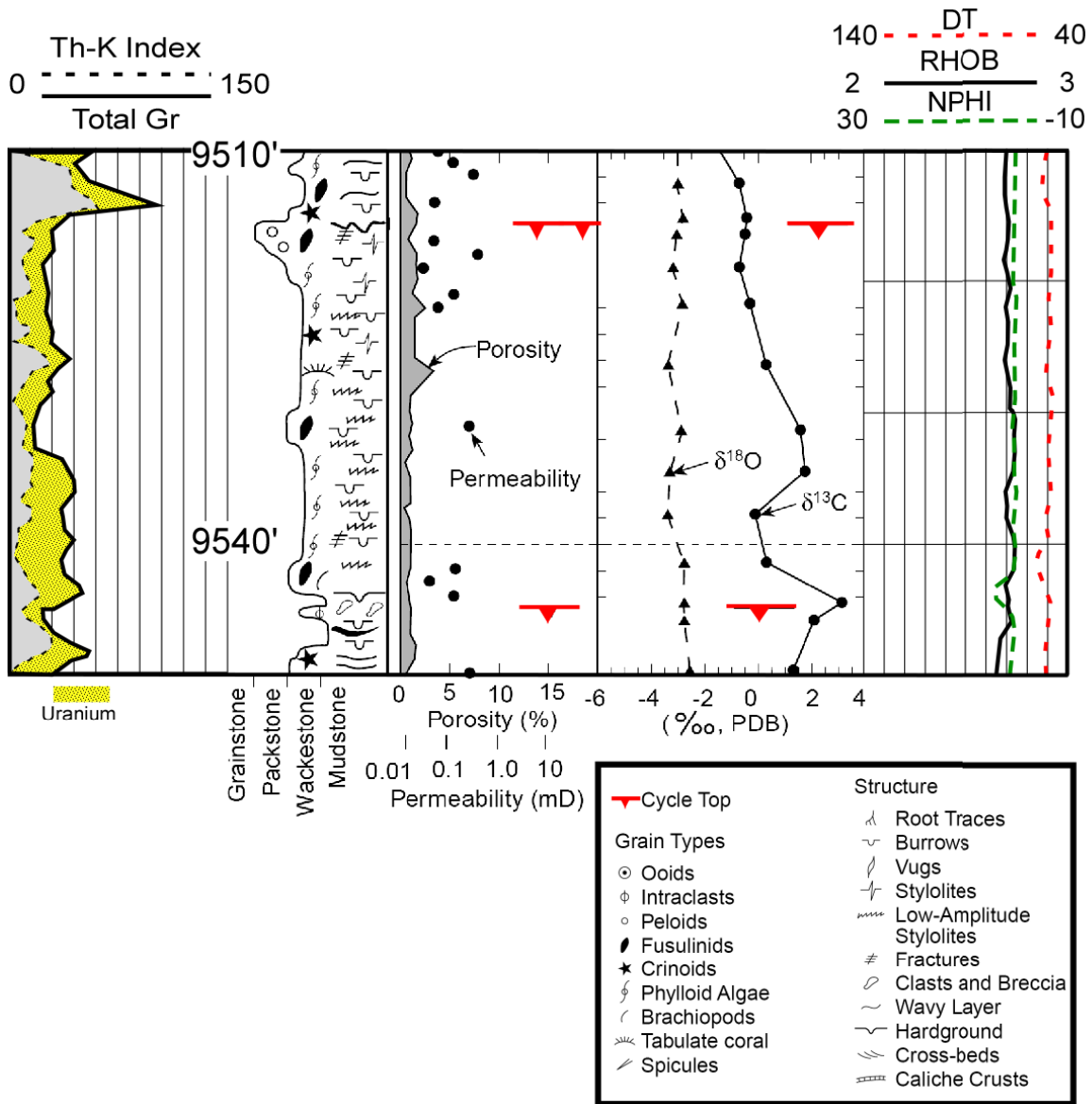


Figure 22. Core description, isotope data, and wireline-log signature of proposed Stage 1 diagenesis event in middle Strawn Formation (Well V#7). Modified from Saller and others (1999a, b). Different Stage 1 surfaces have different spectral gamma responses. Lower total gamma-ray peak centered on 9,540 ft composed primarily of uranium, whereas upper peak at ~9,514 ft has a decided thorium/potassium peak. Note that core and wireline-log porosity are low in entire interval. Permeability (black circles) variable but low <0.5 md. Also note that carbon and oxygen isotopes display marine values. Figure 23 illustrates core-slab photographs of this interval.

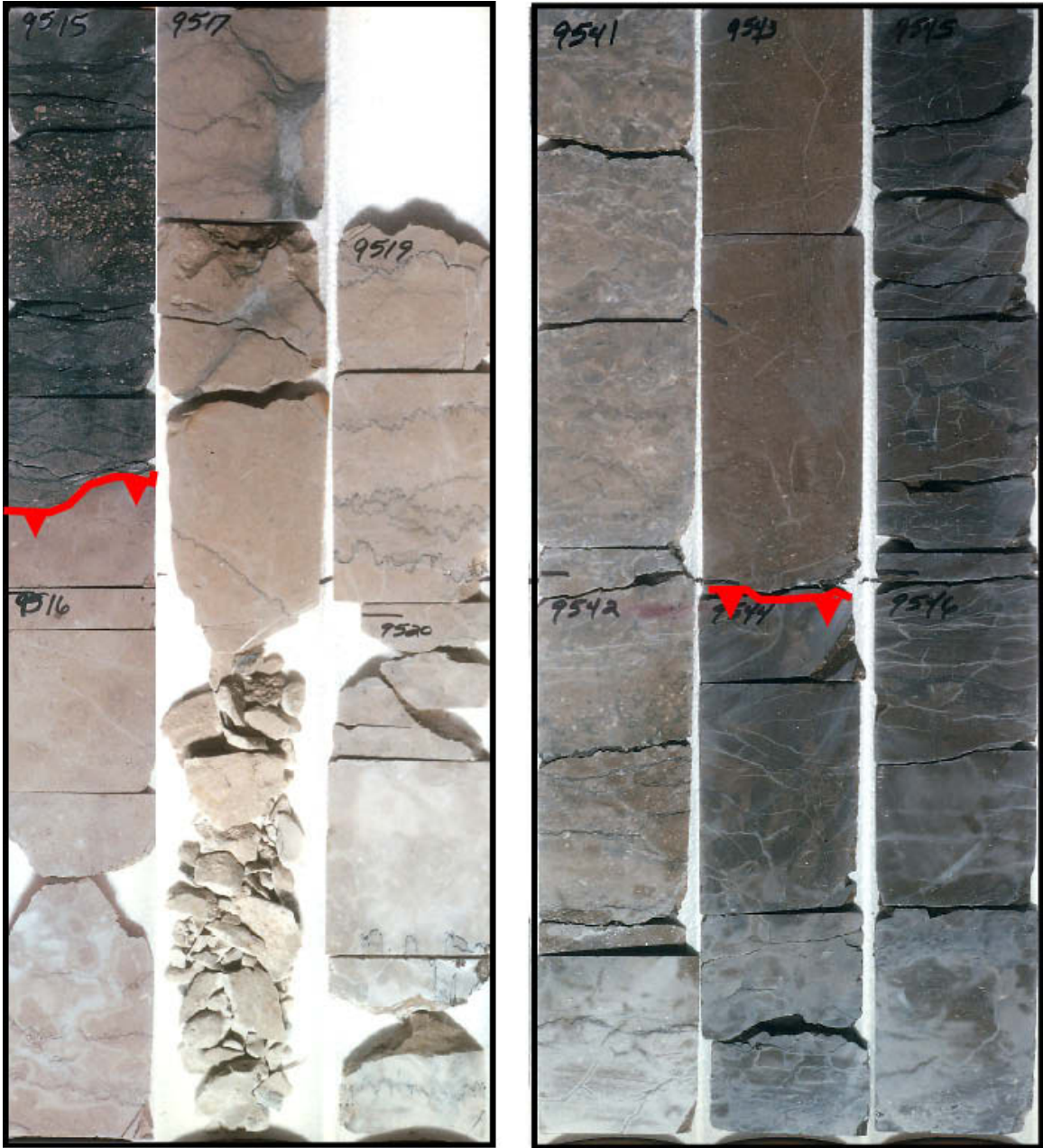


Figure 23. Core photos of Stage 1 Strawn interval in figure 22. Red lines with diamonds are exposure surfaces proposed by Saller and others (1999a, b). In both instances, above the surface can be interpreted as a purely transgressive surface without evidence of exposure. Note that dark fusulinid limestone at about 9,515 ft corresponds to high thorium peak in spectral gamma-ray log.

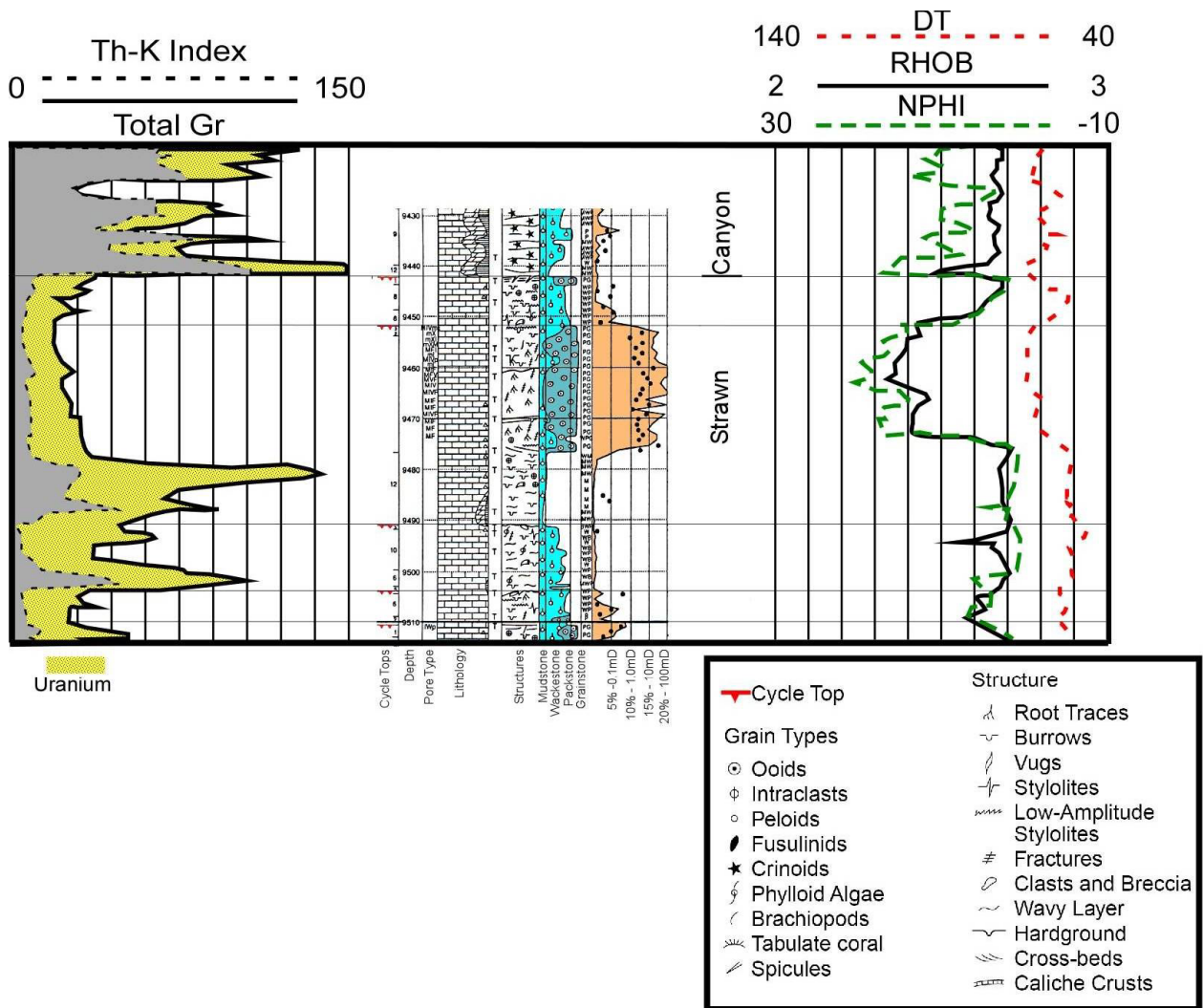


Figure 24. Core description, wireline-log signature, and core-analysis data for a Stage 2 alteration episode. This interval is at the top of the Strawn Formation in Parker X#1 well. Note that there are five cycle tops (each with possible exposure) interpreted by Saller and others, 1999. Exposure event at 9,452 ft 6 inches has no visible manifestation on spectral gamma-ray log. Interval above top of Strawn characterized by high thorium peak, indicating exposure. Total gamma spike at 9,480 ft appears to represent a small flooding or deepening event. In the absence of spectral gamma, exposure surface at 9,440 ft (top of Strawn) would probably be interpreted solely as a flooding event.

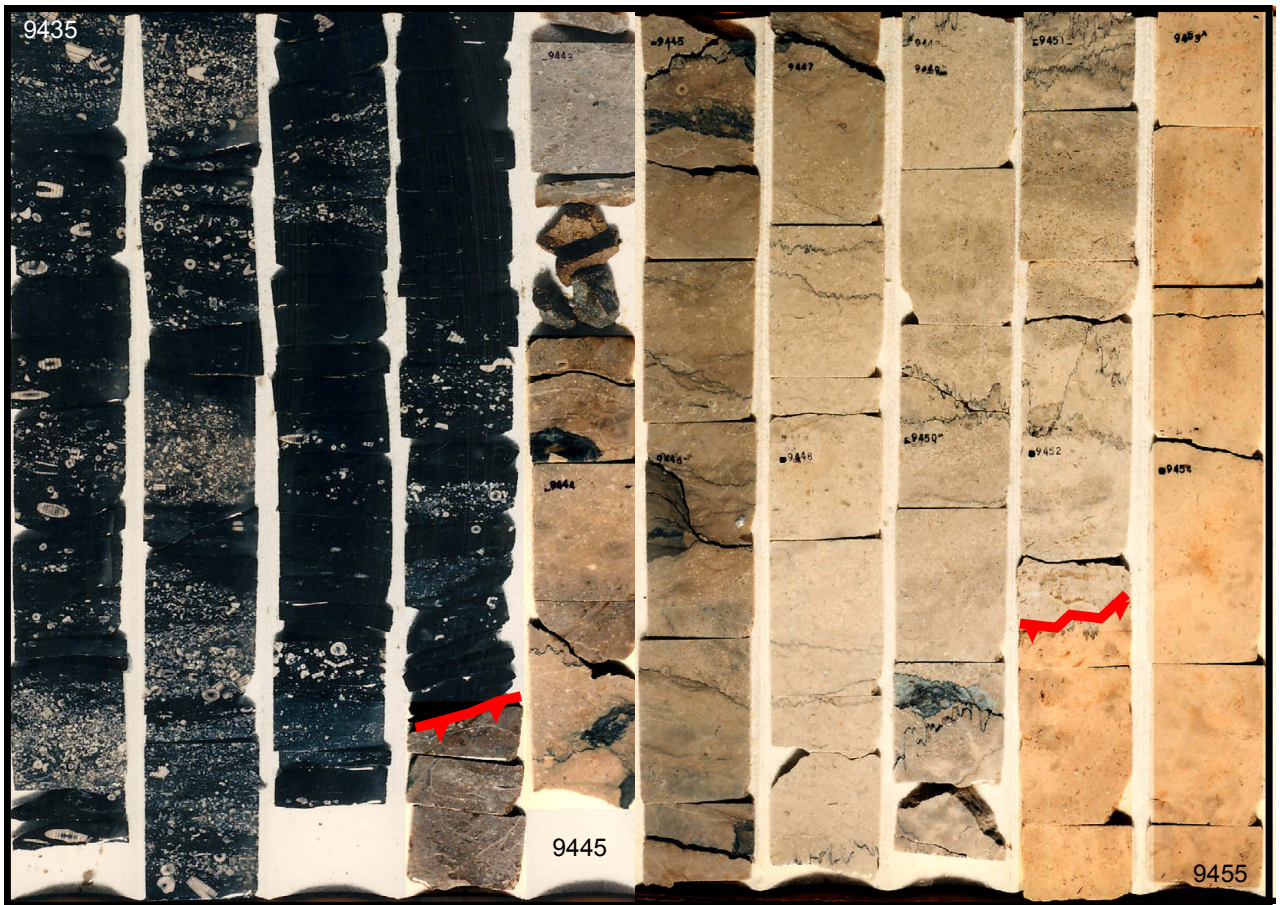


Figure 25. Core photos depicting cycle-top surfaces and facies picked by Saller and others (1999a, b) in the X1 well. Upper dark crinoidal unit corresponds to beginning of the Canyon Formation. Note that high thorium values on spectral gamma ray (fig. 24) correspond only to basal 2 ft of this unit. Interval considered a Stage 2 diagenetic event by Saller and others (1999a, b). Lowermost unit in figure marks beginning of upper Strawn reservoir interval. Judging from core porosity and permeability and wireline-log data, reservoir quality of this interval is good, with a maximum of 20 percent porosity and permeabilities slightly above 10 md. The porosity type found in the reservoir appears to be controlled by facies and grain type, as well as diagenetic alteration during exposure.

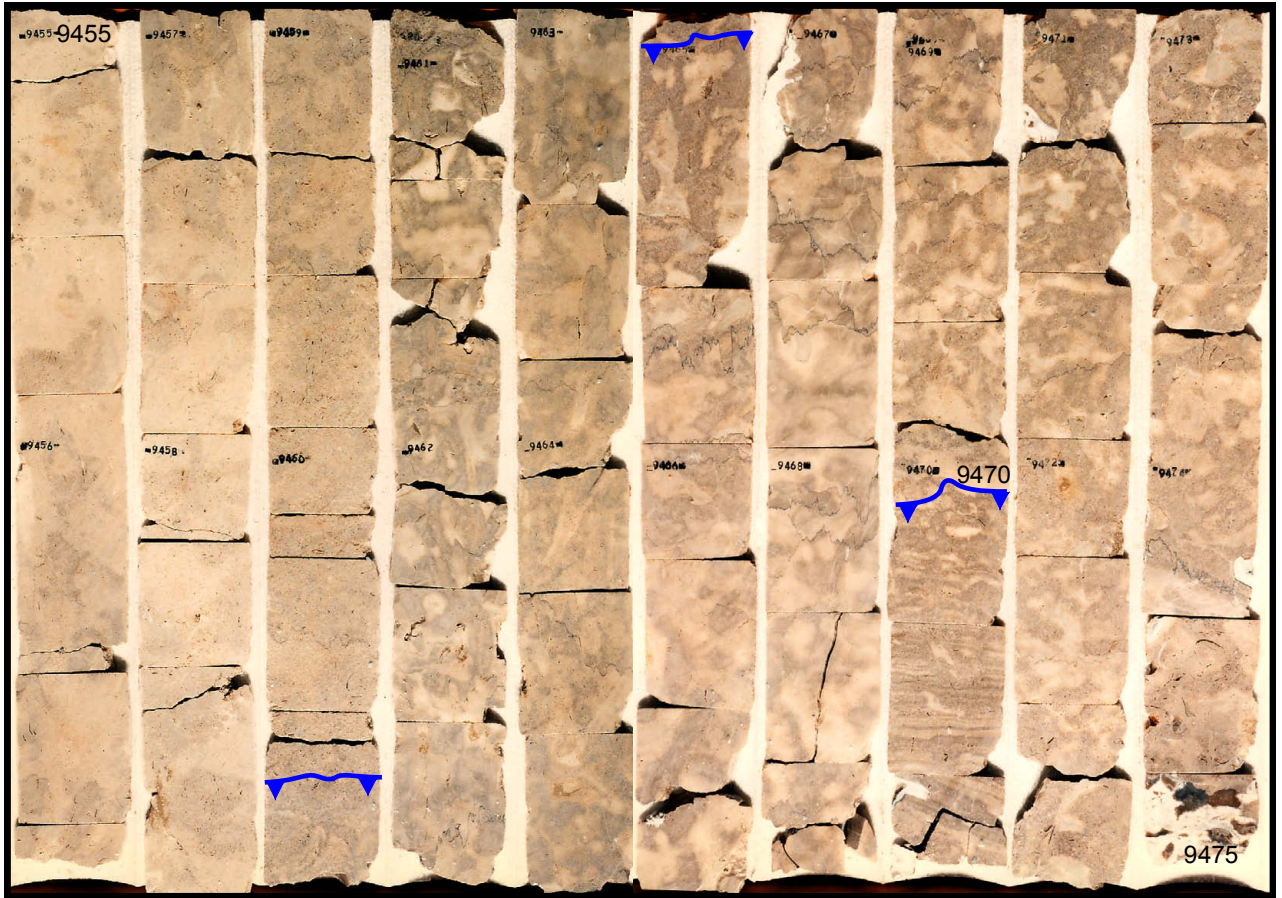


Figure 26. Core-slab photographs of X-1 well illustrating finer scale cycles within reservoir zone and Stage 2 exposure. Note that on the core description and wireline log diagram these facies are not highlighted; however porosity type and overall reservoir quality are affected by these changes. The surface in blue at about 9,470 ft denotes top of laminated facies (peritidal muds?). This facies was identified in another well within the field at the same stratigraphic position and similar wireline-log characteristics. This facies may indicate that the grainstone facies of figure 24 for well X-1 may be split into two cycles, which are separated by a peritidal facies. This type of observation, only possible using core data, has a bearing on lateral and vertical homogeneity of the reservoir interval.

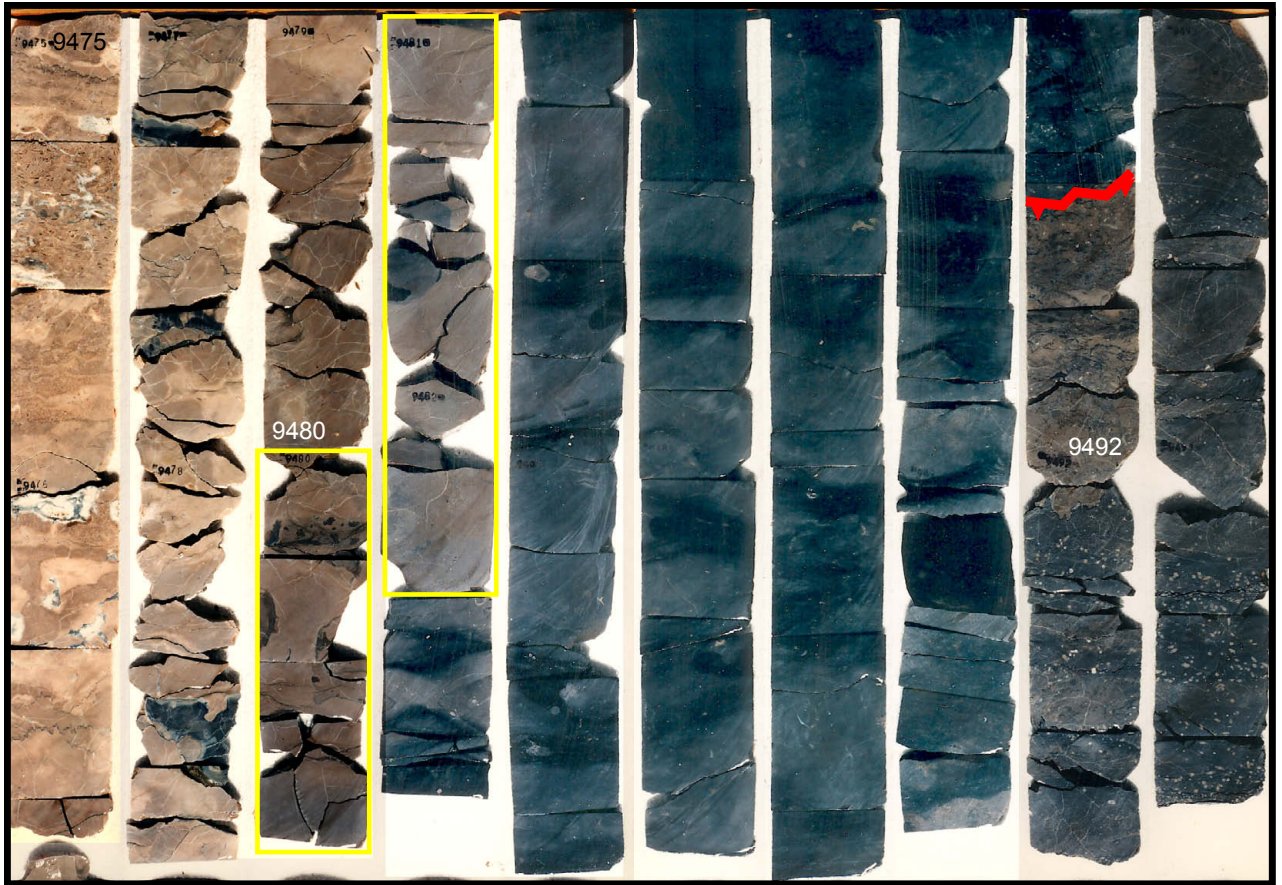
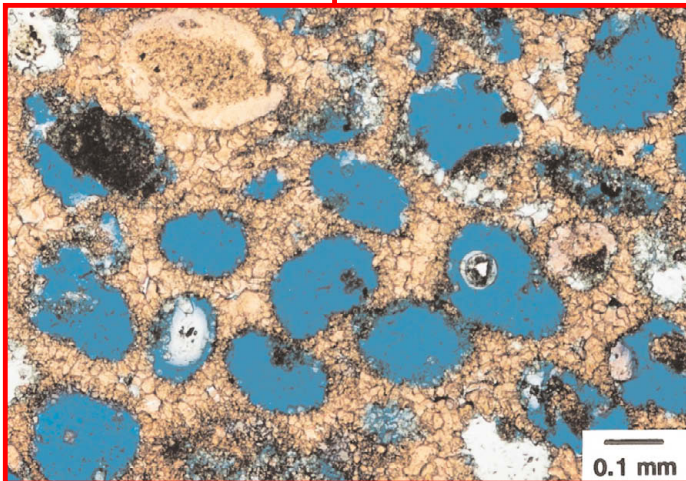
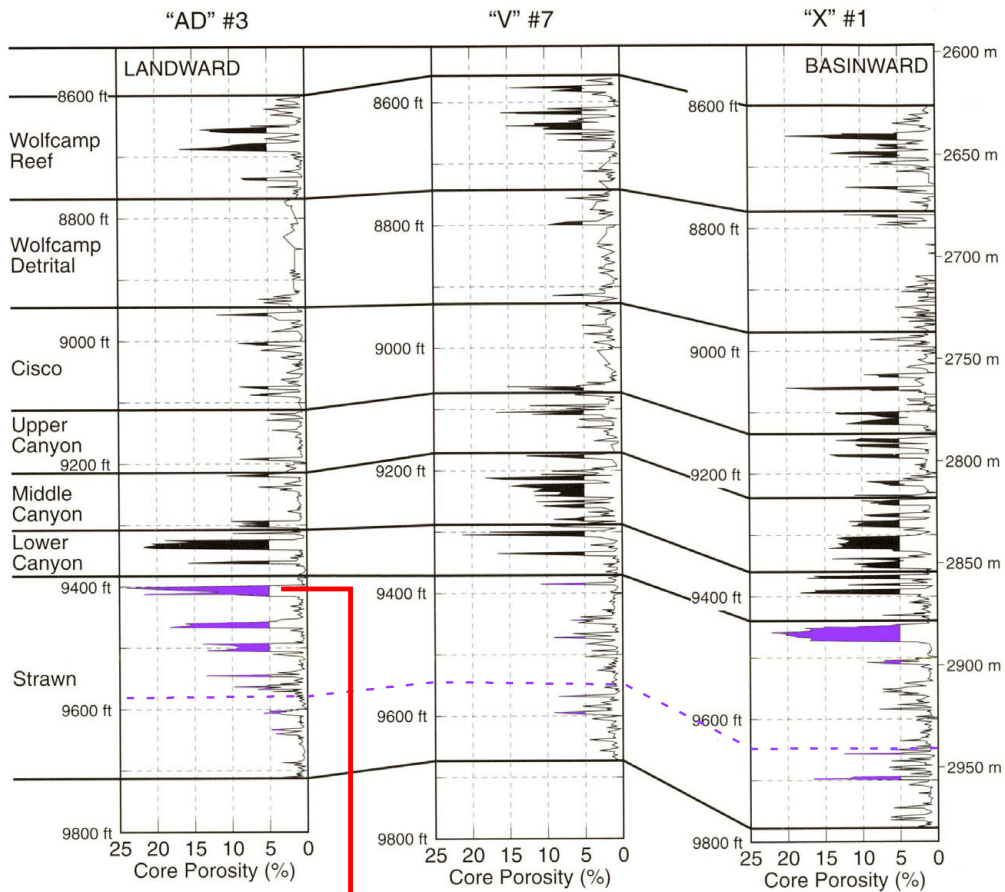


Figure 27. Illustration of lower facies and cycles in figure 24 from 9,475 to 9,495 ft. Yellow boxes outlining facies from 9,480 to 9,482 ft correspond to 2nd-highest total gamma-ray spike in the entire Strawn interval within well X-1. Note that the gamma-ray peak is almost entirely composed of uranium, and the peak does not correspond to the darkest or most “organic-rich” facies. The use of this peak as a possible MSF is highly suspect when viewed in association with core and further highlights that spectral gamma ray should be used for correlation, not total gamma ray.



Porosity= 21.5%
Permeability= 0.99mD

Calcite Cement

Figure 28. Subregional core-porosity correlation in southwest Andrews field area. Porous zones (above 4 percent) in Desmoinesian Strawn highlighted in purple. Thickest reservoir zone underlies sequence boundary and exposure event at top of Strawn. Dashed purple indicates lower, possibly regional, exposure surface under which reservoir intervals in other areas are located (for example, Seminole field, Gaines County, and Kelly-Snyder field, figure 20). Photomicrograph illustrates porosity and permeability associated with Stage 2 diagenesis of upper ooid grainstone package in Strawn (Saller and others, 1999a, b).

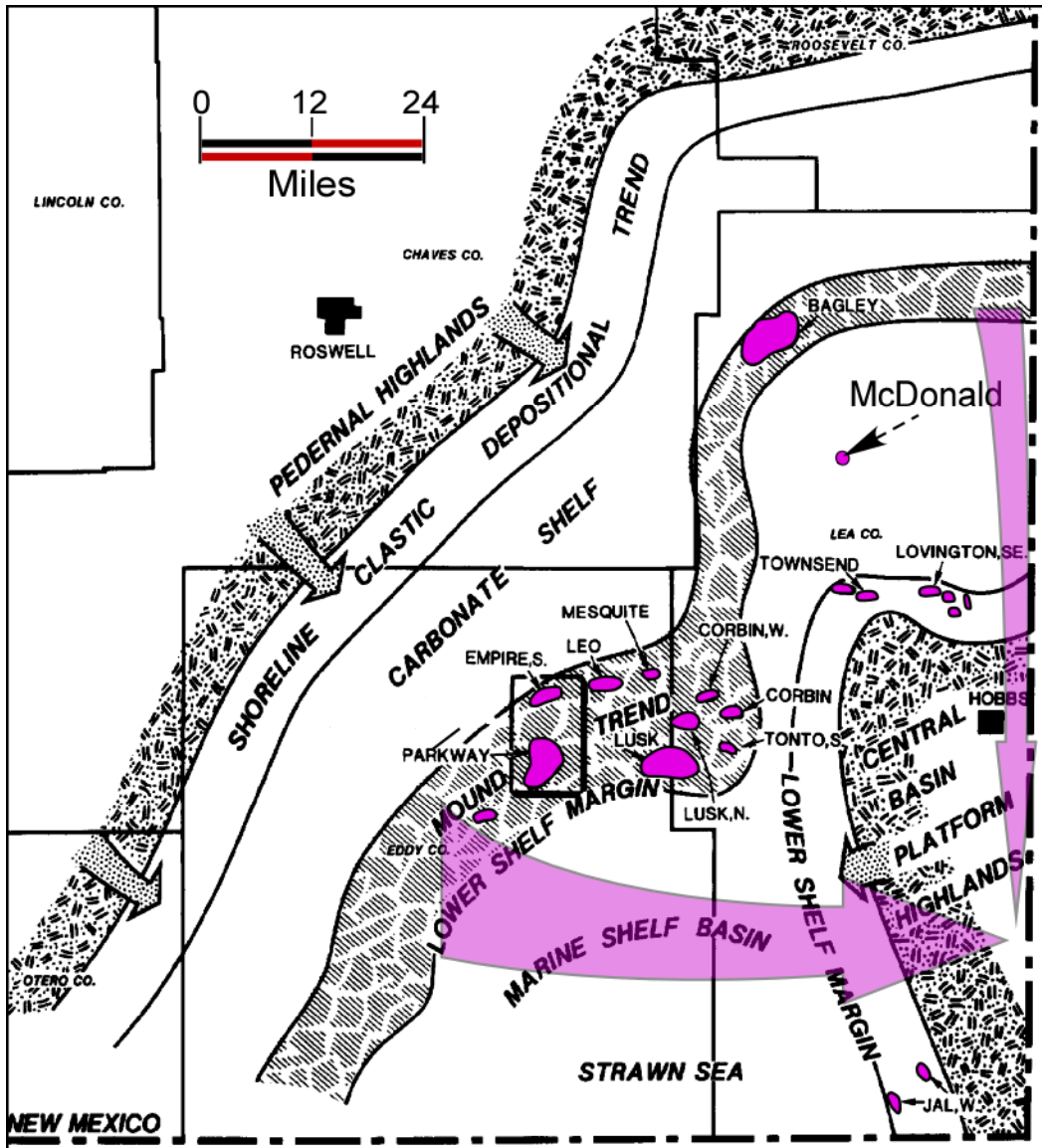


Figure 29. Regional interpretation by James (1985) of mound trend and lower-shelf margin of Strawn Formation during Desmoinesian. Trend likely composed of multiple carbonate bioherms and other facies that were deposited during several lowstand, transgressive, and highstand events. Resultant collage of targets extends much farther eastward onto the Central Basin Platform area, which was not emergent during the Desmoinesian (although it is depicted by James (1985) to be emergent).

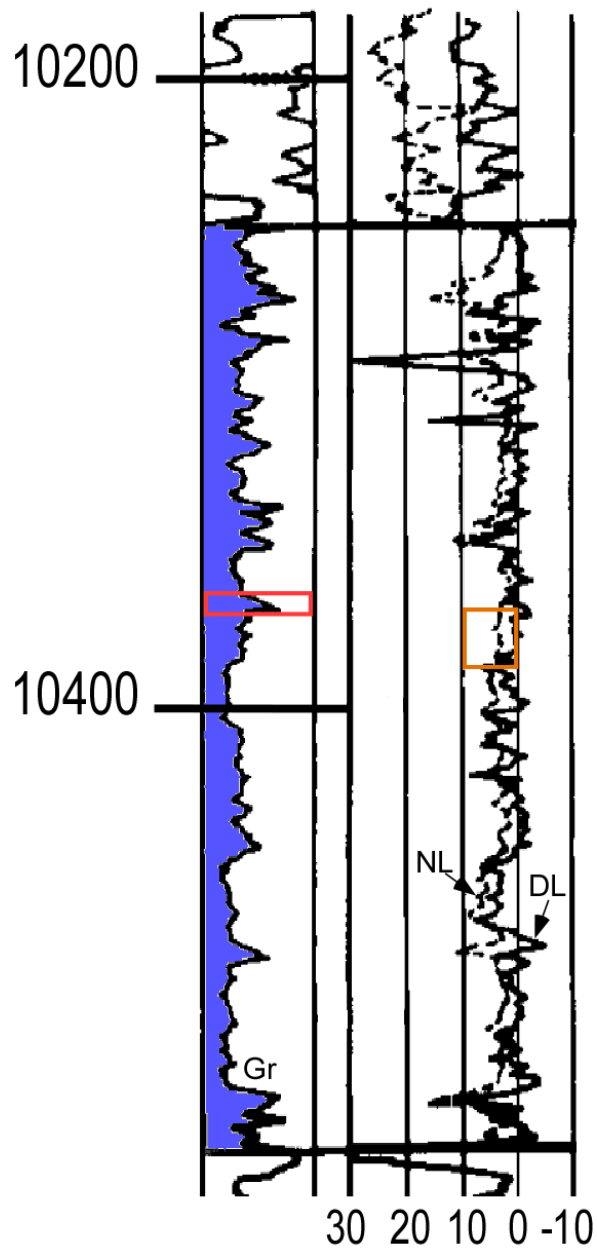


Figure 30. Characteristic gamma-ray and density-neutron log of Desmoinesian-age (Strawn Fm.) carbonates on Northwest Shelf. Southland Royalty Company 1 Parkway State well from Lea County, New Mexico. Strawn Formation Interval, indicated by blue, rests on Atokan sediments and is overlain by Missourian-age Canyon Formation. Gamma-ray spike outlined in red may be of regionally correlative significance. Overall wireline-log profile very similar throughout Permian Basin, with the exception of areas with expanded sections of the 'Upper Strawn.' Within fields such as Block 9 and Southwest Andrews, the highlighted gamma-ray peak contains a high thorium to uranium ratio interpreted as reflecting a possible exposure event below the peak. Area on porosity logs outlined in orange is interval of increased porosity, usually associated with alteration zone below exposure.

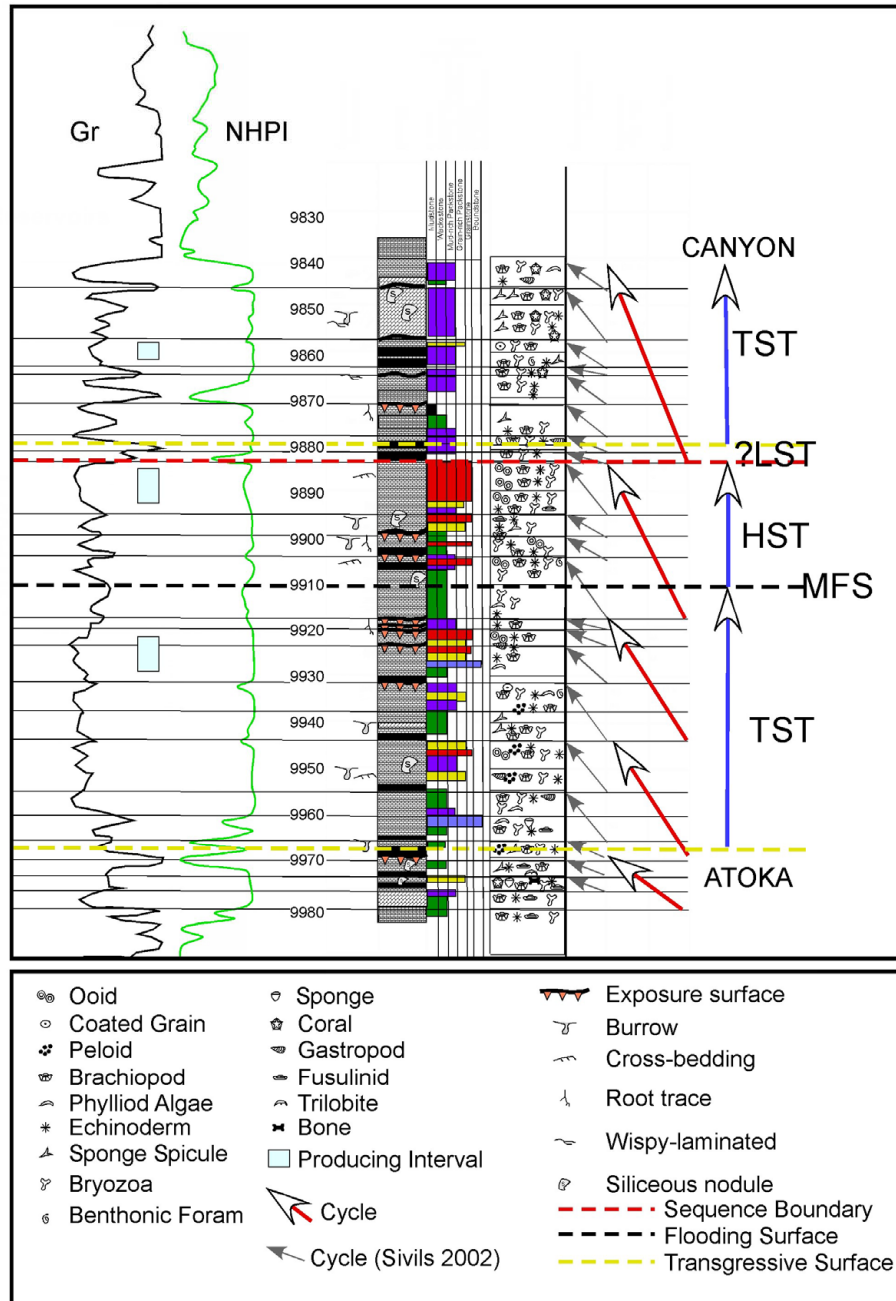


Figure 31. Detailed wireline and sedimentological log Texaco Glasscock "X" Fee #4, St. Lawrence field, Glasscock County. Modified from Sivils (2002). Red arrows on diagram indicate cycles/packages that are thought to be of possible regional scale. Gray arrows indicate 22 upward-shallowing cycles documented by Sivils (2002) for this interval. Sequence stratigraphic framework has been added to original diagram.

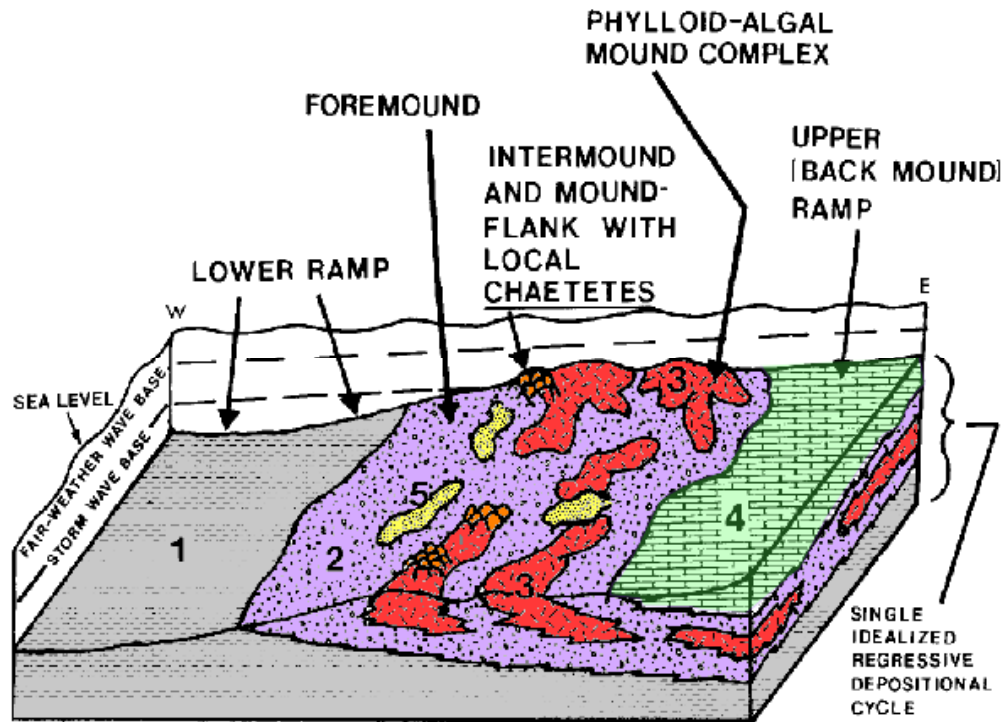


Figure 32. Idealized schematic representation of Goen limestone (patch reef) of Concho County, Eastern Shelf. After Marquis and Laury (1989). Facies tracts labeled 1 through 5 comprise (1) lower ramp (spiculitic mudstones and shales), (2) ramp center, foraminiferal wackestones with (3) localized phylloid-algal and Chaetetes bioherms, (4) upper ramp, bryozoan-coral wackestones, and (5) very fine calcareous sandstone assemblages. Overall Marquis and Laury (1989) thought that deposition represented regression. However, a more regional interpretation indicates that deposition occurred largely during transgression, with minor highstand development.

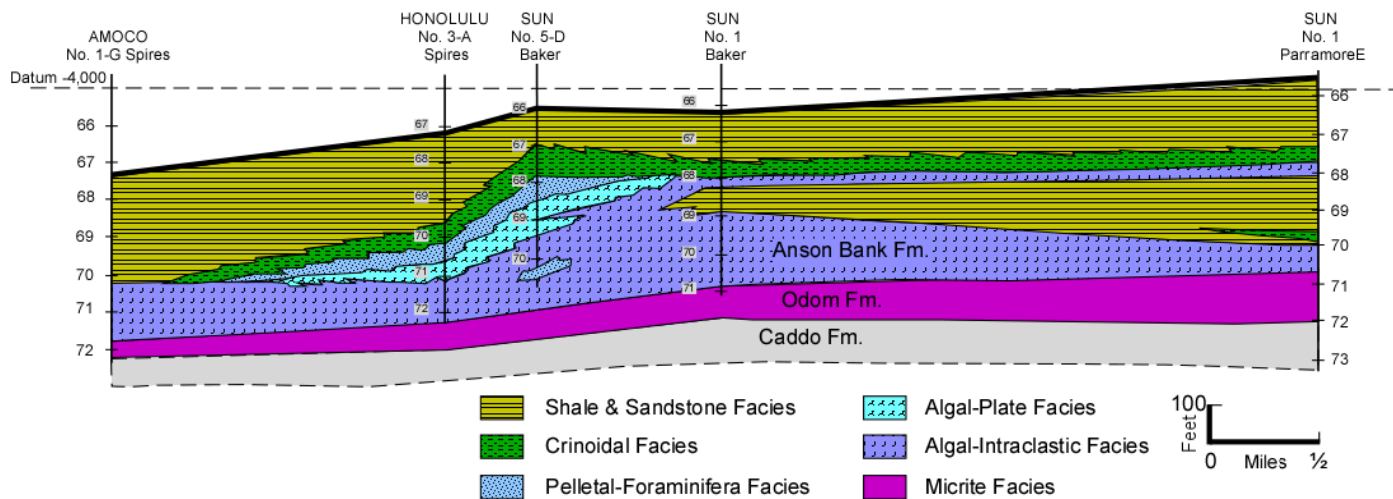


Figure 33. Depositional architecture and facies cross section of Desmoinesian Nena Lucia field, Nolan County. After Mazzullo, 1989). This shelf-margin to rimmed-shelf architecture is prominent on Eastern Shelf from mid-Desmoinesian onward. On diagram, total thickness of the Caddo Formation unknown.

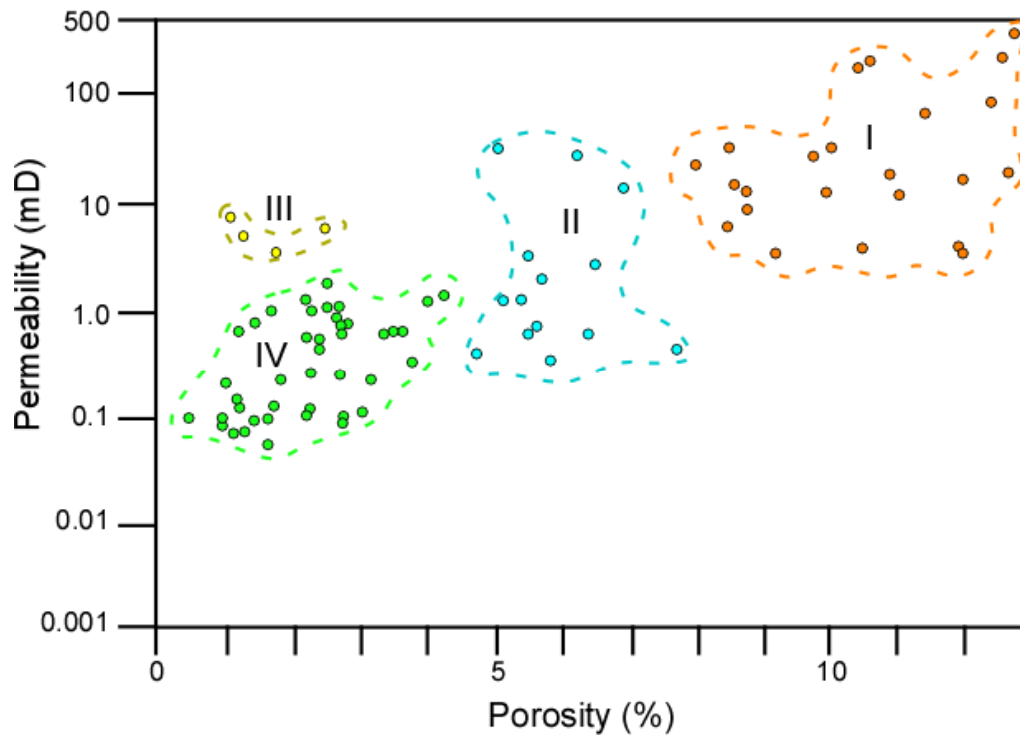


Figure 34. Porosity permeability cross plot for Goen Limestone reservoir. After Marquis and Laury (1989). Type I equals solution-enlarged, algal, moldic, vug, and channel open pores. Type II contains same pore population as Type I but is slightly occluded by later cement. Type III comprises open fracture and channel pores. Type IV contains Type I population of pore types but is dominated by open microporosity.

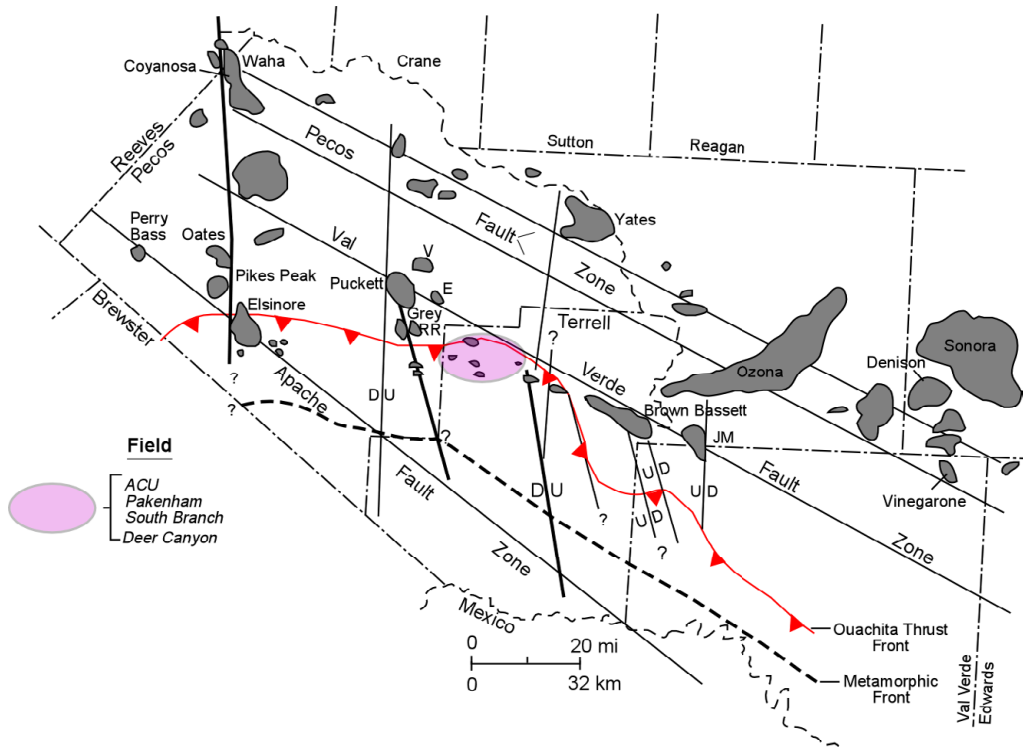


Figure 35. Regional map of the north edge of Val Verde Basin. After Montgomery (1996). Fields highlighted in gray. Most studied region containing Desmoinesian Strawn Formation reservoirs outlined in purple. Region contains ACU, Pakenham, South Branch, and Deer Canyon fields. North edge of Val Verde Basin indicated in red by Ouachita Thrust Front (alternatively called Foreland Thrust).

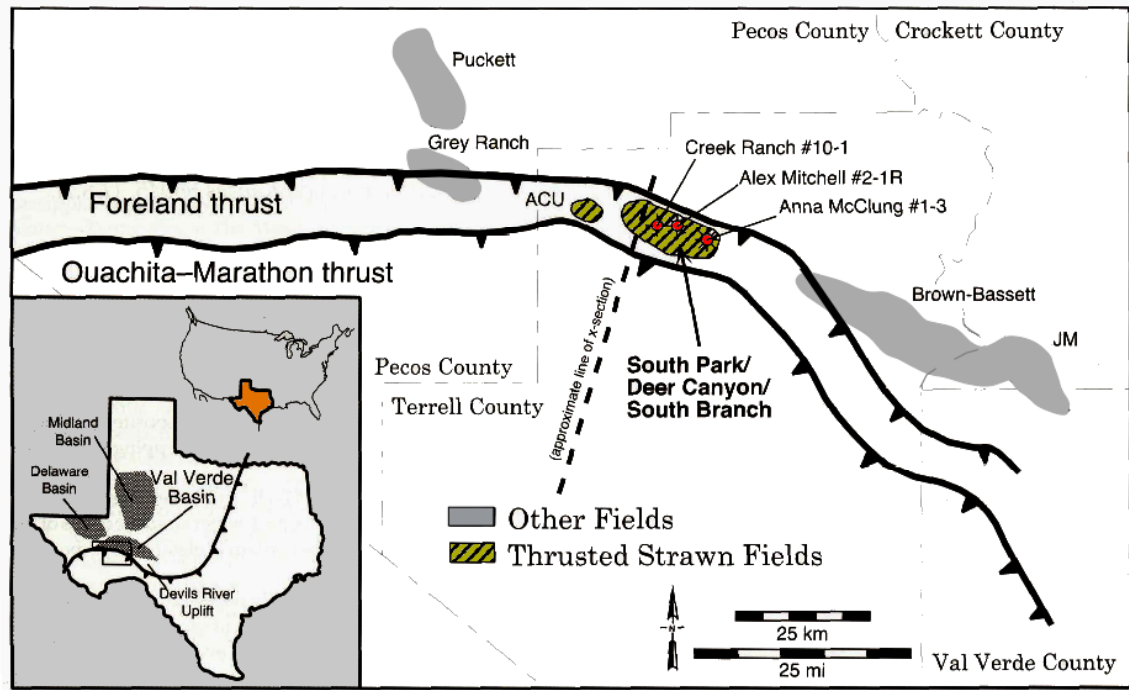


Figure 36. Subregional map illustrating position of thrusted Strawn reservoirs in Val Verde Basin (Terrell County) After Newell and others (2003). Foreland thrust equates to Ouachita Thrust Front in figure 35.

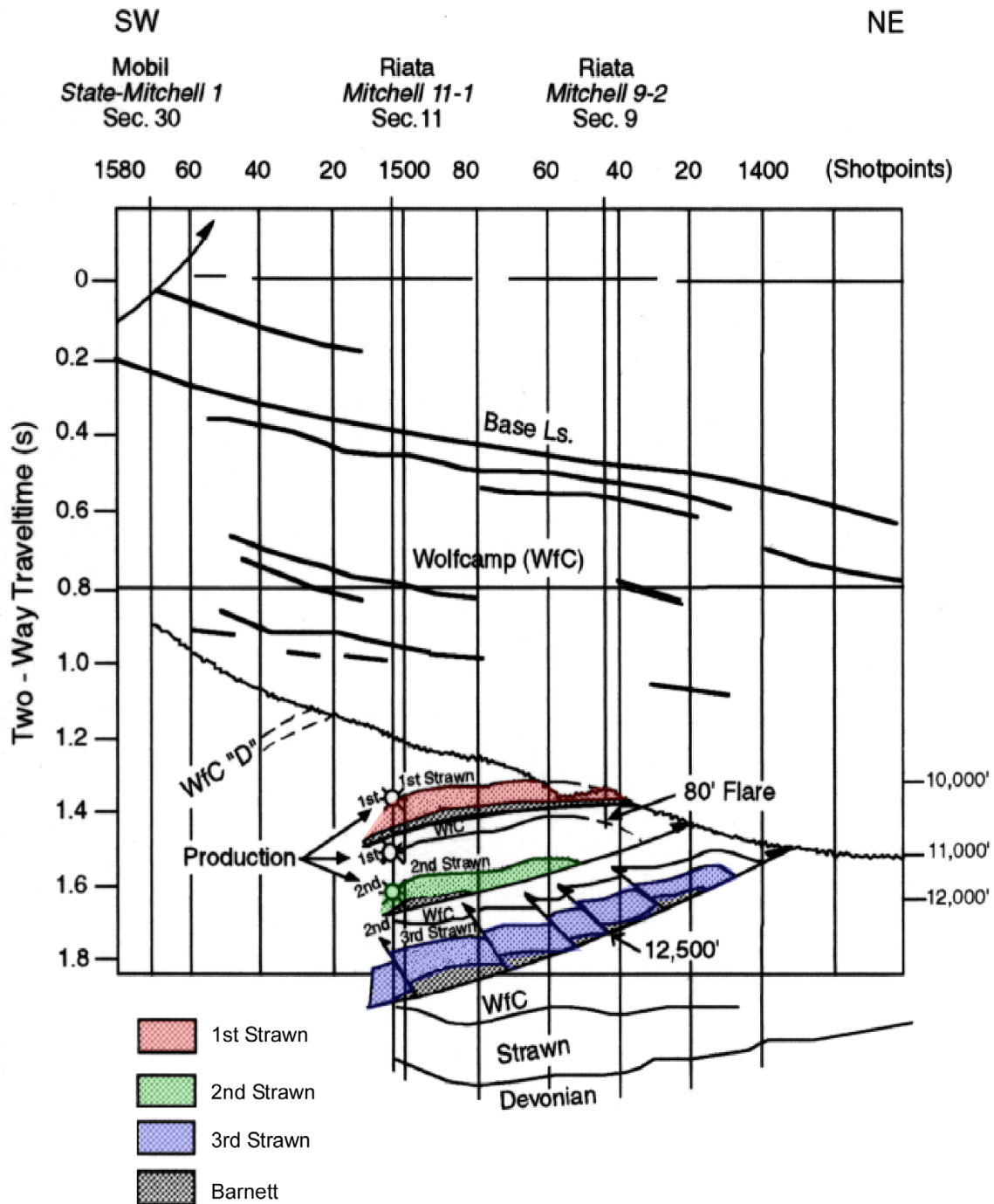


Figure 37. Geologic interpretation of SW-NE seismic line through Pakenham field. After Montgomery (1996). See figure 41 for comparison with uninterpreted seismic line from the same area. Multiple thrust Strawn Formation intervals (for example, 1st-3rd Strawn), as well as a thick allochthonous Strawn interval, are below the basal thrust. Structural complexity within thrust Strawn interval increases downward (fig. 43).

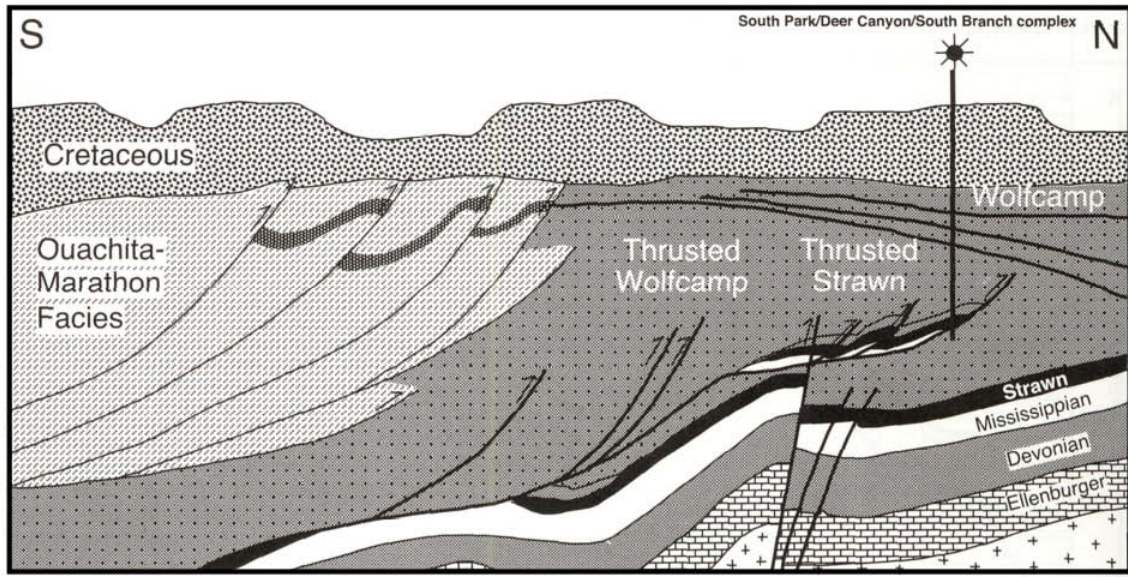


Figure 38. Schematic south-north diagram of Val Verde Basin thrust succession. After Newell and others (2003). There are two main thrust belts. The first contains thrust Mississippian, Strawn Formation, and Wolfcampian sediments and is termed the Foreland Thrust (fig. 36). The second is younger and contains Ouachita-Marathon siliciclastic facies and is termed the Ouachita Marathon Thrust.

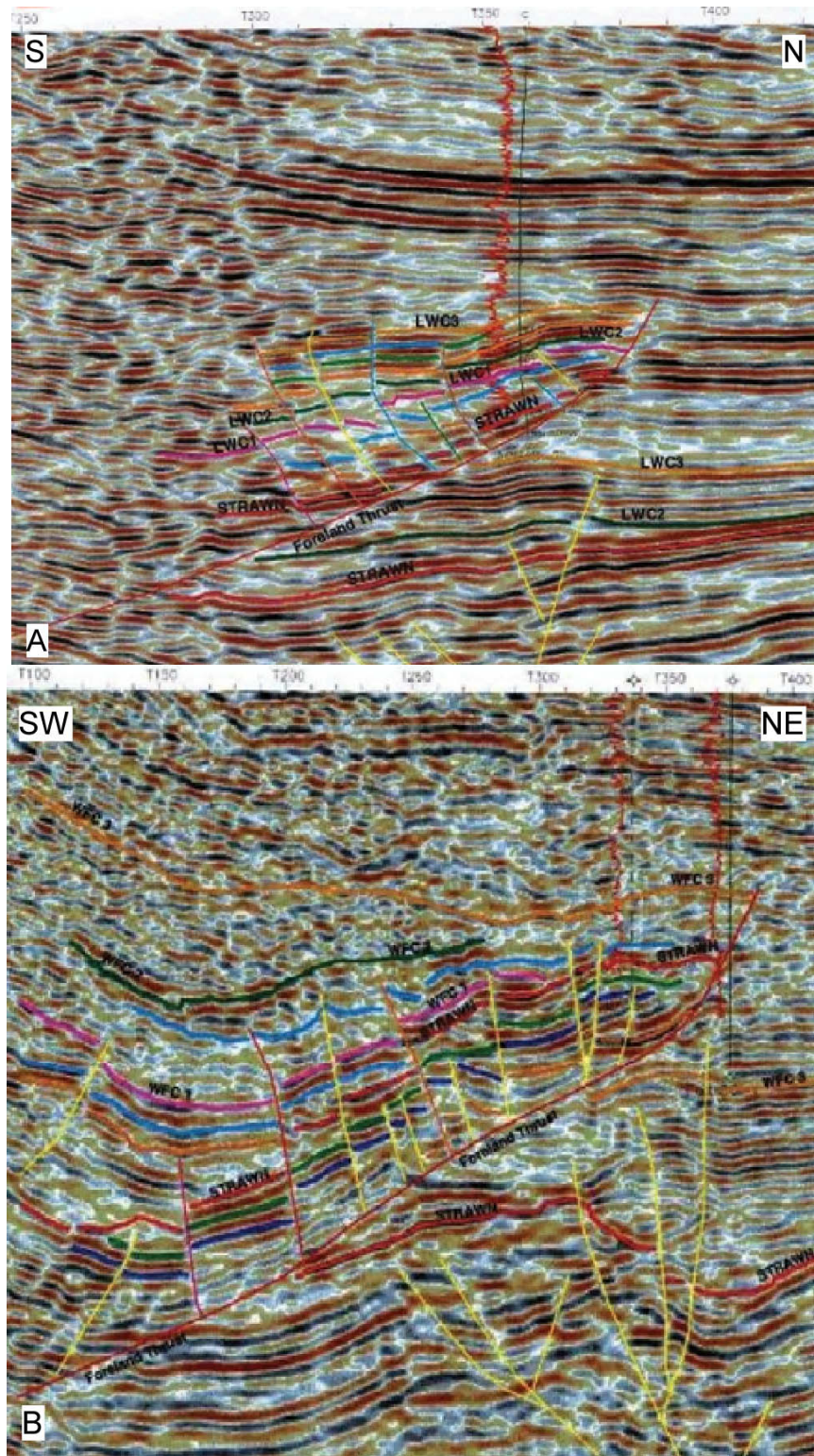


Figure 39. Interpreted (A) N-S and (B) NE-SW seismic lines through South Park area. After Khan and others (2002). Note structural variability between the two seismic lines. The uninterpreted seismic line in figure 41 would lie along strike between lines A and B above. Interpretations above indicate a single thrust interval of Strawn Formation.

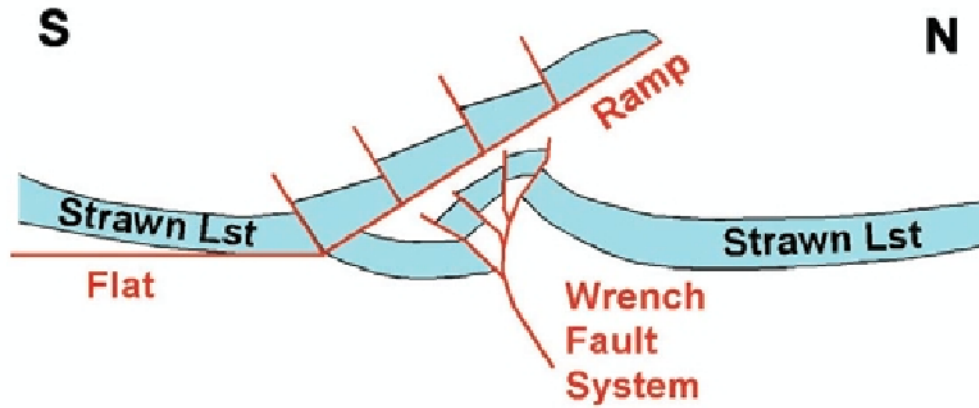


Figure 40. Structural interpretation of Strawn thrust reservoirs in Val Verde Basin. After Khan and others (2002). Model interprets that Strawn interval comprises single overthrust ramp, divided by back thrusts overlying wrench faulted pop-up structures. Model contrasts with those presented by Montgomery (1996) and Newell and others (2003) (figs. 37 and 38).

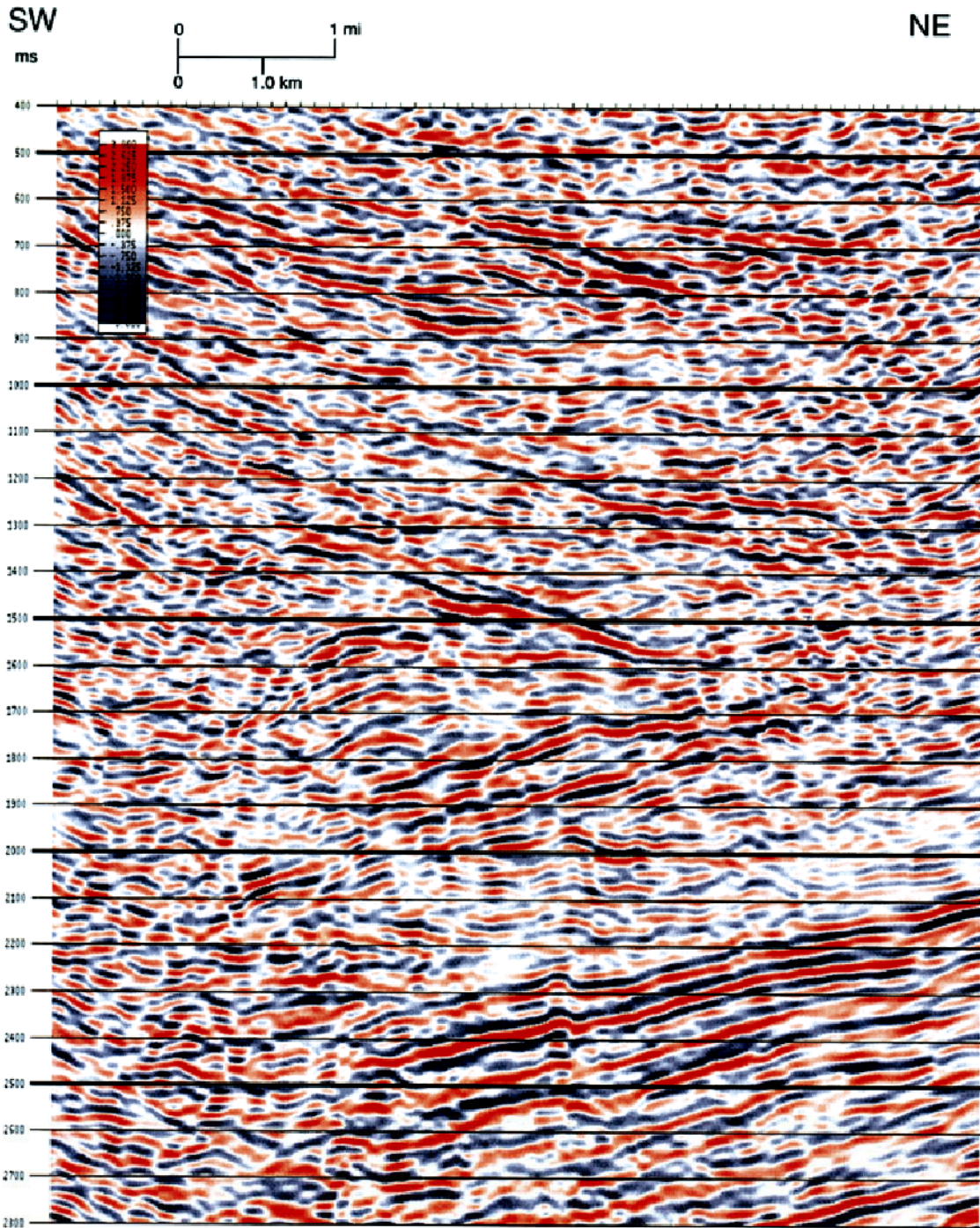


Figure 41. Uninterpreted seismic line trending SW-NE through Pakenham field (Terrell County). Seismic line illustrates structural complexity present in this part of Val Verde Basin. Figure should be compared with figure 37 for geologic and structural interpretation of this area. Figures 39 and 40 illustrate alternative, seismic-based, geologic and structural interpretations of the area.

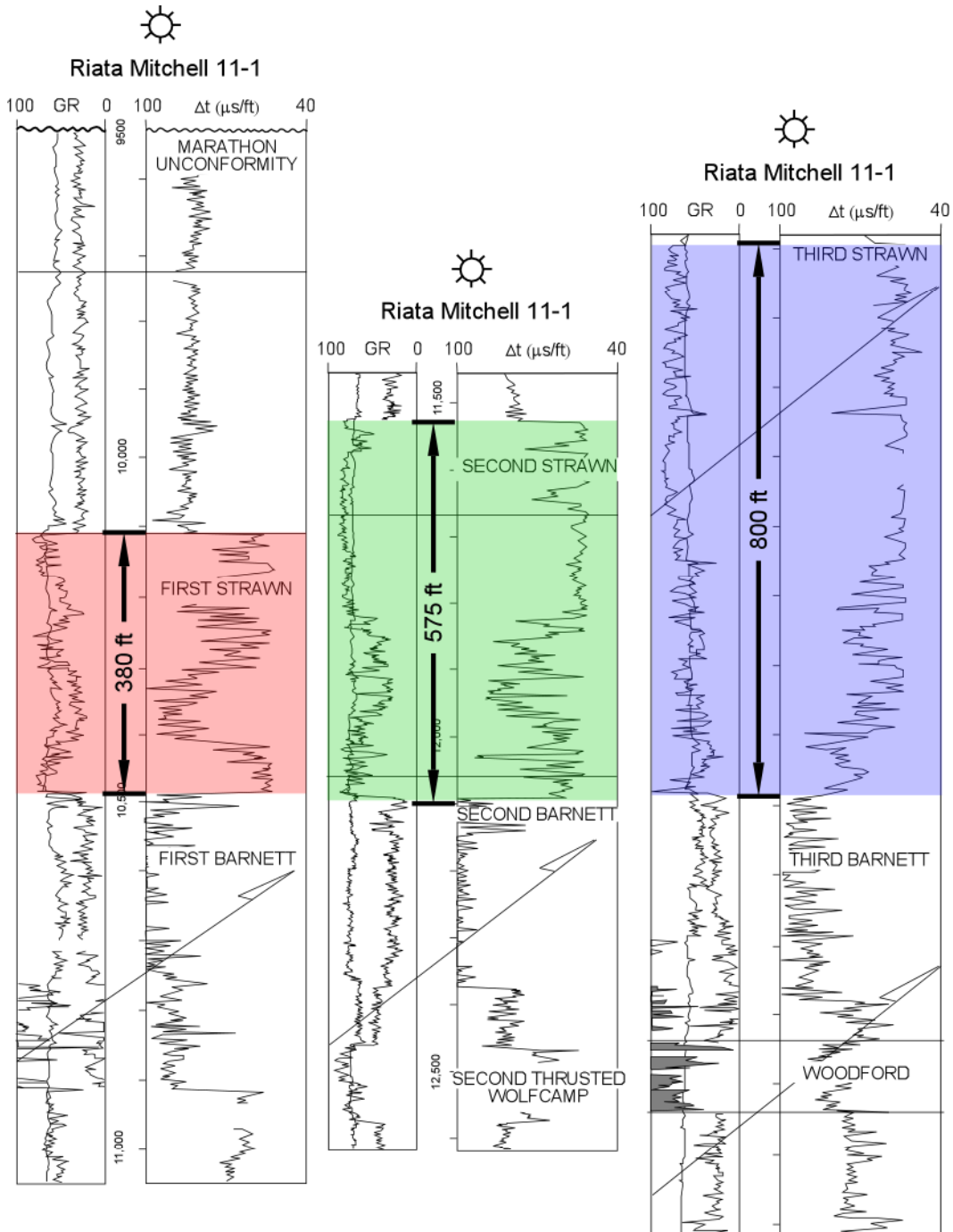


Figure 42. Wireline-log character of Woodford, Barnett, and Strawn Formations in Riata Mitchell 11-1 well (Pakenham field-Tyrell County). Each Strawn interval highlighted by different color (red, green, or blue). Structurally highest Strawn interval the First Strawn. Note that thickness of Strawn increases between first, second, and third Strawn intervals, indicating change in facies type (for example, possible outer-ramp position for First Strawn and inner ramp to mound core in second and third Strawn intervals). Judging from wireline-log character, lower part of all three Strawn intervals similar. Color coding of intervals corresponds to structural interpretations presented in figure 43.

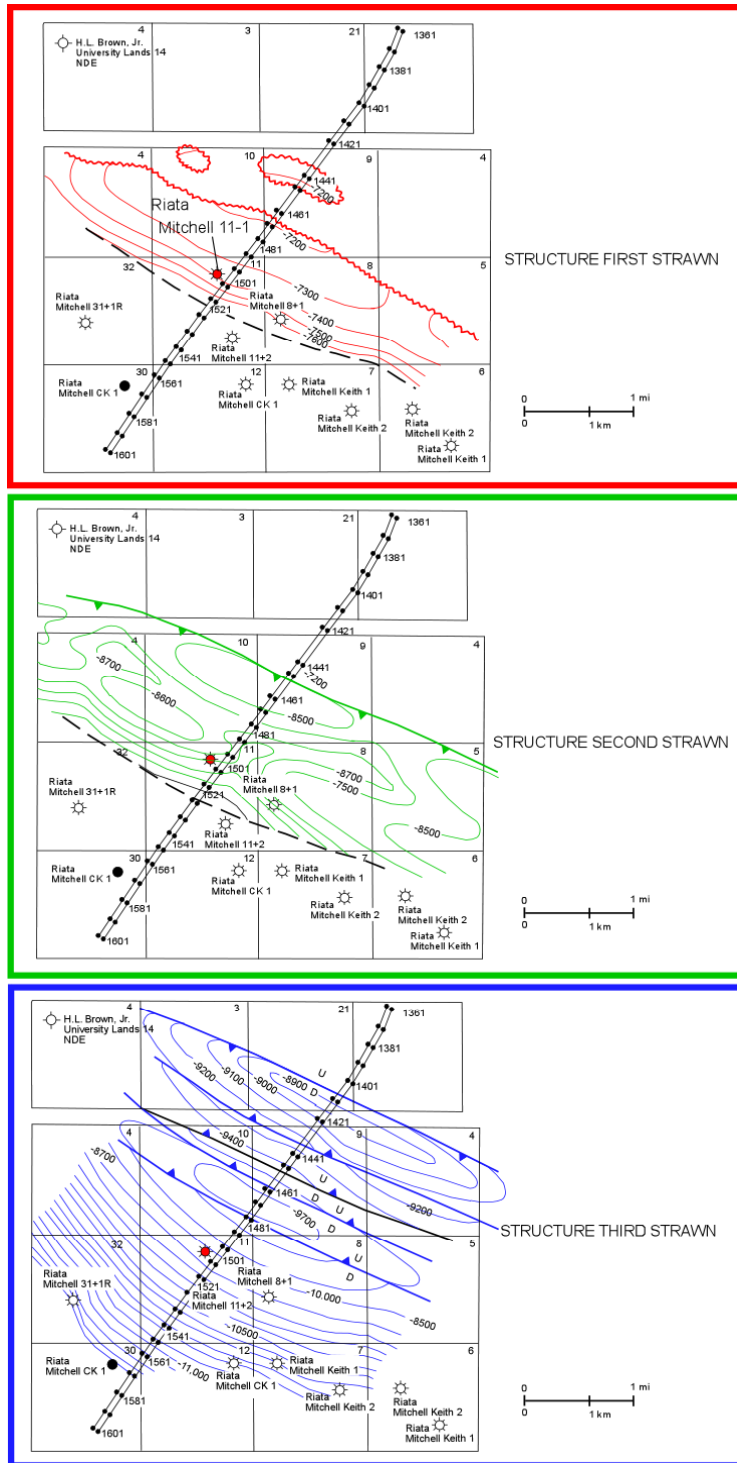


Figure 43. Structural interpretations of Pakenham field (Terrell County) at three Strawn intervals identified in Riata Mitchell 11-1 well (in red). Structural complexity increases with depth (“Third Strawn” most complex). Mounding and structural grain in Second Strawn may be partly depositional in origin. Uppermost Strawn interval has relatively simple closure, whereas lowermost interval has multiple closures in at least five back-thrust structures.

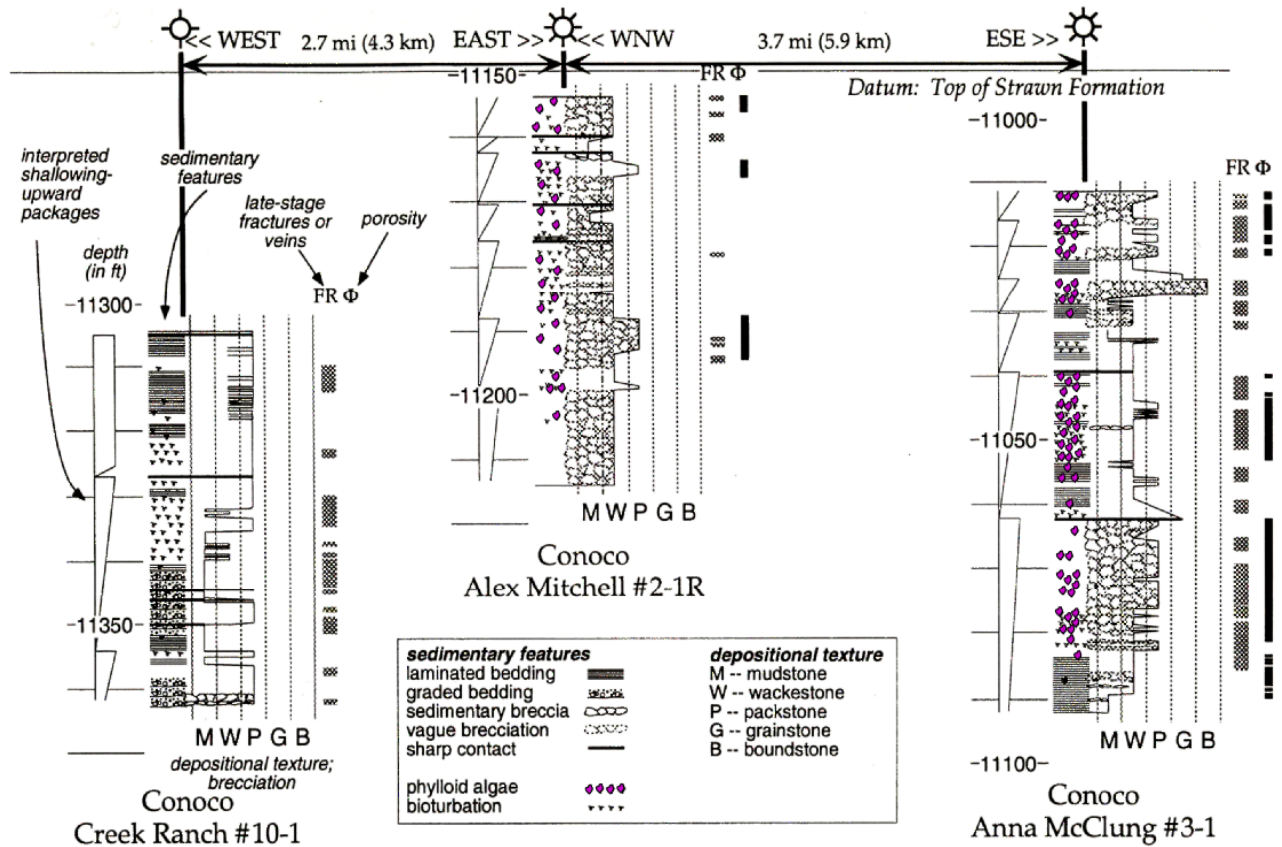


Figure 44. Lithologic description of three wells from South Park-Deer Canyon-South Branch complex of fields (Terrell County) (fig. 36). Creek Ranch #10-1 core dominated by graded packstone to mudstone and very fine grained, laminated packstone to wackestone facies. Both Alex Mitchell #2-1R and Anna McClung #3-1 intervals have coarser sediments containing large proportions of phylloid algae.

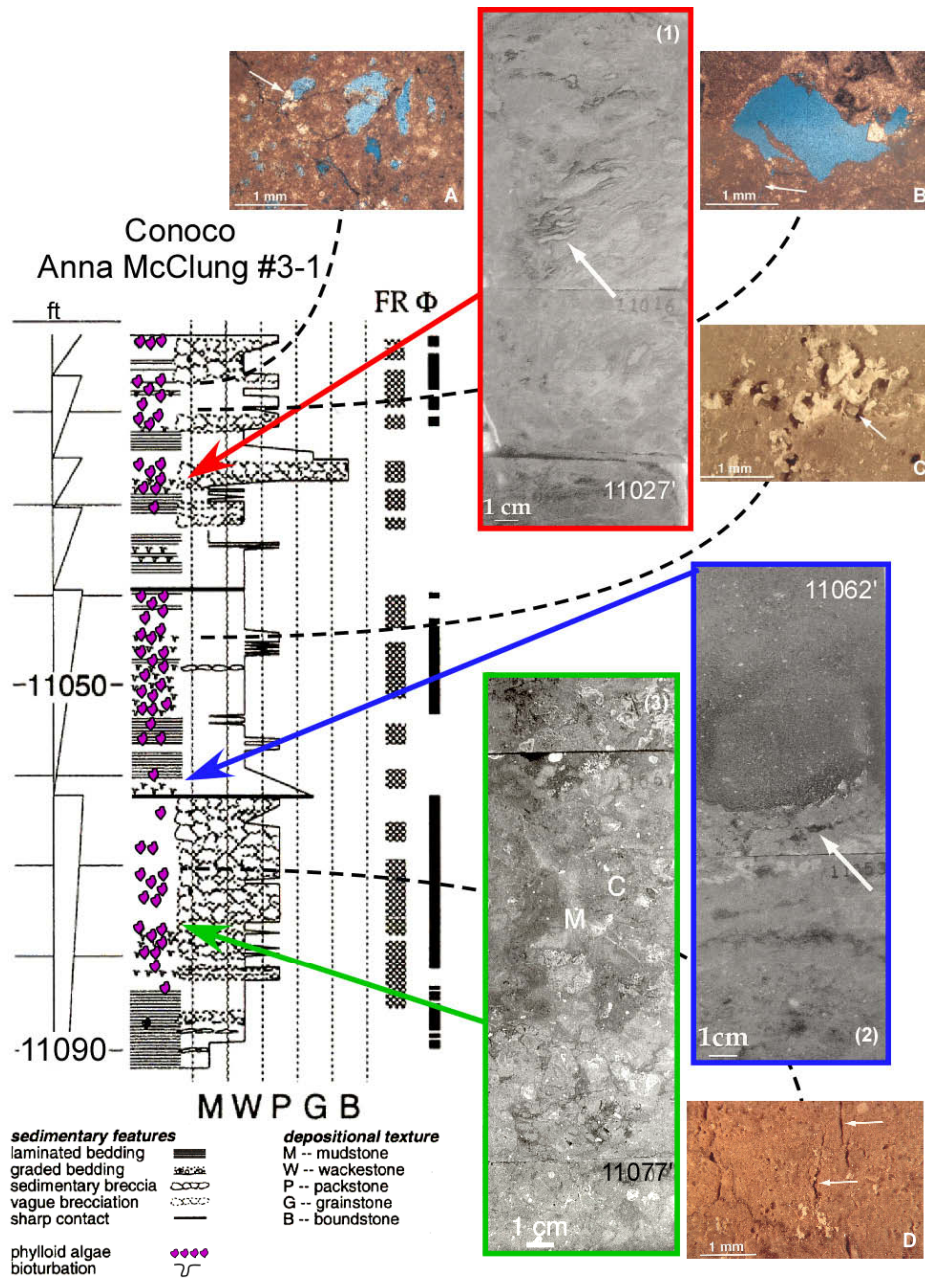


Figure 45. Detailed lithologic description of Anna McClung #3-1 core, with accompanying core photographs and photomicrographs. (1) Core photo of phylloid-algal boundstone (isopachous cement rim on algal plate denoted by arrow). (2) Core photo of cycle contact between underlying packstone facies and overlying very fine grainstone of next cycle (arrow denotes erosion and infilling into packstone). (3) Core photo of “pseudo-breccia” C-clast, M-matrix. (A) Photomicrograph of moldic porosity with dolomite crystal (white arrow) partly filling mold. (B) Photomicrograph of vug porosity with arrow denoting small dissolution-enlarged fracture extending away from vug. (C) Photomicrograph of interconnected solution-enlarged molds occluded by saddle dolomite (arrow). (D) Core photo illustrating solution-enlarged tension gashes (arrow) extending upward from a stylolite. Note that depth on core description is wireline-log depth, and photos of core slabs have been shifted accordingly.

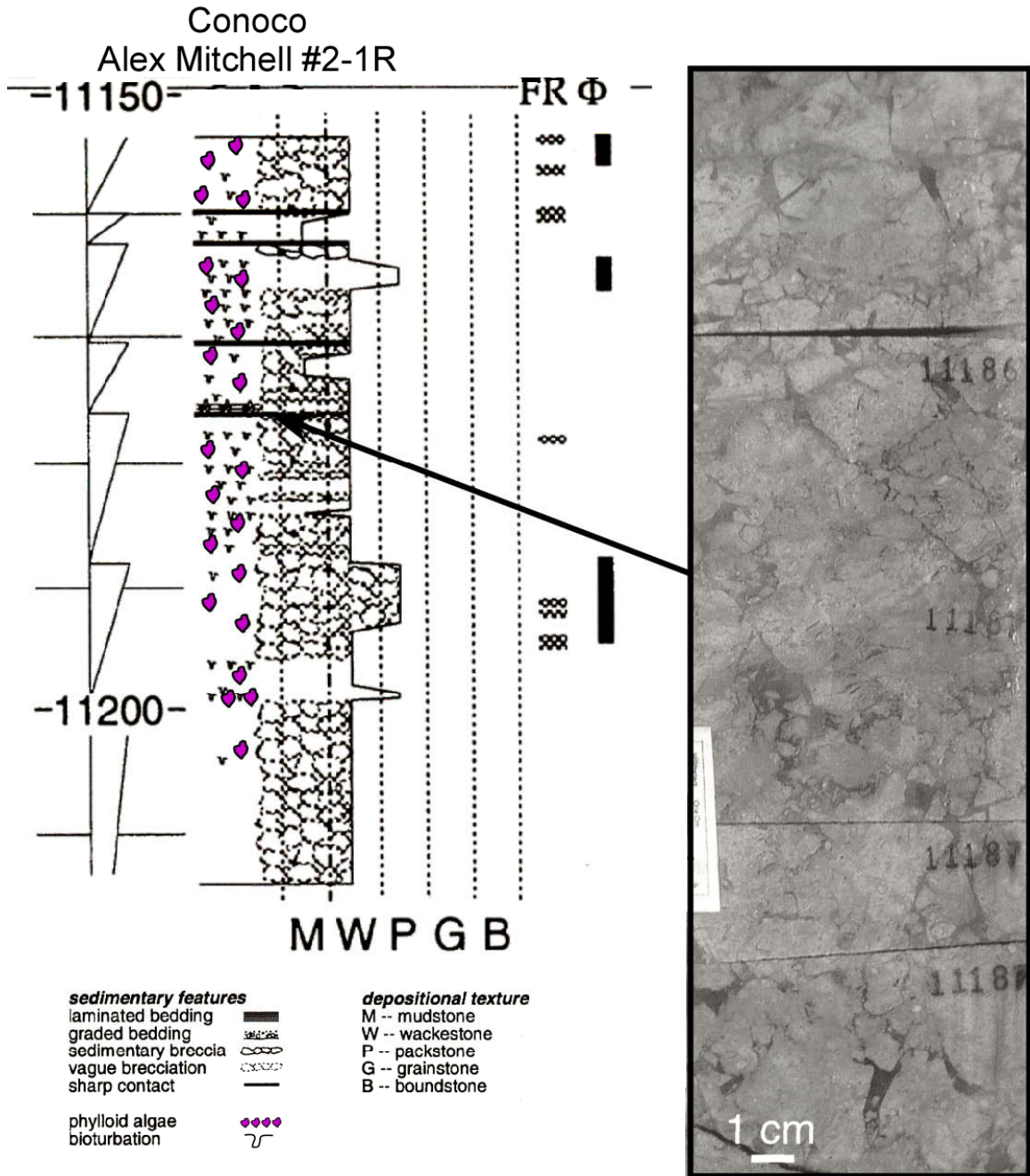
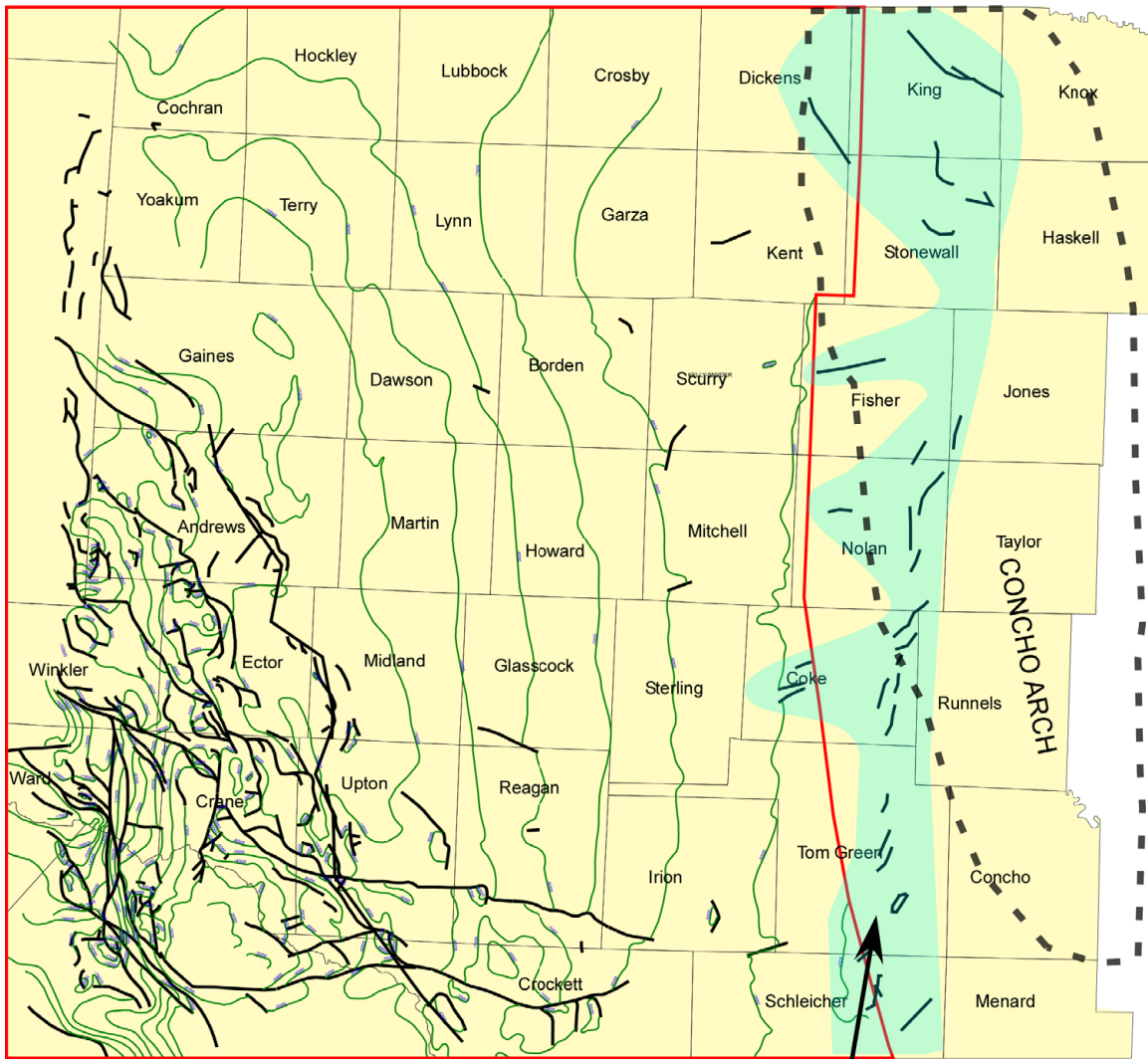


Figure 46. Detailed lithologic description of Alex Mitchell #2-1R core, with accompanying core-slab photograph illustrating brecciated wackestone composed of fitted clasts. Note that depth on core description is wireline-log depth and core-slab photo has been shifted accordingly.



FORT CHADBOURNE FAULT ZONE

Figure 47. Regional structure map of Midland Basin. Green contour lines from top Ellenburger structure. Faults in black derived from Ewing (1983). Fort Chadbourne Fault Zone outlined in blue. Trend of Concho Arch indicated by dashed polygon. Strong correspondence between mid- to late Desmoinesian shelf margin and fault zone.